

Indazole- and Indole-5-carboxamides: Selective and Reversible Monoamine Oxidase B Inhibitors with Subnanomolar Potency

Nikolay Tzvetkov Tzvetkov, Sonja Hinz, Petra Küppers, Marcus Gastreich, and Christa E Müller

J. Med. Chem., **Just Accepted Manuscript** • DOI: 10.1021/jm500729a • Publication Date (Web): 23 Jun 2014

Downloaded from <http://pubs.acs.org> on July 8, 2014

Just Accepted

“Just Accepted” manuscripts have been peer-reviewed and accepted for publication. They are posted online prior to technical editing, formatting for publication and author proofing. The American Chemical Society provides “Just Accepted” as a free service to the research community to expedite the dissemination of scientific material as soon as possible after acceptance. “Just Accepted” manuscripts appear in full in PDF format accompanied by an HTML abstract. “Just Accepted” manuscripts have been fully peer reviewed, but should not be considered the official version of record. They are accessible to all readers and citable by the Digital Object Identifier (DOI®). “Just Accepted” is an optional service offered to authors. Therefore, the “Just Accepted” Web site may not include all articles that will be published in the journal. After a manuscript is technically edited and formatted, it will be removed from the “Just Accepted” Web site and published as an ASAP article. Note that technical editing may introduce minor changes to the manuscript text and/or graphics which could affect content, and all legal disclaimers and ethical guidelines that apply to the journal pertain. ACS cannot be held responsible for errors or consequences arising from the use of information contained in these “Just Accepted” manuscripts.



1
2
3
4
5
6
7
8
9
10
11
12
13
14
15
16
17
18
19
20
21
22
23
24
25
26
27
28
29
30
31
32
33
34
35
36
37
38
39
40
41
42
43
44
45
46
47
48
49
50
51
52
53
54
55
56
57
58
59
60

Indazole- and Indole-5-carboxamides: Selective and Reversible Monoamine Oxidase B Inhibitors with Subnanomolar Potency

Nikolay T. Tzvetkov,^{a,*} Sonja Hinz,^a Petra Küppers,^a Marcus Gastreich,^b and Christa E. Müller^{a,*}

^aPharmaCenter Bonn, University of Bonn, Pharmaceutical Institute, Pharmaceutical Chemistry I, Bonn, Germany

^bBioSolveIT GmbH, An der Ziegelei 79, 53757 St. Augustin, Germany

*To whom correspondence should be addressed: Nikolay Tzvetkov Tzvetkov and Christa E. Müller, PharmaCenter Bonn, Pharmaceutical Institute, Pharmaceutical Chemistry I, An der Immenburg 4, D-53121 Bonn, Germany. Phone: +49-179-5284358 (N.T.T.); +49-228-73-2301 (C.E.M.). Fax: +49-228-73-2567. E-mail: ntzvetkov@uni-bonn.de (N.T.T.); christa.mueller@uni-bonn.de (C.E.M.).

ABSTRACT

1
2
3 Indazole- and indole-carboxamides were discovered as highly potent, selective, competitive and
4 reversible inhibitors of monoamine oxidase B (MAO-B). The compounds are easily accessible by
5 standard synthetic procedures with high overall yields. The most potent derivatives were *N*-(3,4-
6 dichlorophenyl)-1-methyl-1*H*-indazole-5-carboxamide (**38a**, PSB-1491, IC₅₀ human MAO-B 0.386 nM,
7 >25000-fold selective versus MAO-A) and *N*-(3,4-dichlorophenyl)-1*H*-indole-5-carboxamide (**53**, PSB-
8 1410, IC₅₀ human MAO-B 0.227 nM, >5700-fold selective versus MAO-A). Replacement of the
9 carboxamide linker with a methanimine spacer leading to (*E*)-*N*-(3,4-dichlorophenyl)-1-(1*H*-indazol-5-
10 yl)methanimine (**58**) represents a further novel class of highly potent and selective MAO-B inhibitors
11 (IC₅₀ human MAO-B 0.612 nM, >16000-fold selective versus MAO-A). In *N*-(3,4-difluorophenyl)-1*H*-
12 indazole-5-carboxamide (**30**, PSB-1434, IC₅₀ human MAO-B 1.59 nM, selectivity versus MAO-A
13 >6000-fold) high potency and selectivity are optimally combined with superior physicochemical
14 properties. Computational docking studies provided insights into the inhibitors' interaction with the
15 enzyme binding site and a rationale for their high potency despite their small molecular size.
16
17
18
19
20
21
22
23
24
25
26
27
28
29
30
31
32
33
34
35
36
37
38
39
40
41
42
43
44
45
46
47
48
49
50
51
52
53
54
55
56
57
58
59
60

1 KEYWORDS: Alzheimer's disease, carboxamides, docking studies, indazoles, indoles, reversible
2 inhibitors, molecular modeling, monoamine oxidase A and B, neuroprotection, neurodegenerative
3 diseases, Parkinson's disease, physicochemical properties, species differences, structure-activity
4 relationships, synthesis
5
6
7
8
9
10
11
12
13
14
15
16
17
18
19
20
21
22
23
24
25
26
27
28
29
30
31
32
33
34
35
36
37
38
39
40
41
42
43
44
45
46
47
48
49
50
51
52
53
54
55
56
57
58
59
60

INTRODUCTION

1
2
3 Monoamine oxidases (MAO, EC 1.4.3.4) are flavin adenine dinucleotide (FAD) containing enzymes
4
5 localized on the mitochondrial outer membrane, which catalyze the oxidative deamination of biogenic
6
7 amines and monoamine neurotransmitters. Two isoforms of MAO are present in most mammalian
8
9 tissues, MAO-A and MAO-B, distinguished by their substrate and inhibitor selectivity.^{1,2} Epinephrine
10
11 (adrenaline), norepinephrine (noradrenaline), dopamine (DA), tyramine and tryptamine are substrates
12
13 for both isoforms. MAO-A displays higher affinity for the substrates norepinephrine and serotonin
14
15 (5-HT) than MAO-B and is inhibited by low concentrations of clorgyline, whereas MAO-B exhibits
16
17 higher affinity towards phenylethylamine (PEA) and benzylamine, and is potently inhibited by of
18
19 selegiline.^{1,2} The reaction catalyzed by MAO results in the production of hydrogen peroxide (H₂O₂) and
20
21 other reactive oxygen species (ROS), which may contribute to oxidative stress and cell damage.³ The
22
23 protein sequences of MAO-A and MAO-B are ~70% identical.⁴ Both MAO isoforms show regional
24
25 differences in enzyme activity and distribution in the human brain.¹ Highest MAO activity is observed
26
27 in the basal ganglia (striatum) and hypothalamus, whereas the cerebellum and neocortex show low
28
29 levels of MAO activity.⁵ Serotonergic neurons and astrocytes contain predominantly MAO-B, while the
30
31 MAO-A isoform is mainly located in catecholaminergic neurons.⁵ The activity and the expression levels
32
33 of MAO-B in the human brain, but not those of MAO-A, increase with aging and may be associated
34
35 with the loss of dopaminergic neurons in the substantia nigra, where MAO-B is the main form in glial
36
37 cells.⁶ Increased MAO-B activity in the substantia nigra is thus observed in patients with Parkinson's
38
39 diseases (PD).^{2,7} The relationship between oxidative stress and progressive neuronal impairment
40
41 indicates that inhibition of MAO-B activity may have neuroprotective effects.^{6,7}
42
43
44
45
46
47
48
49
50
51

52 Selective irreversible and reversible MAO-A inhibitors are used in the treatment of depression and
53
54 anxiety disorders.⁸ Selective MAO-B inhibitors are currently applied for the therapy of PD, mostly in
55
56 combination with the dopamine prodrug levodopa, to reduce the metabolic degradation of dopamine and
57
58 increase its half-life.^{9,10} Due to their potential neuroprotective effects, MAO-B inhibitors may be useful
59
60

for the treatment of other neurodegenerative diseases as well including Alzheimer's disease (AD).⁹ Recently, MAO-B inhibitors with ancillary activities have been proposed as multi-target drugs for the treatment of PD and AD.^{9,11} Examples for this new strategy include dual-acting acetylcholinesterase (AChE) and MAO inhibitors for AD,^{11,12} dual-acting A_{2A} adenosine receptor (A_{2A} AR) antagonists and MAO-B inhibitors for PD,^{13,14} and triple-target drugs acting as A₁ and A_{2A} AR antagonist in addition to inhibition of MAO-B for the treatment of PD and AD.

Several selective MAO-B inhibitors, including the irreversible inhibitors selegiline (**1**)¹⁵ and rasagiline (**2**)¹⁶ as well as the reversible inhibitor safinamide (**3**)¹⁷, are currently in clinical use for the treatment of PD (for structures, see Figure 1). Selegiline (**1**) is a potent and selective "suicide type" irreversible MAO-B inhibitor (human MAO-B, IC₅₀ = 6.79 nM; human MAO-A, IC₅₀ = 1700 nM)^{17,18} used in combination with levodopa therapy.¹⁹ One major drawback of **1** are side-effects evoked by its amphetamine metabolites.²⁰

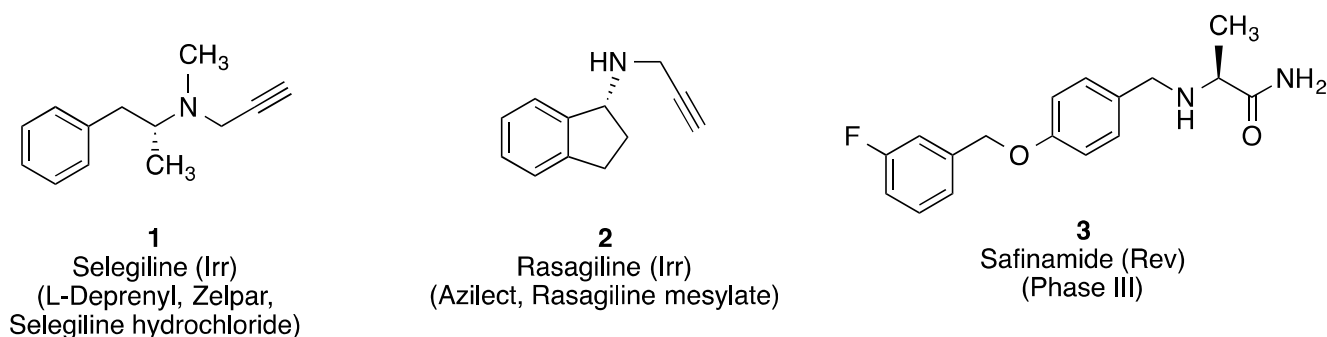


Figure 1. Structures of irreversible (Irr) and reversible (Rev) MAO-B inhibitors in clinical use.

The irreversible MAO-B inhibitor rasagiline (**2**, human brain MAO-B, IC₅₀ = 14.0 nM; human brain MAO-A, IC₅₀ = 710 nM) is not metabolized to amphetamine derivatives and is used for both, monotherapy in early PD and as adjunctive therapy in late-stage patients with PD experiencing motor fluctuations.^{16,21} However, irreversible MAO-B inhibitors may show safety issues and pharmacological side effects.²²

Therefore, selective and reversible inhibition of MAO is believed to be advantageous. For example, the reversible MAO-A inhibitor moclobemide is successfully used to treat depression and anxiety.²³ Reversible MAO-B inhibitors are currently being developed.²⁴ Safinamide (**3**) is such a compound, which is being evaluated in advanced clinical trials as an add-on therapy to dopamine agonists or to levodopa in PD patients with motor fluctuations.²⁵ Besides MAO-B inhibition (human brain MAO-B, $IC_{50} = 9.0$ nM; human brain MAO-A, $IC_{50} = 45$ μ M) it shows additional mechanisms of action including inhibition of DA reuptake, inhibition of excessive glutamate release²⁶, and sodium channel inhibition.²⁷

A wide range of MAO-B inhibitors with common structural features has been developed to date (for examples, see Figure 2).^{28,29,30,31,32} These include small mono- or disubstituted heterobicyclic compounds such as the 2,5-disubstituted indole **4**, 5-nitroindazole (**5**), 7-[(3-chlorobenzoyloxy)]-4-[(methylamino)methyl]coumarin (**6**), isatine (**7**) and its C5-substituted analogues (*E*)-5-styrylisatin (**8**) and 5-(4-phenylbutyl)isatin (**9**). The 2-propargylamine-substituted compound **4** is an irreversible MAO-B inhibitor that is similarly potent as selegiline (**1**).²⁹ MAO-B inhibitor **4** was found to exhibit neuroprotective effects in several in vivo models of PD.³³

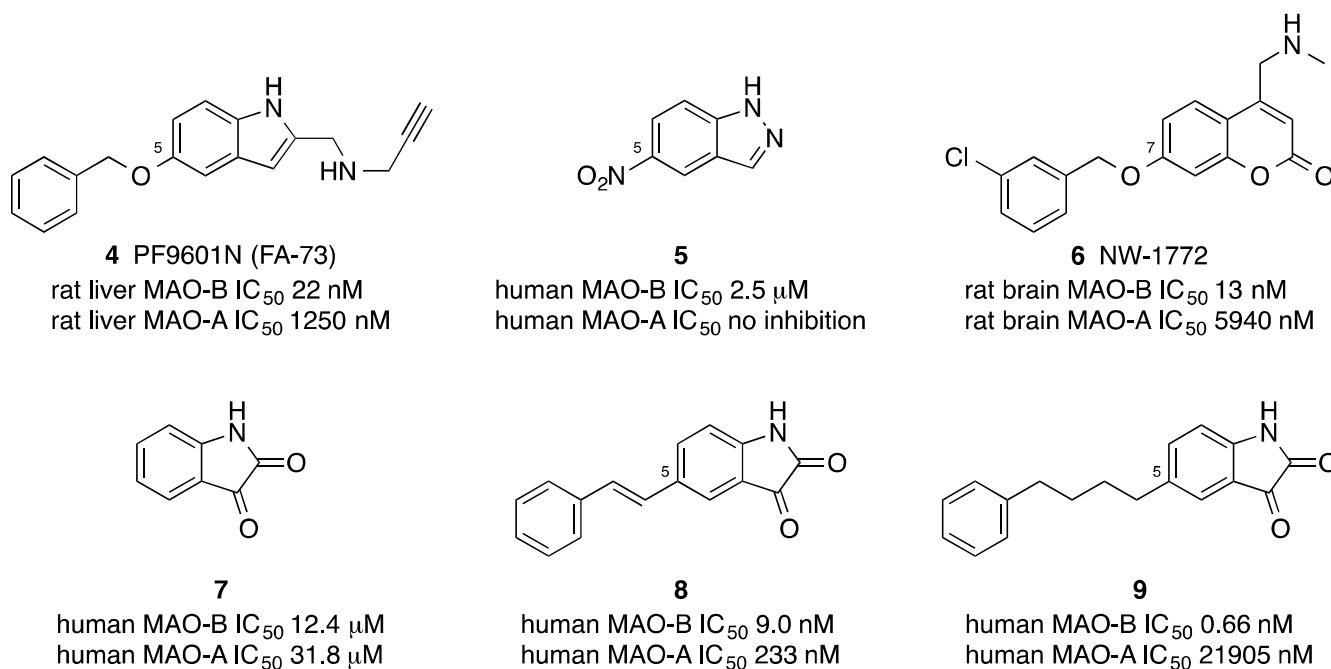


Figure 2. Structures and potencies of previously described MAO-B inhibitors.^{11,29-32}

Compound **5** was described as the most potent MAO-B inhibitor within the class of nitroindazoles.^{11,30}

Recently, aminocoumarin derivative **6** has been identified as a promising clinical candidate with high MAO-B inhibitory activity and suitable pharmacokinetic properties.³¹ Another small molecule, isatin (**7**), is a weak inhibitor of human MAO-B ($IC_{50} = 31.8 \mu M$), but its C5-substituted analogues **8** and **9** are more potent, reversible MAO-B inhibitors.³²

Due to the promising pharmacological properties combined with only minor side effects of selective, reversible MAO-B inhibitors,⁹ we aimed at developing such inhibitors with improved properties. In the present study, novel classes of most potent irreversible MAO-B inhibitors were discovered, namely indazole-5-carboxamides (designated class I), indole-5-carboxamides (class II) and (indazol-5-yl)methanimine derivatives (class III). The new compounds were evaluated at rat and human MAO A and B, and optimized in order to improve their MAO-B affinity and selectivity, as well as their physicochemical and drug-like properties. Computational studies were performed to understand their binding modes and to explain their exceedingly high affinities.

RESULTS AND DISCUSSION

Compound Design. Our design of novel classes of MAO-B inhibitors was based on the general formula **I** containing a heterobicyclic ring system linked to a phenyl moiety as displayed in Figure 3 (L = linker, R = H or halogen, and Het = heterocycle). The pharmacophore in **I** labeled in red incorporates the key structural features found in all previously described MAO-B inhibitors **4–9** (cf. Figure 2). For simplification, we divided **I** into two scaffold fragments representing the common structural motifs (building blocks) used for the construction of these MAO-B inhibitors.

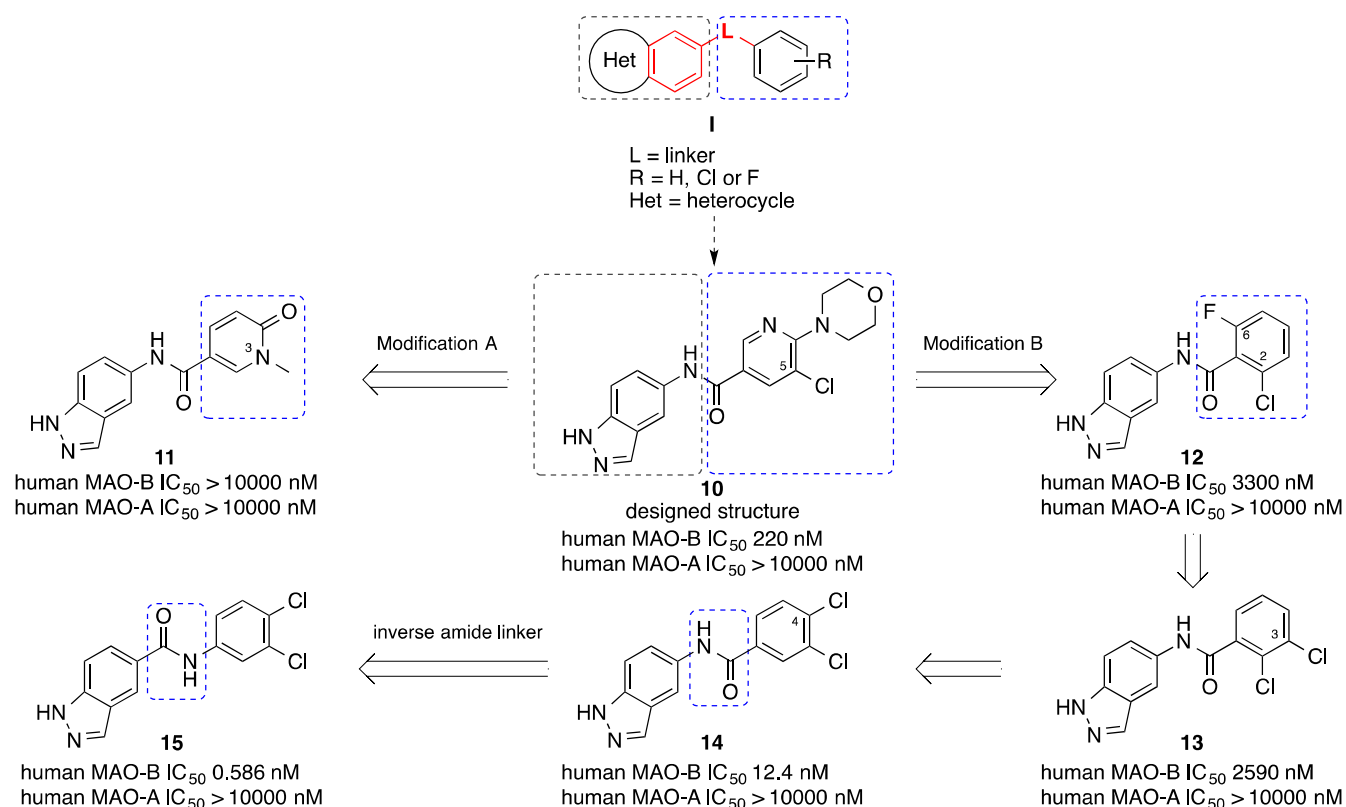


Figure 3. Rational design strategy to obtain MAO-B inhibitor **10**, and further structural optimization to obtain class I MAO-B inhibitor **15**.

1 We prepared and evaluated only 6 compounds (**10-15**) in our rational design strategy to obtain a
2 compound with the desired high, subnanomolar potency and MAO-B selectivity. In order to design the
3 initial compound **10**, we studied the core structural characteristics of the known MAO-B inhibitors
4 considering their potential for further scaffold variation, novelty and accessibility (see Figure 2).
5 Structure-activity relationship (SAR) examination for MAO-B potency and selectivity showed that
6 electron-rich spacers such as a double bond, an ether, or a methylamine group were well tolerated by
7 MAO-B, while C3- to C4-alkyl linkers led to less potent and less selective compounds. Since linkers
8 like C1- to C4-alk(en)yl (**8** and **9**) or ethers (**3**, **4** and **6**) are already well-established in a number of
9 structures with MAO-B activity, we decided to replace these by an amide group in **10**. Furthermore, C5-
10 substitution in several heterobicyclic motifs has been observed to be beneficial for potent, reversible
11 MAO-B inhibitors.³² Except for the coumarine derivative **6**, which is substituted at position 7, the
12 MAO-B inhibitors **4**, **5**, **8**, and **9** are C5-substituted (see Figure 2). Based on previous studies targeted
13 towards dual A_{2A} adenosine receptor antagonists / MAO-B inhibitors,³⁴ we conjugated a 5-chloro-
14 substituted morpholinopyridine motif (blue box) at the C5 position of an indazole moiety (gray box) to
15 obtain compound **10**. The 5-chloro-6-morpholinopyridine was selected as a bioisosteric replacement of
16 halogen-substituted phenyl residues due to its polarity and favorable physicochemical properties.
17
18
19
20
21
22
23
24
25
26
27
28
29
30
31
32
33
34
35
36
37
38
39

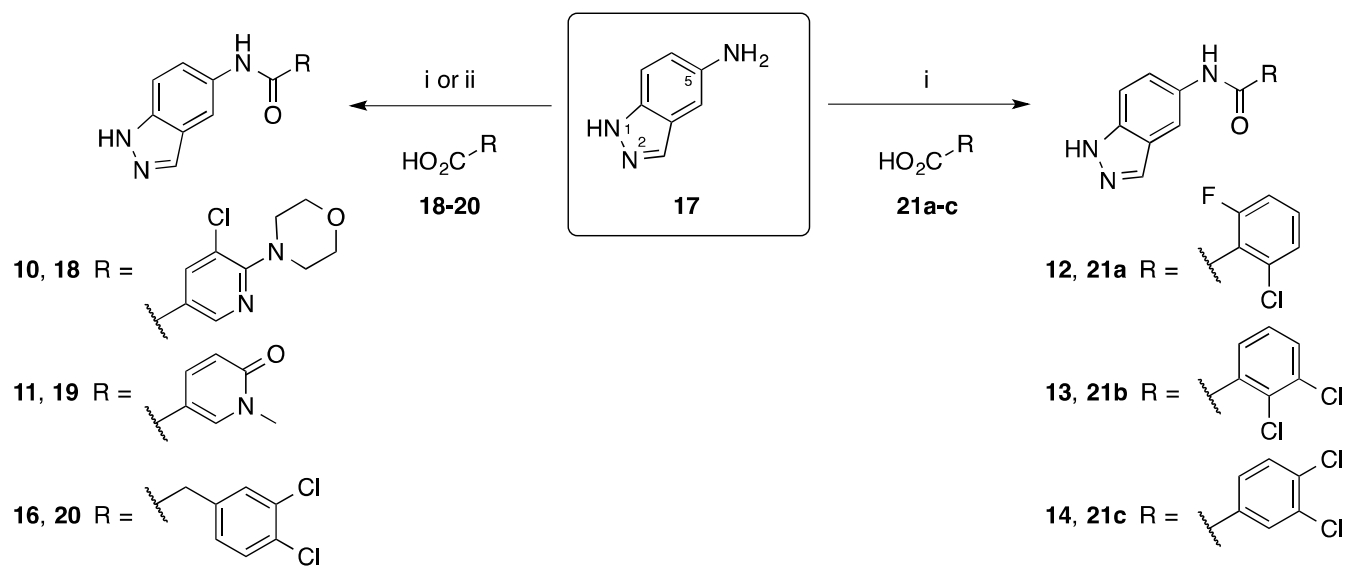
40 Similar to the benzyloxy group in the potent MAO-B inhibitors safinamide (**3**) and compound **4**, the
41 bulky moiety in **10** may extend through the substrate cavity into the entrance cavity of the bipartite
42 active site of human MAO-B.³⁵ In fact, the first compound **10** designed through a rational design
43 strategy provided a moderate inhibitory activity at human MAO-B in the high nanomolar range (IC₅₀
44 220 nM) being 45-fold selective for MAO-B over MAO-A. These results encouraged further
45 exploration within the series of indazole-containing compounds related to **10**. In the next step, we
46 performed a systematic modification of **10** by introducing a hydrophilic 1-methyl-pyridone moiety
47 (modification A) or a more lipophilic 2-chloro-6-fluorophenyl ring (modification B), respectively, to
48 obtain compounds **11** and **12** (Figure 3). While **11** showed no activity at all, compound **12** exhibited
49
50
51
52
53
54
55
56
57
58
59
60

1 lower potency than the parent **10** with a micromolar IC_{50} value of 3.30 μ M at human MAO-B.
2
3 Compound **12** was subsequently modified with 2,3- and 3,4-dichloro substituents at the phenyl ring to
4
5 obtain **13** and **14**, respectively. The chlorine substituent at the aryl C3 position was kept constant. Both
6
7 compounds showed progressive improvement of MAO-B inhibition from micromolar (**13**, human
8
9 MAO-B, IC_{50} 2.59 μ M) to low nanomolar potency (**14**, human MAO-B, IC_{50} 12.4 nM). The choice of
10
11 the 3,4-dichlorophenyl-substitution pattern appeared to be essential for obtaining very high MAO-B
12
13 inhibitory activity. Finally, we obtained a further dramatic increase in MAO-B inhibitory potency by
14
15 inverting the amide linker leading to compound **15**. Thus, we developed indazole-5-carboxamides as a
16
17 new structural class of extraordinarily potent MAO-B inhibitors (designated class I). *N*-(3,4-
18
19 dichlorophenyl)-1*H*-indazole-5-carboxamide (**15**) was evaluated at rat and human MAO-A and B: it was
20
21 identified as a highly potent inhibitor (20-fold more active than **14**) with remarkable selectivity for the
22
23 MAO-B-isoform (human MAO-B, IC_{50} 0.586 nM; human, MAO-A, IC_{50} >10000 nM) surpassing the
24
25 activity of all recently developed MAO-B-selective inhibitors. The indazol-5-carboxamide scaffold
26
27 subsequently served as a starting point for the design, synthesis and biological evaluation of a number of
28
29 compounds, many of them with MAO-B inhibitory activity in the subnanomolar range and significantly
30
31 improved physicochemical properties. We also prepared two additional classes of MAO-B inhibitors
32
33 differing from **15** either by replacement of the 5-substituted indazole by a 5-substituted indole
34
35 (designated class II), or by exchange of the amide connection by a methanimine linker (class III).
36
37
38
39
40
41
42
43
44

45 **Chemistry.** All new compounds of the present study were prepared by amide coupling reactions,³⁶
46
47 *N*-alkylation³⁷ and iminoalkylation reactions³⁸ using a variety of reagents and conditions as illustrated in
48
49 Schemes 1-5. Amide coupling was performed by reaction of the differently substituted carboxylic acids
50
51 **18-20**, **21a-c**, **22**, **39**, and **50-52** with substituted amines **17**, **23a-k**, **25**, or aminopyridine **24**,
52
53 respectively. With the exception of carboxylic acids **18** and **19**, all building blocks used for the
54
55 syntheses of the final products were commercially available. Amide coupling was conducted in the
56
57 presence of Hünig's base (*N,N*-diisopropylethylamine, DIPEA), using the condensation reagent *O*-
58
59
60

(benzotriazol-1-yl)-*N,N,N',N'*-tetramethyluronium tetrafluoroborate (TBTU) in acetonitrile or, alternatively, by applying 1-ethyl-3-(3-dimethylaminopropyl)carbodiimide hydrochloride (EDC-HCl) as a coupling reagent in methanol.³⁴ In general, amide coupling reactions were performed at room temperature for several hours. The conversion of the starting materials was monitored by thin-layer chromatography (TLC) or by high performance liquid chromatography (HPLC) coupled to an ultraviolet (UV) detector and to electrospray ionisation mass spectrometry (ESI-MS) analysis. Products **10-14** and **16** were obtained as shown in Scheme 1. Compound **14** had previously been described,^{36,39} but in the present study we used different reaction conditions to obtain **14** in higher yields. The carboxylic acids **18** and **19** were prepared by two- or three-step reaction procedures according to published procedures (for details see Supporting Information). A methylene group in **16** was introduced in order to study an extension of the spacer between the 3,4-dichloro-phenyl ring and the indazole moiety.

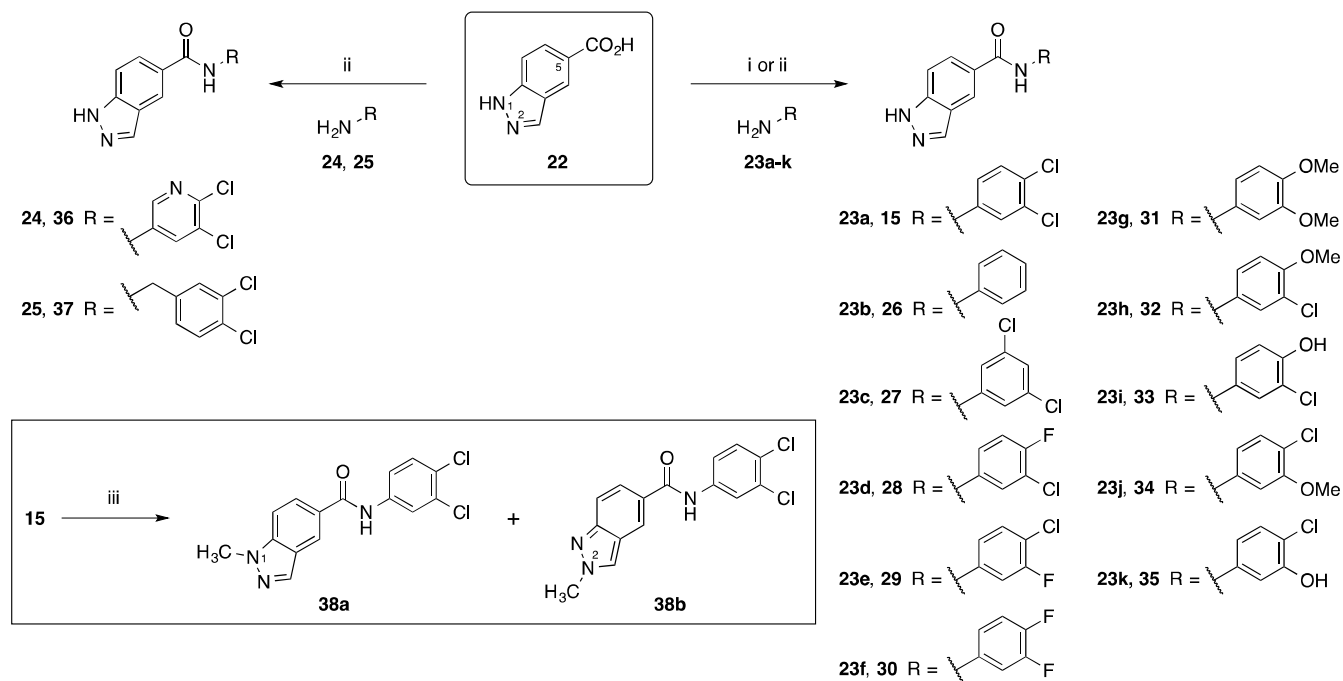
Scheme 1. Synthesis of indazol-5-yl-amides **10-14** and **16**^a



^aReagents and conditions: (i) for **10-14**:³⁹ carboxylic acid **18**, **19** or **21a-c** (1.0 equiv.), 5-amino-1*H*-indazole (**17**, 1.0 equiv.), TBTU/DIPEA (1.2 equiv.), acetonitrile, RT, 3-72 h, yield 23–73%; (ii) for **16**: 2-(3,4-dichlorophenyl)acetic acid (**20**, 1.0 equiv.), 5-amino-1*H*-indazole (**17**, 1.0 equiv.), EDC-HCl (1.1 equiv.), methanol, RT, 3-4 h, yield 56% (**16**).

The preparation of indazole-5-carboxamides **15**, **26-37** and **38a-b** is depicted in Scheme 2. The compounds were prepared by amide coupling reaction of commercially available 1*H*-indazole-5-carboxylic acid (**22**) with differently substituted anilines and related amines (**23a-k**, **24**, **25**). In order to investigate the impact of the substitution pattern of the phenyl ring on biological activity, we introduced a broad variety of substituents mainly in the 3- and 4-position including halogen atoms, methoxy and hydroxyl functions. To introduce structural diversity in position N1 or N2 of the indazole moiety, **15** was alkylated with methyl iodide yielding a 3:1 mixture of N1-/N2-methylated products **38a** and **38b** (Scheme 2). The reaction occurred in the presence of potassium carbonate in *N,N*-dimethylformamide (DMF) at room temperature and the reaction time was optimized by monitoring of the conversion.³⁷ The mixture of **38a** and **38b** was separated by column chromatography. The structure determination of **38a** and **38b** was carried out by heteronuclear multiple bond correlation (HMBC) NMR in combination with ¹H and ¹³C NMR spectroscopy.

Scheme 2. Synthesis of indazole-5-carboxamides **15**, **26-37** and **38a-b**^a



^aReagents and conditions: (i) for **15**, **32** and **34**: 1*H*-indazole-5-carboxylic acid (**22**, 1.0 equiv.), differently substituted anilines **23a,h,j** (1.0 equiv.), TBTU/DIPEA (1.2 equiv.), acetonitrile, RT, 3-72 h, yield 11–30%; (ii) for **15**, **26-31**, **33**, and **35-37**: 1*H*-indazole-5-carboxylic acid (**22**, 1.0 equiv.),

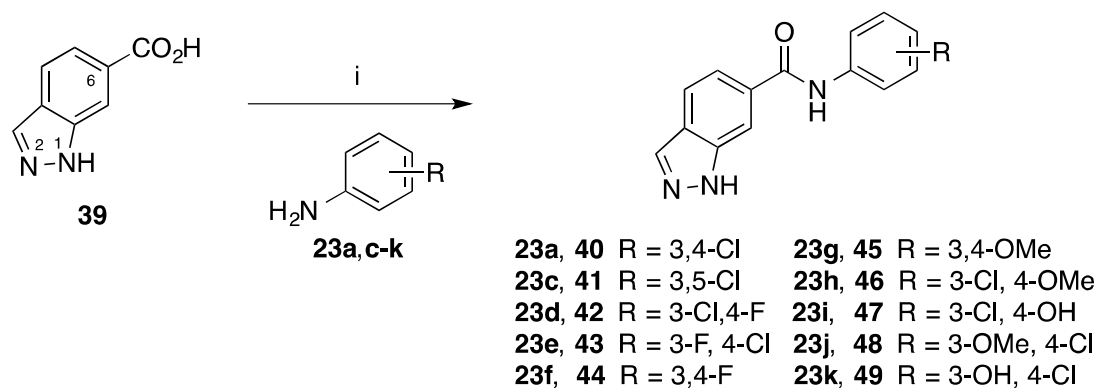
differently substituted anilines **23a-g,i,k**, **24** and **25** (1.0 equiv.), EDC-HCl (1.1 equiv.), methanol, RT, 3-4 h, yield 18-67%; (iii) *N*-(3,4-dichlorophenyl)-1*H*-indazole-5-carboxamide (**15**, 1.0 equiv.), MeI (1.3–2.0 equiv), K₂CO₃ (1.3 equiv), DMF, RT, 16–20 h, yield 47% (**38a**) and 9% (**38b**).

In order to increase the compounds' polarity and water-solubility, we introduced a bioisosteric replacement for the 3,4-dichloro-phenyl residue, namely a 3,4-dichloropyridine moiety (compound **36**).

An extension of the spacer between the indazole core and the substituted phenyl ring was introduced in **37** by coupling of **22** with the corresponding 3,4-dichlorobenzylamine (**25**).

Indazole-6-carboxamides **40-49**, which represent 6-substituted analogues or isomers of the indazole-5-carboxamides (**15**, **27-35**) described above were obtained by coupling of 1*H*-indazole-6-carboxylic acid (**39**) with anilines **23a,c-k** as shown in Scheme 3. This set of compounds was prepared in order to investigate the role of the indazole nitrogen atoms for MAO-B inhibition, in particular, the supposed role (and position) of the NH as a hydrogen bond donor in protein binding.

Scheme 3. Synthesis of indazole-6-carboxamides **40-49**^a

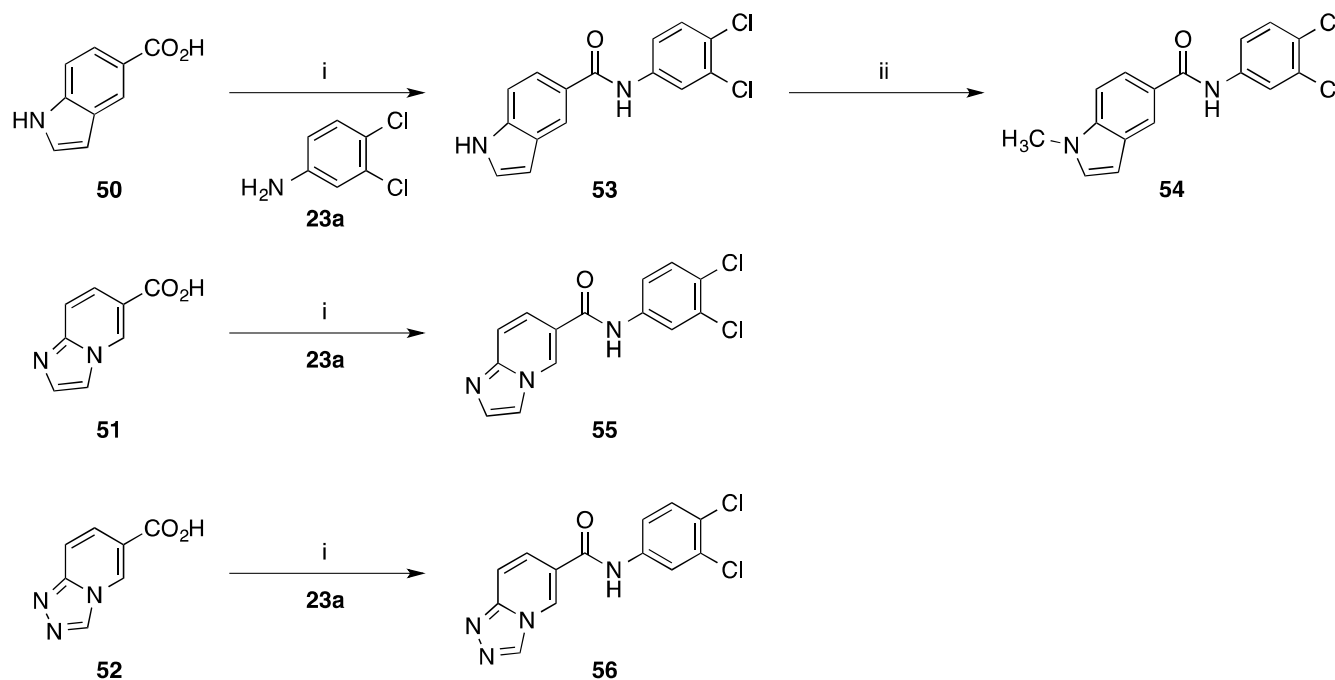


^aReagents and conditions: (i) 1*H*-indazole-6-carboxylic acid (**39**, 1.0 equiv.), differently substituted anilines **23a,c-k** (1.0 equiv.), EDC-HCl (1.1 equiv.), methanol, RT, 3-4 h, yield 22–71%.

Replacement of the indazole ring of **15** by an indole, an imidazo[1,2-*a*]pyridine, or a [1,2,4]triazolo-[4,3-*a*]pyridine moiety led to compounds **53**, **55** and **56** (Scheme 4). These were synthesized in order to create diversity of the heterobicyclic core via variation of the electronic properties of the ring system while keeping the 3,4-dichlorophenyl substituent of lead structure **15** constant. Furthermore, alkylation

of **53** was performed by *N*-alkylation with methyl iodide under mild reaction conditions yielding **54** (Scheme 4).

Scheme 4. Synthesis of indole-5-carboxamides **53** and **54** and *N*-(3,4-dichlorophenyl)carboxamide derivatives **55** and **56**^a

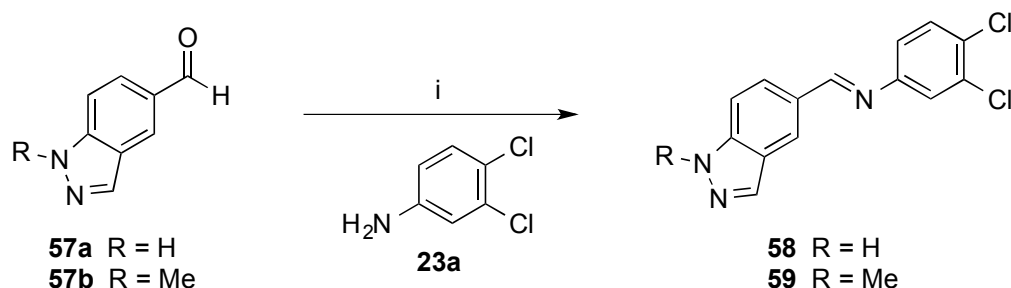


^aReagents and conditions: (i) carboxylic acids **50-52** (1.0 equiv.), 3,4-dichloroaniline (**23a**, 1.0 equiv.), EDC-HCl (1.1 equiv.), methanol, RT, 3-4 h, yield 17–36%; (ii) *N*-(3,4-dichlorophenyl)-1*H*-indole-5-carboxamide (**53**, 1.0 equiv.), MeI (1.3–2.0 equiv), K₂CO₃ (1.3 equiv), DMF, RT, 16–20 h, yield 68%.

Finally, the amide group was replaced by an imine linker. For the preparation of **58** and **59**, aldehydes **57a,b** were reacted with 3,4-dichloroaniline **23a** in the presence of a catalytic amount of acetic acid in ethanol under reflux (Scheme 5).⁴⁰ The chemical stability of product **59** was investigated by LC/ESI-MS and compared to that of amide **54**. For this purpose we analyzed stock solutions of the compounds in DMSO (10 mM), which had been prepared for biological testing and kept for 70 days at room temperature (for details see Supporting Information, Figures S3, S4 and Table S2). We observed that the imine **59** was relatively stable and showed only moderate degradation under these conditions (15% hydrolysis), while the amide **54** was found to be completely stable. Imines **58** and **59** will offer further opportunities for modification to obtain more stable compounds: e.g. in analogy to the preparation of

1 safinamide (**3**), the imine double bond may be reduced to an aminoalkyl group.⁴⁰ Molecular mechanics
2 calculations showed that the formation of the *E*-isomer was favoured over the *Z*-diastereomer (for
3 details, see Supporting Information, Figure S5). NMR analyses (¹H and ¹³C) confirmed the sole
4 formation of the *E*-isomer. However, the possibility of an *E/Z*-isomerization of **58**, e.g. after exposing it
5 to daylight in dilute solution, cannot be excluded.⁴¹

14 **Scheme 5.** Synthesis of 3,4-dichlorophenyl-substituted (1*H*-indazol-5-yl)methanimines **58** and **59**^a



27 ^aReagents and conditions: (i) 1*H*-indazole- or 1-methyl-1*H*-indazole-5-carboxaldehyde (**57a,b**, 1.0
28 equiv.), 3,4-dichloroaniline (**23a**, 1.0 equiv.), acetic acid (0.2 equiv.), ethanol, reflux, 1-24 h, yields:
29 89% (**58**) and 90% (**59**).
30
31
32
33

34 Our synthetic strategy to obtain novel classes of MAO-B inhibitors provides several advantages. These
35 include easy accessibility of the final products by only one or two steps using commercially available
36 starting materials. The procedures allow the possibility for broad structural variation in the last step, and
37 the preparation of compound libraries for fast analysis of SARs. Moreover, the procedures will enable
38 simple scale-up from milligram amounts to large, multigram or even kilogram quantities.
39
40
41
42
43
44
45
46
47

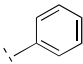
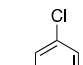
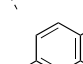
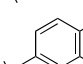
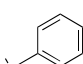
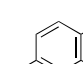
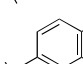
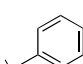
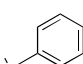
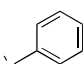
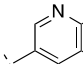
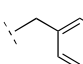
48 The new compounds were isolated by column chromatography and subsequently re-crystallized to
49 obtain pure products. All final products were fully characterized by NMR spectroscopy (¹H and ¹³C) and
50 mass spectrometry (LC/ESI-MS) and their structures were confirmed. The purity of all compounds was
51 determined by HPLC-UV to be at least 95% (see Experimental Section and Supporting Information).
52
53
54
55
56
57
58
59
60

1
2
3
4
5
6
7
8
9
10
11
12
13
14
15
16
17
18
19
20
21
22
23
24
25
26
27
28
29
30
31
32
33
34
35
36
37
38
39
40
41
42
43
44
45
46
47
48
49
50
51
52
53
54
55
56
57
58
59
60

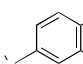
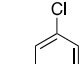
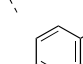
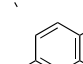
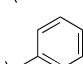
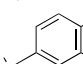
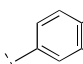
Monoamine Oxidase Inhibition Studies. The compounds were investigated for inhibition of human and rat MAO-A and MAO-B using recombinant enzymes (human) expressed in baculovirus-infected insect cells,⁴² and mitochondria-enriched rat liver fractions as sources for the rat MAO isoforms, respectively. Enzyme inhibition assays of reference and test compounds at human MAO-A and MAO-B were performed by a fluorescence-based assay with the substrate *p*-tyramine measuring the production of hydrogen peroxide formed as a by-product of the enzymatic deamination reaction (also see Experimental Section and Supporting Information).⁴³ The inhibitors clorgyline for MAO-A and selegiline for MAO-B were used to block the respective isoenzyme in rat liver fractions for determining selective inhibition of the other isoenzyme. The selective inhibitors were also used as positive controls in human recombinant MAO-A and MAO-B assays, respectively. Determined inhibitory potencies (IC₅₀ values) for reference inhibitors and all new synthesized compounds are collected in Table 1.

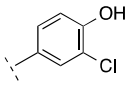
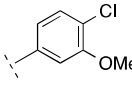
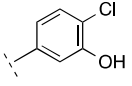
Table 1. Inhibitory Potencies of Compounds at Monoamine Oxidases

IC₅₀ ± SEM (nM)^a			
Compd.	MAO-A (h= human, r= rat)	MAO-B (h= human, r= rat)	Selectivity index (SI)^b
Standard inhibitors			
Selegiline (1)	1700 (human brain) ¹⁸ 944 (rat brain) ¹⁸	6.59 ± 1.09 (h) 9.97 ± 1.33 (r) 6.79 (human brain) ¹⁸ 3.63 (rat brain) ¹⁸	>250
Rasagiline (2)	710 (human brain) ¹⁸ 412 (rat brain) ¹⁸	14.0 (human brain) ¹⁸ 4.43 (rat brain) ¹⁸	>50
Safinamide (3)	45000 (human brain) ⁴⁴ 580000 (rat brain) ²⁷	5.18 ± 0.04 (h) 18.0 ± 4.9 (r) 9.0 (human brain) ⁴⁴ 98 (rat brain) ²⁷	5000
5-Carboxamidoindazole derivatives 10-16			
10	 >10000 (h) >10000 (r)	220 ± 23 (h) 1990 ± 110 (r)	>9
11	 >10000 (h) >10000 (r)	>10000 (h) >10000 (r)	–
12	 >10000 (h) >10000 (r)	3300 ± 400 ^c (h) >10000 (r)	–
13	 >10000 (h) >10000 (r)	2590 ± 410 (h) >10000 (r)	–
14	 >10000 (h) >10000 (r)	12.4 ± 0.2 (h) 138 ± 18 (r)	806
16	 >10000 (h) >10000 (r)	882 ± 61 (h) >10000 (r)	>11
Indazole-5-carboxamides 15, 26-38 (class I inhibitors)			
15	 ≥10000 (h) >10000 (r)	0.586 ± 0.087 (h) 1.43 ± 0.11 (r)	17065

1	26		>10000 (h) >10000 (r)	117 ± 13 (h) 708 ± 34 (r)	>86
2					
3	27		<10000 (h) >10000 (r)	2.75 ± 0.40 (h) 2.73 ± 0.21 (r)	3636
4					
5					
6	28		>10000 (h) >10000 (r)	0.679 ± 0.044 (h) 2.36 ± 0.17 (r)	14727
7					
8					
9	29		<10000 (h) >10000 (r)	0.668 ± 0.053 (h) 2.61 ± 0.68 (r)	14970
10					
11	30		>10000 (h) >10000 (r)	1.59 ± 0.16 (h) 8.89 ± 0.05 (r)	6289
12	(PSB-1434)				
13					
14	31		>10000 (h) >10000 (r)	185 ± 21 (h) 1400 ± 56 (r)	>54
15					
16					
17	32		>10000 (h) >10000 (r)	3.42 ± 0.28 (h) 21.9 ± 3.4 (r)	2924
18					
19	33		>10000 (h) <10000 (r)	123 ± 16 (h) 941 ± 51 (r)	>81
20					
21					
22	34		8790 ± 200 (h) >10000 (r)	4.36 ± 0.08 (h) 43.1 ± 4.2 (r)	2016
23					
24					
25	35		3000 ± 122 (h) >10000 (r)	37.5 ± 7.3 (h) 385 ± 9 (r)	80
26					
27	36		<10000 (h) <10000 (r)	5.42 ± 0.20 (h) 26.6 ± 1.5 (r)	1845
28					
29					
30	37		>10000 (h) >10000 (r)	388 ± 52 (h) 837 ± 28 (r)	>25
31					
32					
33	38a	see structure above	>10000 (h) >10000 (r)	0.386 ± 0.052 (h) 1.32 ± 0.09 (r)	25906
34	(PSB-1491)				
35					
36	38b	see structure above	420 ± 24 (h) 1740 ± 60 (r)	1.44 ± 0.41 (h) 22.5 ± 0.6 (r)	292
37					
38					

Indazole-6-carboxamides 40-49

	R			
40		3310 ± 288 (h) <10000 (r)	67.1 ± 9.1 (h) 466 ± 39 (r)	>49
41		>10000 (h) >10000 (r)	335 ± 11 (h) 423 ± 13 (r)	>29
42		>10000 (h) >10000 (r)	234 ± 38 (h) 1070 ± 44 (r)	>42
43		>10000 (h) >10000 (r)	316 ± 29 (h) 2670 ± 152 (r)	>31
44		>10000 (h) >10000 (r)	1300 ± 176 (h) <10000 (r)	>7
45		>10000 (h) >10000 (r)	>10000 (h) >10000 (r)	–
46		>10000 (h) >10000 (r)	1280 ± 141 (h) <10000 (r)	8

1	47		>10000 (h) <10000 (r)	<10000 (h) 3280 ± 174 (r)	–
2					
3	48		>10000 (h) >10000 (r)	2760 ± 973 (h) >10000 (r)	4
4					
5	49		>10000 (h) >10000 (r)	6220 ± 825 (h) >10000 (r)	2
6					
7					
8					
9	Indole-5-carboxamides 53 and 54 (class II inhibitors)				
10		R			
11	53	H	1300 ± 68 (h) 6790 ± 121 (r)	0.227 ± 0.039 ^c (h) 1.01 ± 0.16 (r)	5727
12	(PSB-1410)				
13	54	Me	>10000 (h) >10000 (r)	2.26 ± 0.16 (h) 1.11 ± 0.11 (r)	4425
14					
15					
16					
17					
18	Imidazopyridine 55 and triazolopyridine 56				
19		R			
20	55	see structure above	>10000 (h) >10000 (r)	141 ± 12 (h) 1140 ± 108 (r)	71
21					
22	56	see structure above	>10000 (h) >10000 (r)	2270 ± 246 (h) >10000 (r)	>4
23					
24					
25					
26	(Indazol-5-yl)methanimines 58 and 59 (class III inhibitors)				
27		R			
28	58	H	<10000 (h) >10000 (r)	0.612 ± 0.065 (h) 3.69 ± 0.17 (r)	16340
29					
30	59	Me	<10000 (h) >10000 (r)	1.03 ± 0.09 (h) 4.55 ± 0.31 (r)	9709
31					
32					
33					

^a n = 3, unless otherwise noted. ^b SI = IC₅₀(human MAO-A)/IC₅₀(human MAO-B). ^c n = 4.

1 **Structure-Activity Relationships at Monoamine Oxidase B.** The biological evaluation of 37 novel
2 compounds at human and rat MAO-A and -B enzymes resulted in the identification of highly potent,
3 specific MAO-B inhibitors from three related chemical series: indazole-5-carboxamides (class I,
4 compounds **15**, **26-38a** and **38b**); indole-5-carboxamides (class II, **53** and **54**); and (indazol-5-
5 yl)methanimines (class III, **58** and **59**). Most of these compounds contain a disubstituted phenyl moiety
6 attached to the heterobicyclic core structure by an amide or an imine linker. Among the tested
7 compounds, 29 showed high inhibition of MAO-B ranging from submicromolar to subnanomolar
8 potency. The majority of potent compounds showed high selectivity for MAO-B without noticeable
9 inhibitory activity at MAO-A.
10
11
12
13
14
15
16
17
18
19
20
21
22
23

24 5-Chloro-*N*-(1*H*-indazol-6-yl)-6-morpholinonicotinamide (**10**) showed a moderate inhibitory activity at
25 human MAO-B (IC₅₀ 220 nM), and was significantly weaker at the rat enzyme (IC₅₀ 1990 nM, 9-fold).
26 Considering the hydrophobic character and the bipartite structure of the active site of the human MAO-
27 B enzyme and the binding mode of known inhibitors,^{35,44,45} the bulky and polar 6-morpholino-
28 substituted pyridine moiety of **10** might be too large, e.g. as compared to the reference inhibitors **1-3**.
29 Therefore, we focused on reducing the molecular mass and also introduced more lipophilic residues into
30 the target structures. In fact, the introduction of the smaller, but more polar *N*-methylpyridone residue
31 (compound **11**) abolished MAO inhibition completely. Better results were obtained by introducing a
32 phenyl ring substituted with electron-withdrawing groups (mainly F and Cl). Introduction of a 2-chloro-
33 6-fluoro- or a 2,3-dichloro-substituted phenyl ring resulted in compounds **12** and **13** which were weaker
34 than **10** indicating that *ortho*-phenyl substituents were not well tolerated. To evaluate the importance of
35 *meta,para*-substitution at the phenyl ring, we evaluated the dichloro-substituted isomer **14**. Compared to
36 the lead structure **10**, 3,4-dichlorophenyl derivative **14** showed a remarkable, 18-fold improvement in
37 MAO-B inhibition (human, IC₅₀ = 12.4 nM; rat, IC₅₀ = 138 nM). Thus, **14** was the first highly potent
38 and selective MAO-B inhibitor within the series of *N*-(indazo-5-yl)benzamide derivatives. The structure
39 of **14** indicated that a lipophilic 3,4-disubstituted phenyl ring and a carboxamide linker might be
40
41
42
43
44
45
46
47
48
49
50
51
52
53
54
55
56
57
58
59
60

1 favorable when connected to the indazole C5-position. In order to further study the role of the linker, we
2 introduced a methylene group between the aromatic ring and the amide carbonyl group producing
3 (indazol-5-yl)acetamide derivative **16**. The elongation of the linker led to a 71-fold decrease in potency
4 (human, IC₅₀ 882 nM) in **16** compared to the corresponding benzamide derivative **14**. At the rat
5 orthologue **16** was virtually inactive. Because of this result, we decided to keep the carboxamide linker
6 for connecting the two ring systems. However in the next series of compounds we inverted the
7 carboxamide function by connecting indazole-5-carboxylic acid with aniline derivatives (compounds **15**
8 and **26-38**). This modification of the linker provided a new class of extraordinarily potent and selective
9 MAO-B inhibitors some of which displayed subnanomolar potency. Indazole-5-carboxamide derivative
10 **15** exhibited 9-fold higher inhibitory activity at human MAO-B than the standard inhibitor safinamide
11 (**3**); it was 21-fold more potent than its isomer **14**. Compound **15** exhibited a slight preference for human
12 versus rat MAO-B (human MAO-B, IC₅₀ 0.586 nM; rat MAO-B, IC₅₀ 1.43 nM) and did not inhibit rat
13 and human MAO-A at a high concentration of 10000 nM. We therefore considered *N*-(3,4-
14 dichlorophenyl)-1*H*-indazole-5-carboxamide (**15**) as a new lead structure for further structural variations
15 to explore the SARs of this new class of MAO-B inhibitors. The corresponding derivative without
16 substituents at the phenyl ring (compound **26**) led to decreased inhibition (human MAO-B, IC₅₀ 117
17 nM; rat MAO-B, IC₅₀ 708 nM). 3,5-Dichlorophenyl-substitution (compound **27**) resulted in a potent
18 compound which was only 2-5-fold less potent than the 3,4-dichlorophenyl-substituted analogue **15**
19 (human MAO-B, IC₅₀ 2.75 nM; rat MAO-B, IC₅₀ 2.73 nM). It should be noted that **27** was the only
20 compound of the present series that showed no species differences. Thus, *meta*- and *para*-substituents at
21 the phenyl ring appeared to be crucial for high inhibitory activity at MAO-B. Following this
22 observation, we subsequently introduced different substituents in the 3- and 4-position of the phenyl
23 ring. 3-Chloro-4-fluoro- or 4-chloro-3-fluoro-substitution (compounds **28** and **29**) led to remarkably
24 potent inhibitors of human MAO-B (**28**, IC₅₀ 0.679 nM; **29**, IC₅₀ 0.668 nM), comparable to the potency
25 of the parent compound, the dichlorophenyl derivative **15**. The 3,4-difluoro-phenyl substituent provided
26 MAO-B inhibitor **30**, which was similarly potent (IC₅₀, human MAO-B 1.59 nM); it was approximately
27
28
29
30
31
32
33
34
35
36
37
38
39
40
41
42
43
44
45
46
47
48
49
50
51
52
53
54
55
56
57
58
59
60

1
2
3
4
5
6
7
8
9
10
11
12
13
14
15
16
17
18
19
20
21
22
23
24
25
26
27
28
29
30
31
32
33
34
35
36
37
38
39
40
41
42
43
44
45
46
47
48
49
50
51
52
53
54
55
56
57
58
59
60

6-fold less potent at the rat enzyme ($IC_{50} = 8.89$ nM). In contrast, the introduction of 3,4-dimethoxy-substitution at the phenyl ring (compound **31**, IC_{50} human MAO-B 185 nM) was not as well tolerated by MAO-B leading to a >300-fold decrease in potency compared to the dichlorophenyl derivative **15**. Consequently, we continued by replacing only one of the 3,4-chloro substituents in **15** with a methoxy or hydroxyl group (compounds **32-35**). While two methoxy substituents had been unfavourable with regard to MAO-B inhibition, the exchange of only one chloro substituent of **15** for a methoxy group (compounds **32** and **34**) was tolerated and resulted in an only slight reduction in inhibitory potency. Both, the 3-chloro-4-methoxyphenyl (**32**) and the 4-chloro-3-methoxyphenyl derivatives (**34**) were almost equipotent at human MAO-B (**32**, IC_{50} human MAO-B 3.42 nM; **34**, human MAO-B IC_{50} 4.36 nM). At rat MAO-B, both compounds were less potent (**32**, rat MAO-B, IC_{50} 21.9 nM; **34**, rat MAO-B, IC_{50} 43.1 nM). In contrast, a hydroxyl instead of a methoxy residue in the same position of the phenyl ring resulted in a significant decrease in affinity (**33**, human MAO-B, IC_{50} 123 nM; **35**, human MAO-B, IC_{50} 37.5 nM). In contrast to the methoxy-substituted analogues, we observed a preference for the 3-OH (**35**) versus the 4-OH substitution (**33**) with regard to MAO-B affinity. Our SARs thus revealed that electron-donating groups such as OMe and OH resulted in lower MAO-B inhibitory activity than electron-withdrawing substituents (e.g., Cl and F) at one or both, *para*- and *meta*-position of the phenyl ring in lead structure **15**. In order to enhance water-solubility of this relatively lipophilic series of MAO-B inhibitors, the benzene ring of **15** was bioisosterically replaced by a 5,6-dichloropyridine residue (compound **36**). The resulting indazole-5-carboxamide derivative **36** exhibited high MAO-B inhibition (human MAO-B, IC_{50} 5.42 nM; rat MAO-B, IC_{50} 26.6 nM) even though somewhat weaker than that of lead structure **15**. Introduction of a 3,4-dichloro-substituted benzyl moiety to probe a linker extension (compound **37**) led to a considerable decrease in MAO-B inhibitory potency (human MAO-B, IC_{50} 388 nM; rat MAO-B, IC_{50} 837 nM), in analogy to the effect observed for the indazol-5-yl-acetamide homolog **16**. Because of the high MAO-B inhibitory potency and selectivity of compound **15**, we used the 3,4-dichlorophenyl and the carboxamide linker as fixed motifs for further modification of the C5-substituted indazole unit. As a next step we introduced a methyl substituent on one of the indazole

1 nitrogen atoms resulting in isomers **38a** and **38b**. Methylation at the indazole N1 position (**38a**) slightly
2 increased potency at MAO-B, providing the best inhibitor of the present series (human MAO-B, IC₅₀
3 0.386 nM; rat MAO-B, IC₅₀ 1.43 nM). Compound **38b**, an N2-methylated regioisomer of **38a**, was less
4
5
6
7 potent than its N1-substituted analogue and than the unmethylated lead structure **15**, but it still showed
8
9 high MAO-B inhibitory potency (human MAO-B, IC₅₀ 1.44 nM). Its affinity for the human enzyme
10
11 was 15-fold higher than that for the rat enzyme (rat MAO-B, IC₅₀ 22.5 nM), being one of the
12
13 compounds that showed major species differences. Moreover, **38b** was also identified as the only
14
15 example in all series having notable inhibitory activity at MAO-A (human MAO-A, IC₅₀ 420 nM; rat
16
17 MAO-A, IC₅₀ 1740 nM). Thus, the N2-methyl substitution of the indazole moiety was found to be
18
19 beneficial for MAO-A inhibition, although **38b** was still >290-fold selective for human MAO-B over
20
21 human MAO-A. Our results indicate that the indazole NH is not required as a hydrogen bond donor, and
22
23 the binding pocket of MAO-B is able to accommodate substituents like methyl groups at indazole N1 or
24
25 N2. The high potency of compounds **15**, and **27-30** shows that 3,4-disubstituted phenyl-5-
26
27
28
29
30
31
32
33
34
35
36
37
38
39
40
41
42
43
44
45
46
47
48
49
50
51
52
53
54
55
56
57
58
59
60
amidindazoles represent a new class of highly potent and selective MAO-B inhibitors, which may be
suitable for further development as diagnostic or therapeutic drugs.

Further systematic SAR analysis led us to investigate a small set of C6-connected indazole-
carboxamides (**40-49**) with the same substitution pattern as the corresponding isomeric indazole-5-
carboxamides (compounds **15**, **27-35**). Compared to the indazole-5-carboxamides, the corresponding
indazole-6-carboxamides displayed greatly reduced MAO-B inhibition. Only 3,4- or 3,5-
halogenophenyl-substituted indazole-6-carboxamide derivatives (i.e., **40-44**) possessed some, although
only moderate, inhibitory activity at human MAO-B, whereas methoxy- or hydroxyl-substituted
compounds (**45-49**) were inactive or only very weakly active. The most potent compound in the
indazole-6-carboxamide series was the 3,4-dichlorophenyl-substituted derivative **40** (human MAO-B,
IC₅₀ 67.1 nM; rat MAO-B, IC₅₀ 466 nM). However, **40** was still 115-fold (human MAO-B) and 326-
fold (rat MAO-B) less potent than the related indazole-5-carboxamide analogue **15**. The 3,5-

1 dichlorophenyl derivative **41** had a moderate inhibitory effect (human MAO-B, IC₅₀ 335 nM; rat MAO-
2 B, IC₅₀ 423 nM). Similar potencies were observed for the corresponding 4-fluoro- and 3-fluoro-
3 substituted analogues **42** and **43**, which were moderately active only at the human, but not at the rat
4 MAO-B (**42**, human MAO-B, IC₅₀ 234 nM; **43**: human MAO-B, IC₅₀ 316 nM). Within the class of
5 indazole-6-carboxamides, in which the position of the indazole NH is altered in comparison with the
6 indazole-5-carboxamide series, the MAO-B potency decreased in the same rank order as observed for
7 the more potent indazole-5-carboxamide isomers (**15** and **27-35**): 3,4-di-Cl ≈ 3-F, 4-Cl ≈ 4-F, 3-Cl >
8 3,5-di-Cl > 3-Cl, 4-OMe ≈ 3-OMe, 4-Cl > 3-Cl, 4-OH ≈ 3-OH, 4-Cl. One exception was the 3,4-
9 difluoro-substituted compound **44**, which was less potent than expected (compare to **30**).
10
11
12
13
14
15
16
17
18
19
20
21
22
23

24 In order to further explore the heterobicyclic part in the so far most potent series of indazole-5-
25 carboxamides, the indazole residue was replaced by different heterobicycles resulting in compounds **53**-
26 **56**, while the 3,4-dichloro-substituted phenyl ring of **15** was kept constant. Replacement of the indazole
27 by an indole residue (compound **53**) resulted in an extremely high MAO-B inhibitory potency (human
28 MAO-B, IC₅₀ 0.227 nM; rat MAO-B, IC₅₀ 1.01 nM) showing only weak inhibition of MAO-A (human
29 MAO-A, IC₅₀ 1300 nM; rat MAO-A, IC₅₀ 6790 nM). Thus, the indole derivative **53** was 3-fold more
30 potent than the indazole-5-carboxamide analogue **15** at human MAO-B; it represents the most potent
31 MAO-B inhibitor of all compounds investigated. The activity of its *N*-methylated derivative **54** at
32 human MAO-B was 10-fold lower (IC₅₀ 2.26 nM). Based on their high bioactivity, which was
33 comparable or even superior to the indazole-5-carboxamide series, the indole-5-carboxamides **53** and **54**
34 may as well be considered as suitable candidates for further drug development (class II MAO-B
35 inhibitors).
36
37
38
39
40
41
42
43
44
45
46
47
48
49
50
51
52
53
54

55 Next, we continued with the modification of the indazole residue by replacing it by an
56 imidazo[1,2-*a*]pyridine or a [1,2,4]triazolo[4,3-*a*]pyridine moiety (compounds **55** and **56**). In
57 comparison to the indazole-5-carboxamides and the indole-5-carboxamides, compounds **55** and **56**
58
59
60

1 showed a large decrease in inhibitory activity at MAO-B. The 3,4-dichloro-phenyl-substituted
2 imidazo[1,2-*a*]pyridine-6-carboxamide (**55**) containing a bridge nitrogen atom had only moderate
3 potency at the human (IC₅₀ 141 nM) and rat MAO-B (IC₅₀ 1140 nM), while the
4 [1,2,4]triazolo[4,3-*a*]pyridine motif of **56** led to an almost complete loss of activity. This indicates that
5 the position of the nitrogen atom (N1) present in the indazole and indole moieties is essential for MAO-
6 B binding and has a strong impact on potency. A second nitrogen atom is well tolerated only in the
7 neighboring position (e.g., N2-position of the indazole). Introduction of a third nitrogen atom
8 (compound **56**) resulted in a virtually complete loss of MAO-B inhibitory activity (cf. docking studies
9 below).

10 Finally, the carboxamide linker in the 3,4-dichlorophenyl-substituted indazole derivate **15** was replaced
11 by an imine function producing Schiff bases **58** and **59**. Both compounds showed similarly high
12 MAO-B inhibitory potencies as the corresponding indole-5-carboxamides (**53** and **54**). The
13 unsubstituted indazole derivative **58** (human MAO-B, IC₅₀ 0.612 nM; rat MAO-B, IC₅₀ 3.69 nM) was
14 slightly more potent at MAO-B than its N1-methyl-substituted derivative **59** (human MAO-B, IC₅₀ 1.03
15 nM; rat MAO-B, IC₅₀ 4.55 nM).

16 From all 37 tested compounds, 29 were found to be potent inhibitors of MAO-B. In the series of
17 indazole-5-carboxamide derivatives (**15**, **27-38a**, **38b**), all compounds were found to be active at
18 MAO-B. The highest inhibitory potencies were achieved with the compounds containing a 3,4-
19 dihalogenophenyl residue (**15**, **28** and **29**) and an *N*-unsubstituted or an N1-methylated indazole core
20 (**38a**) inhibiting MAO-B in the subnanomolar range. These compounds are significantly more potent
21 than the current irreversible (selegiline, rasagiline) and reversible (safinamide) standard MAO-B
22 inhibitors (>13-fold). In the classes of indole-5-carboxamides (class II, **53** and **54**) and (indazol-5-
23 yl)methanimines (class III, **58** and **59**) selective MAO-B inhibitors with similarly high potencies as
24 those of the best indazole-5-carboxamides (class I derivatives) were discovered. The most potent
25

1 MAO-B inhibitor of the whole series was indole-5-carboxamide **53** (class II inhibitor), which contains a
2
3 3,4-dichlorophenyl residue. It inhibits human MAO-B with subnanomolar potency and was found to be
4
5 23-fold more potent than the standard inhibitor safinamide (**3**). The optimized structural features were a
6
7 5-indazole or a 5-indole moiety connected to a lipophilic, substituted phenyl ring through a polar linker
8
9 with a length of two atoms.
10

11
12
13
14 **Species Selectivity.** Significant species differences and moderate correlations between human and rat
15
16 IC_{50} values were previously described for other classes of MAO-B inhibitors.^{14,28,46} Therefore, all new
17
18 compounds were tested at human as well as rat MAO-A and MAO-B in order to assess potential species
19
20 differences. Since most compounds were inactive at MAO-A, species differences at MAO-A could only
21
22 be noticed for very few compounds. However, for many compounds major species differences in the
23
24 inhibitory potencies at MAO-B could be observed. With the exception of **27** and **54**, which were
25
26 virtually equipotent at rat and human MAO-B, the potency of the compounds at human MAO-B was
27
28 generally higher (5.2-fold on average, with compound **38b** showing the highest deviation of
29
30 approximately 1.2 log units between IC_{50} values at human and rat MAO-B) than at the rat orthologue.
31
32 The plot of all determined pIC_{50} values at rat MAO-B versus pIC_{50} values at human MAO-B gave a
33
34 linear regression with a slope = 1.00, y-intercept = -0.67 and $R^2 = 0.89$, thus displaying a clear
35
36 correlation between rat and human MAO-B enzyme inhibitory activity (for details, see Figure S8,
37
38 Supporting Information). Nonetheless it appears to be indispensable to determine MAO-B inhibition not
39
40 only at the human enzyme, but also at the species used for preclinical studies.
41
42
43
44
45
46
47
48
49

50 **Mechanism of Monoamine Oxidase B Inhibition.** The goal of the present study was to prepare novel
51
52 reversible MAO-B inhibitors. Reversible inhibition is expected to have considerable advantages
53
54 compared to irreversible inhibition, as discussed above. To investigate whether the indazole-5-
55
56 carboxamides (class I compounds) are reversible or irreversible inhibitors of human MAO-B, we
57
58 performed reactivation experiments with the representative human MAO-B inhibitor **15**. For this
59
60

purpose, the inhibition of reactivated human MAO-B by **15** was evaluated at a concentration that represents its IC_{80} value versus *p*-tyramine as a substrate. The enzyme activity of **15** was measured for 22 min in the presence of low concentration of the substrate *p*-tyramine (10 μ M pre-incubation) followed by a large increase in substrate concentration (to 1.0 mM). The irreversible inhibitor selegiline **1** and the reversible inhibitor safinamide **3** were tested as reference inhibitors (Figure 4).

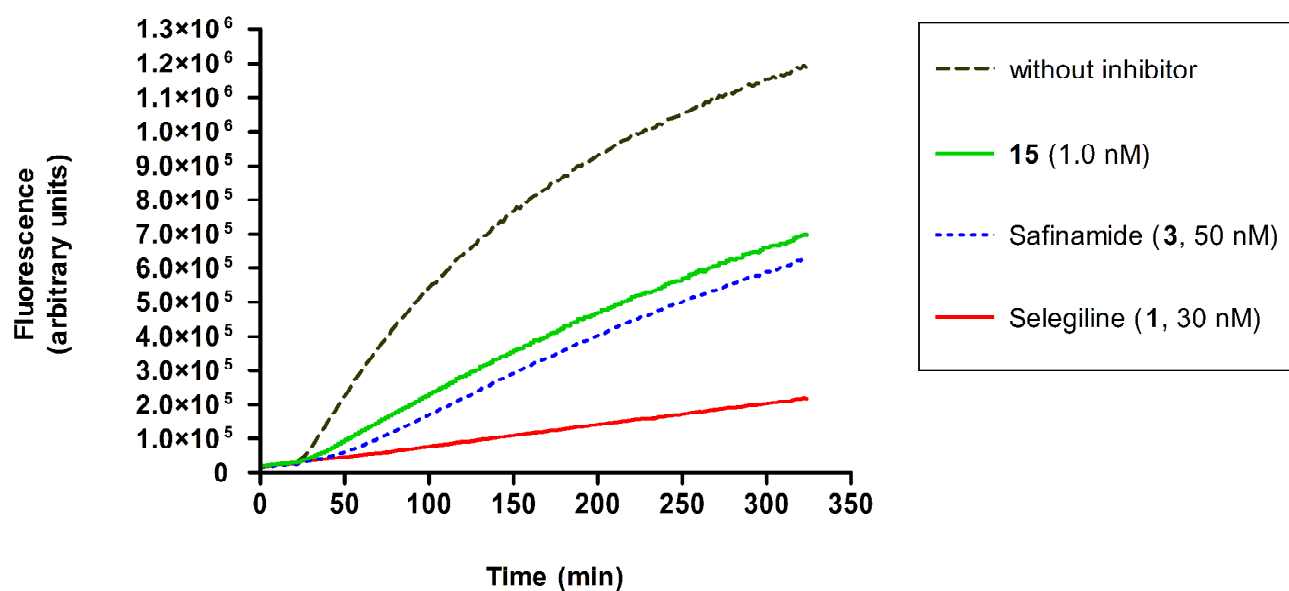


Figure 4. Reactivation of MAO-B: recombinant human MAO-B enzyme was treated under assay conditions with inhibitor **15** at a concentration that presents its IC_{80} value (1.0 nM) in the presence of the substrate *p*-tyramine. The irreversible MAO-B inhibitor selegiline (**1**) and the reversible inhibitor safinamide (**3**) were applied at concentrations of 30 nM and 50 nM, respectively. After a pre-incubation period of 22 min, the substrate concentration was increased from 10 μ M to 1.0 mM, and the fluorescence was measured over a period of 5 h.

1 In case of a reversible inhibition, after pre-incubation followed by an increase in the substrate
2 concentration, the MAO-B inhibitor will be replaced by the competing excess of *p*-tyramine and a
3
4 subsequent enzyme reactivation can be observed. In the experiment with the inhibitor **15**, an elevated
5
6 fluorescence can be detected after increasing the *p*-tyramine concentration indicating, that **15** acts as a
7
8 reversible MAO-B inhibitor. The measurements with the reversible reference inhibitor safinamide **3**
9
10 clearly showed the expected reversible mode of interaction with MAO-B, which is proven by an
11
12 elevation of the fluorescence after increasing the substrate concentration, similar as that observed for **15**.
13
14 In contrast, in the experiment with the irreversible inhibitor selegiline (**1**) the residual activity was not
15
16 significantly enhanced after increasing the substrate concentration. These experiments clearly indicate
17
18 that the indazol-5-carboxamides are reversible inhibitors of MAO-B. This was expected since they do
19
20 not contain any reactive moieties.
21
22
23
24
25
26
27

28 To further examine the interaction mode of the indazol-5-carboxamides with the binding site of
29
30 MAO-B, the type of enzyme inhibition was determined by Michaelis-Menten kinetic experiments. For
31
32 this purpose, the initial rates of the MAO-B-catalyzed oxidation of *p*-tyramine at six different substrate
33
34 concentrations in the absence and in the presence of three different concentrations of the selected
35
36 representative inhibitor **15** were measured. The results are depicted in Figure 5. Michaelis-Menten
37
38 kinetic parameters K_m and V_{max} of human MAO-B inhibition were determined in the presence and
39
40 absence of inhibitor **15**. The maximal velocity (V_{max}) remained almost constant at different
41
42 concentrations of **15**, whereas the Michaelis constant (K_m) rose with increasing inhibitor concentrations.
43
44 The Lineweaver-Burk plots for different concentrations of **15** were linear and intersected at the y-axis
45
46 with the plot for the uninhibited enzyme. In addition, a Dixon plot was calculated (see Figure S9,
47
48 Supporting Information). The obtained results indicate that the indazol-5-carboxamides are competitive
49
50 MAO-B inhibitors.
51
52
53
54
55
56
57
58
59
60

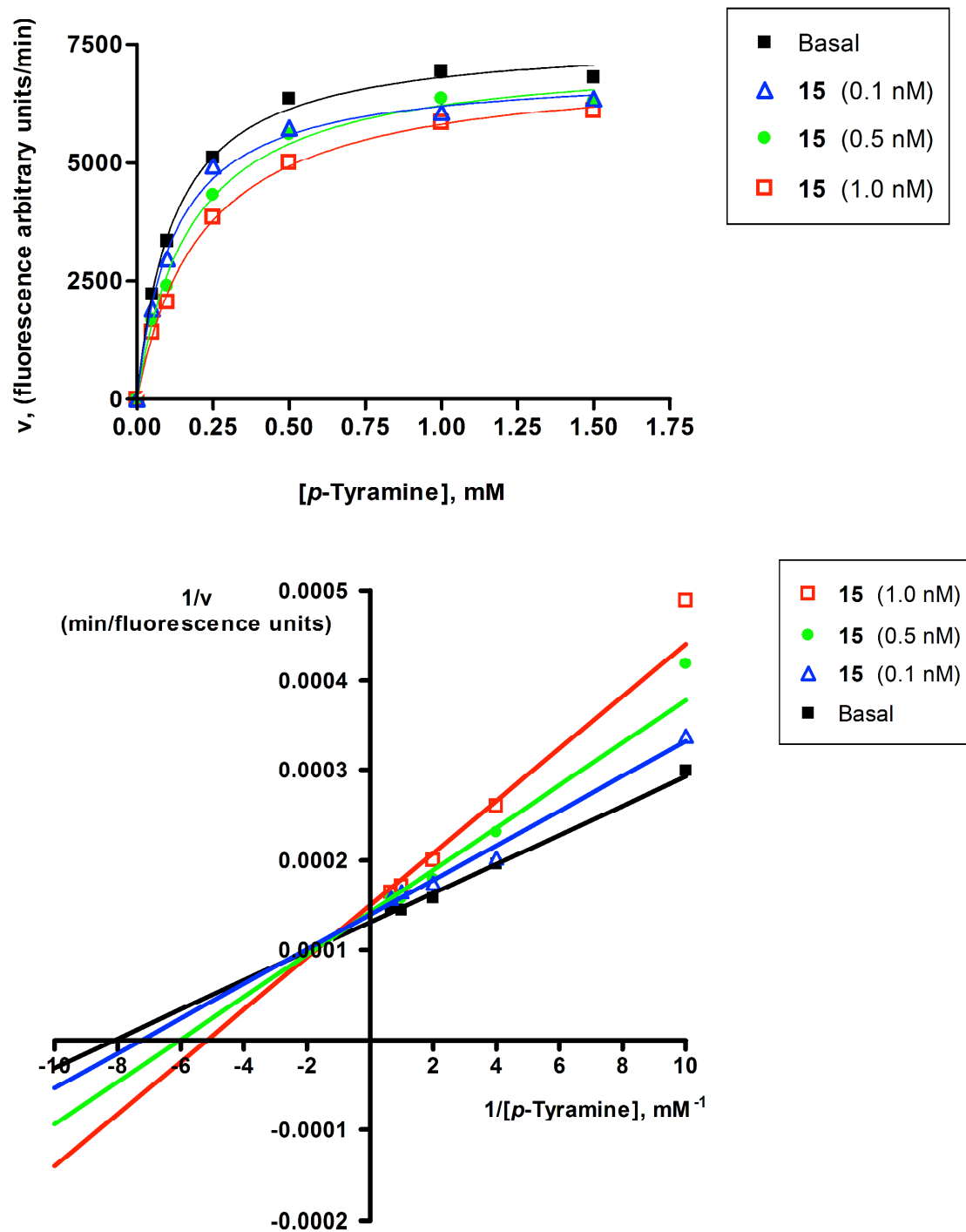


Figure 5. Mode of MAO-B inhibition: saturation curves (top) and Lineweaver-Burk plot (bottom) of the inhibition of recombinant human MAO-B enzyme by different concentrations of **15** (0, 0.1, 0.5, and 1.0 nM) in the presence of *p*-tyramine (0.05, 0.1, 0.25, 0.5, 1.0, and 1.5 mM) as a substrate. In the Lineweaver-Burk plot the reciprocal MAO-B inhibitory activity was plotted against the reciprocal substrate concentration (double reciprocal plot, $n = 2$).

Molecular Modeling Studies. The structure-activity relationship analyses of indazole-5- and indazole-6-carboxamide analogs provided useful information about the main structural features determining their MAO-B inhibitory potency. A detailed examination of their potential binding modes revealing the most significant interactions within the substrate binding site of MAO-B might provide additional information including an explanation for the observed preference in inhibitory potency of C5- versus C6-substituted indazole derivatives. Therefore we selected the structurally related compounds **15** and **40** for docking studies. While **15** is one of the most potent MAO-B inhibitors investigated here, compound **40** was found to bind with considerably weaker affinity. The modeling study was particularly focused on the estimation of main interactions taking place at (i) the indazole NH function, (ii) the carboxamide linker and (iii) the 3,4-dichloro-substituted phenyl ring. We carried out docking experiments of **15** and **40** followed by a HYDE-based selection of the top (FlexX-scored) solutions using the X-ray co-crystal structure of human MAO-B with the reference inhibitor safinamide **3** (PDB code 2V5Z, see Experimental Section).^{44,47} The docking simulations were performed with conformationally relaxed ligands using a LeadIT software. Overall, the docking studies reproduced the experimentally found binding modes and activities of several ligands well (we tested with a small set of structurally different compounds).⁴⁷ While treating protein protons and N \leftrightarrow O flips flexible, the HYDE module in LeadIT was utilized to evaluate the accuracy of the predicted ligand/enzyme interactions. Following standard procedures, the ligand and safinamide complexes obtained from the initial dockings were post-optimized using HYDE technology.⁴⁸ The automatized yet visual scoring method was recently developed to rapidly compute estimations of binding affinities; previous experience has shown its usefulness to improve the selection of correct poses from dockings. Furthermore, there appears convergence when selecting n = 32 binding poses per ligand.⁴⁹ Docking studies with LeadIT give strong indication that **15** and **40** occupy the same substrate cavity space as previously determined for safinamide.⁴⁴ In each docking case, the ligand molecule could be unambiguously modeled in the electron density binding region, assuming that both ligands do not covalently bind with the flavine (FAD) cofactor in contrast to some irreversible MAO-B inhibitors like selegiline and rasagiline.⁴⁵

However, there were significant differences in the binding modes of **15** and **40** at the active site of human MAO-B. In general, from the ligand perspective of **15**, the docking model led to the proposal that the binding pocket of human MAO-B can be divided into three different sub-pockets inside the protein: a heterocyclic binding pocket anchored in the “substrate cavity” in close to the FAD cofactor (hydrophobic region I, S1), a postulated H-interacting linker region, and a highly lipophilic halogen binding pocket (hydrophobic region II, S2) positioned in the “entrance” cavity (Figure 6).⁴⁵

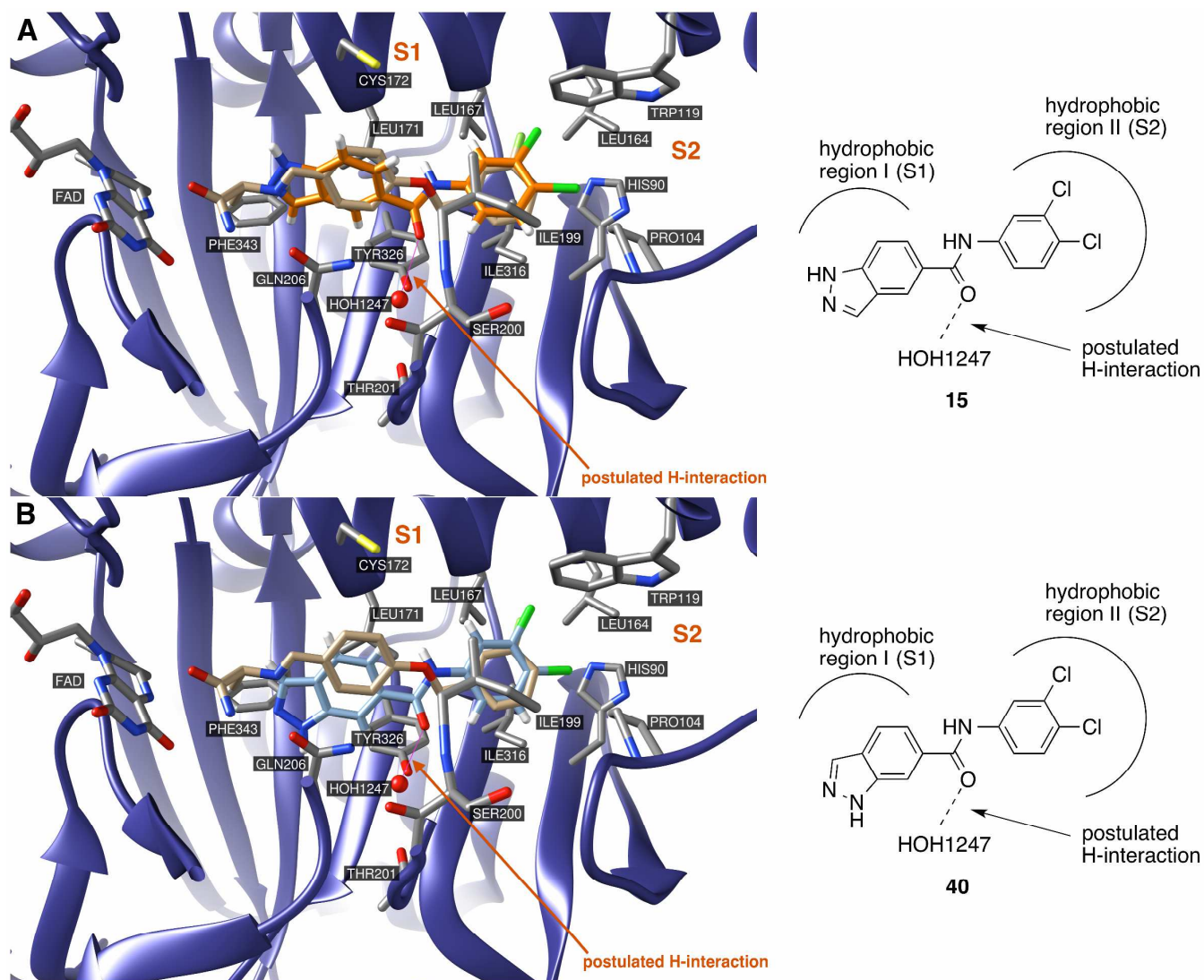


Figure 6. Predicted binding modes of **15** (A) and **40** (B) in the human MAO-B (PDB code: 2V5Z) active site. The ligands and the co-crystallized safinamide **3** are colored in orange, light blue and broken white, respectively. For clarity, only the relevant residue side chains are shown in gray. Clipping planes have been used for better visibility. All structures are represented as stick models. The postulated H-bond interactions between the carbonyl group and the water molecule HOH1247 are displayed as pink lines.⁵⁰

1 The heterocycle-binding site of the pocket is limited by the FAD cofactor; however, some space remains
2 unoccupied by **15**. The aromatic part of the indazole ring shows a π - π arrangement with the amide plane
3 of TYR326 below and CYS172 above the plane. In addition, slightly more distant, but still within the
4 distance limitations for hydrophobic contacts, LEU171 interacts with the indazole moiety too. The
5 carboxamide linker of **15** plays a remarkable role. It forms the basis for the only obvious hydrogen bond
6
7 ‘anchor’: a well-formed interaction to HOH1247 (CO---HOH1247 = 2.04 Å). Such an interaction was
8
9 also observed for the 6-substituted analogs, for which **40** served as an example. Below the ligand amide
10 linker, there is a π - π -type arrangement with TYR326, which itself (using its hydroxyl-group) showed
11 another interaction to HOH1247, eventually rendering this water molecule even more conserved
12 (protein-HOH1247 interaction not shown). In the back of the groove, in the region of the carboxamide
13 linker there is the side chain of LEU171, which maintains the hydrophobic character of that part
14 rendering the amide placement favorable there. Finally, the 3,4-dichlorophenyl substituent of the ligand
15 occupies a strongly hydrophobic binding pocket in which it is placed with considerable affinity gain by
16 releasing water molecules (hydrophobic effect). There are a multitude of hydrophobic amino acids
17 contributing (notably leucin and isoleucin residues), the most important ones being ILE316 (below),
18 PRO104 (hydrophilic side, limiting the pocket), ILE199 (top right), ILE198 (above paper plane), and
19 ILE199 (above paper plane, not shown to improve visibility). The upper right ‘roof’ of the pocket is
20 formed by the TRP119 ring system with the closest distance to any of the halogen atoms being
21 approximately 3.5 Å. Summarizing our findings, we can conclude that (i) the indazole side of **15** is
22 dominated by hydrophobic contacts, (ii) the carboxamide linker exhibits a hybrid feature providing an
23 H-bond acceptor - the carboxylic oxygen - and serving as a hydrophilic anchor, while additionally using
24 its π -character to form hydrophobic interactions, and (iii) the 3,4-dichlorophenyl side is dominated by
25 hydrophobic interactions (halogen binding pocket, HBP). In agreement with the HYDE analysis
26 (compare below), the binding is heavily dominated by hydrophobic contacts, and therefore, it appears to
27 be largely entropy-driven, owing most of its strength to the release of water molecules from the
28
29
30
31
32
33
34
35
36
37
38
39
40
41
42
43
44
45
46
47
48
49
50
51
52
53
54
55
56
57
58
59
60

1 hydrophobic environments. There is only a single H-bond anchor mediating this type of interaction
2
3 between protein and ligand.
4
5
6

7 In the case of the 6-substituted indazole **40**, the situation is similar (Figure 6). The heterocyclic moiety
8 of the binding groove is limited by the FAD cofactor. The back of this part of the binding site is
9 represented by the phenyl part of PHE343. It is oriented in a herringbone-like arrangement with respect
10 to the pyrazole part of the indazole moiety. On the other side, i.e., below the pyrazole, we find the amide
11 side chain of GLN206 forming a stacking interaction. Moving further to the right, another hydrophobic
12 contact can be made out: LEU171 and GLN206 are forming a sandwich orientation with the phenyl part
13 of the indazole moiety. Moreover, similarly to the docking results for **15**, the oxygen atom of the
14 carboxamide linker interacts with HOH1247 (CO---HOH1247 = 2.15 Å), which itself bridges to
15 GLN206-amine and the ILE199 backbone-carbonyl groups. The 3,4-dichlorophenyl moiety of the
16 binding situation in **40** closely resembles the one of the above-mentioned complex of **15** in 2V5Z.
17
18
19
20
21
22
23
24
25
26
27
28
29
30

31 In summary, we observed that this class of compounds is likewise dominated by binding through
32 replacing water molecules. The only relevant H-bond is formed by the central linker of the molecule,
33 however this very water molecule is highly coordinated also by protein residues, making it more
34 essential for overall binding. One route to further optimization of these classes of compounds might be
35 to replace HOH1247, e.g., by a suitable alkyl substituent. However, this would lead to even more
36 lipophilic compounds. Finally, docking studies are in line with a proposal of a non-covalent binding
37 mode to human MAO-B, typically associated with reversible inhibitory activity. This finding is in
38 agreement with the experimentally confirmed reversible mechanism of action for **15**.
39
40
41
42
43
44
45
46
47
48
49
50
51

52 **HYDE Visual Binding Assessment of 5- versus 6-Substituted Indazoles.** Comparing compounds **15**
53 and **40**, it is difficult to understand why the C5-substituted indazoles exhibit higher affinity towards
54 human MAO-B than the C6-substituted analogues (about two log units difference between **15** compared
55
56
57
58
59
60

1
2
3
4
5
6
7
8
9
10
11
12
13
14
15
16
17
18
19
20
21
22
23
24
25
26
27
28
29
30
31
32
33
34
35
36
37
38
39
40
41
42
43
44
45
46
47
48
49
50
51
52
53
54
55
56
57
58
59
60

to **40**). To find plausible explanations we subjected both compounds in their docked conformations to a HYDE Visual Affinity Assessment (Figure 7).

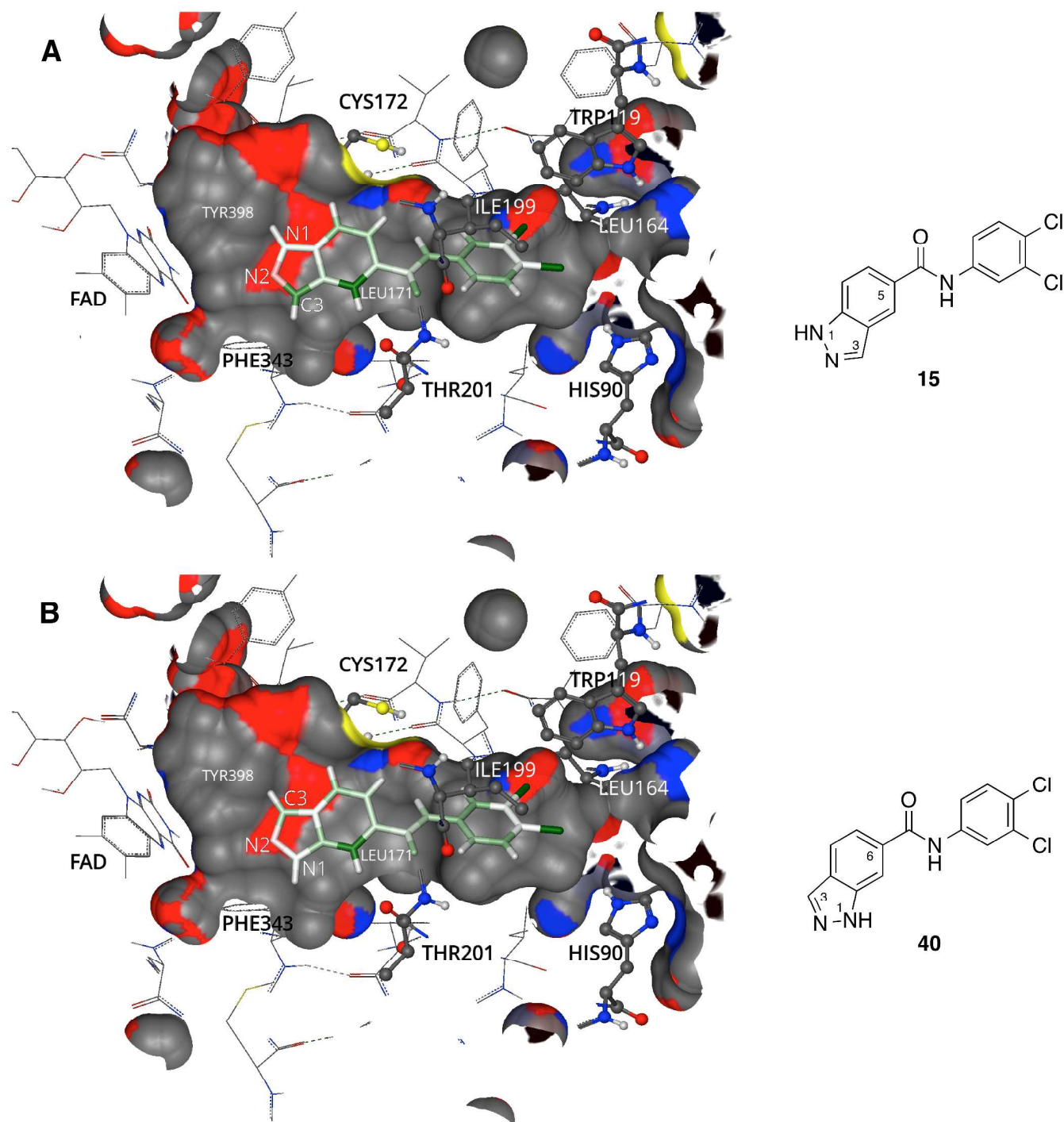


Figure 7. Compounds **15** (**A**) and **40** (**B**) placed within the PDB 2V5Z cavity in a HYDE Visual Affinity Assessment (ligands rendered in stick model with atom coloring by HYDE: green = favorable, red = unfavorable for affinity; the relevant ligand atoms C3, N1 and N2 are labeled in white, atoms of LEU171 and TYR398 behind the binding site surface). The surface has been colored by the respective amino acid elements; clipping planes have been used to enhance visibility and therefore not all atoms are visible for all residues and FAD.⁴⁷

1 When comparing the two substitution scenarios, distinct differences become visible. In the case of **40**,
2 the indazole N1 atom (lower center) essentially has no contribution to affinity. Besides the fact that the
3 modeling shows no H-bond contribution, the desolvation penalty for this atom amounts to
4 approximately 0.5 kJ/mol. This is slightly overcompensated by the desolvation gain from the binding
5 site (around 1.0 kJ/mol), totaling to a negligible contribution overall (HYDE shows it in almost white
6 coloring). The neighboring N2 atom exhibits a somewhat higher desolvation penalty (approximately 1.0
7 kJ/mol), while the enzyme binding site behaves indifferently; furthermore, there is again no bond
8 formed which could overcompensate the loss from desolvation penalties, so that the overall contribution
9 stays at roughly 1.0 kJ/mol in the view of a HYDE analysis. While the halogen-phenyl part and the
10 carboxamide linker stay similarly favorable with respect to their affinity contributions, the situation
11 changes for the 5-membered ring in the indazole moiety in **15** and its surroundings. Here, the placement
12 of a more hydrophobic atom in the binding groove around the lower part of the indazole-5-ring is
13 obviously especially favorable (PHE343, TYR398, FAD). According to the ligand docking, the C3-
14 position in the C5-substituted indazoles occupies that very spatial region which is occupied by the N2 in
15 the C6-substituted analogs. This is a subtle yet distinct effect and entails higher affinity. According to
16 the HYDE calculations, the C3 atom at this position now contributes with a desolvation gain of about
17 3.5 kJ/mol, whereas the N2 atom is not able to overcompensate this, given its desolvation penalty of
18 almost 2.0 kJ/mol. The N1 atom also contributes indirectly, inducing a receptor desolvation contribution
19 of about 0.5 kJ/mol, and therefore, overall, a positive contribution of the three relevant atoms of
20 approximately 4.0 kJ/mol occurs, giving a strong pointer to the origins of the enhanced activities for the
21 5-substituted indazoles. Furthermore, taking into account that the only remaining atom contributing
22 slightly unfavorably in the 5-substituted indazoles is N2, it appears natural that further optimization of
23 this class of compounds could proceed from, for example, a vector at this very N2 position. This
24 assumption is experimentally confirmed by compound **38b**, which contains a methyl group at the N2-
25 position in the indazole moiety and was not only well tolerated by human MAO-B, but also showed a
26 moderate activity for the human MAO-A isoenzyme. Further, a hydrophilic substitution should make
27
28
29
30
31
32
33
34
35
36
37
38
39
40
41
42
43
44
45
46
47
48
49
50
51
52
53
54
55
56
57
58
59
60

1 this atom less accessible for water, entailing a “quenching” of desolvation effects, and therefore, an
2 improvement of affinity.
3

4
5 In conclusion, the 5- and 6-substituted indazoles **15** and **40** exhibit different binding affinities based on
6 their different entropic contributions (hydrophobic effects) to the total binding energy. The visual
7 analyses with HYDE provide indications that the C5-substituted indazole **15** contributes with almost 1.5
8 kcal/mol at its C3 position. In contrast, the C6-substituted analog **40** has no favorable desolvation
9 contribution by any atom in the same spatial area (whereas the remaining molecular parts keep their
10 contributions constant). In this more hydrophobic region, a nitrogen atom (N1 position in **40**) is present
11 and, with respect to desolvation effects, the difference between the bonded and unbonded states amounts
12 to zero. That means, the N5 atom is assumed to be solvated in both the unbound and bound states;
13 consequently, the affinity contribution from desolvation effects – being the difference in ΔG between
14 these two states – is not affected. In addition, it does not form any hydrogen bonds, and therefore, its
15 contribution to the overall affinity can essentially be neglected. Summarizing, HYDE was able to help
16 understanding activity differences by visualization and quantification of effects of (de)hydration and H-
17 bonds.
18
19
20
21
22
23
24
25
26
27
28
29
30
31
32
33
34
35
36
37

38 **Physicochemical Properties.** Based on their potent and selective inhibition of MAO-B, 14 compounds
39 were selected for further evaluation (**15**, **27-36**, **38a**, **38b**, **53**, **54**, **58**, and **59**; see Table 1). The selection
40 criteria included inhibitory potency towards human MAO-B with an IC_{50} of <10 nM and greater than
41 1000-fold selectivity for MAO-B over MAO-A. To evaluate the drug-likeness of the selected
42 compounds, we calculated several physicochemical parameters, including lipophilicity (clogP),
43 topological polar surface area (*t*PSA), and ligand-lipophilicity efficiency (LLE),^{51,52,53} and compared
44 them to the reference MAO-B inhibitors **1-3** (Table 2).
45
46
47
48
49
50
51
52
53
54
55
56
57
58
59
60

Table 2. Physicochemical Properties of Selected Compounds and Reference MAO-B inhibitors

Compd.	M _R	pIC ₅₀	N ^a	clogP ^b	tPSA (Å ²) ^b	LLE ^c
Selegiline (1)	187	8.18	14	2.85	3.24	5.33
Rasagiline (2)	171	7.85 ^d	13	2.30	12.0	5.55
Safinamide (3)	302	8.29	22	2.48/2.20 ^e	64.4	5.81
15	306	9.23	20	3.60	57.8	5.63
27	306	8.56	20	3.60	57.8	4.96
28	289	9.17	20	3.13	57.8	6.04
29	289	9.17	20	3.13	57.8	6.04
30	273	8.88	20	2.67	57.8	6.13
32	301	8.47	21	2.83	67.0	5.64
34	301	8.36	21	2.83	67.0	5.53
36	307	8.27	20	2.60	70.7	5.67
38a	320	9.41	21	3.72	46.9	5.69
38b	320	8.84	21	4.08	46.9	4.76
53	305	9.64	20	4.37	44.9	5.27
54	319	8.65	21	4.60	34.0	4.05
58	290	9.21	19	4.38	41.0	4.83
59	304	8.99	20	4.50	32.0	4.49

^aN, number of heavy atoms. ^bCalculated by the Instant JChem program (Version 6.0.2), ChemAxon, 2013, (<http://www.chemaxon.com>). ^cLLE: ligand-lipophilicity efficiency = pIC₅₀ – clogP. ^dData from ref. 18. ^eData obtained from *CINAPS Dossier: Safinamide 3/29/2009*, National Institute of Neurological Disorders and Stroke (NINDS), Bethesda, USA, 2009.

The clogP value was in all cases lower than 5, which is in agreement with the well known rule-of-5 for drug-likeness.^{54,55} Compounds **28-30**, **32**, **34** and **36** exhibit a clogP value of less or about 3, which is considered as optimal for perorally administered drugs being in the same range as the reference drugs **1-3**. Compounds **28-30**, **32** and **34** have lower molecular weight (M_R) than the reference drug safinamide (**3**). Moreover, all selected compounds are more potent at human MAO-B than the reference drugs **1-3**. The mean number of the heavy atoms for the new compounds was always lower (HA_{mean all} = 20.3) than that of the reversible standard MAO-B inhibitor safinamide (**3**, HA_{SAF} = 22), but higher than that of the irreversible MAO-B inhibitors **1** and **2** containing 14 and 13 non-hydrogen atoms,

1
2
3
4
5
6
7
8
9
10
11
12
13
14
15
16
17
18
19
20
21
22
23
24
25
26
27
28
29
30
31
32
33
34
35
36
37
38
39
40
41
42
43
44
45
46
47
48
49
50
51
52
53
54
55
56
57
58
59
60

respectively (see Table 2). In general, most of the new MAO-B inhibitors appear to have optimal physicochemical parameters for allowing oral bioavailability ($\log P$ 2–4, $M_R < 400$ and $tPSA$ 50–90 \AA^2).⁵⁶ Together with $\text{clog}P$ and M_R , the PSA is used to assess the compound's ability to cross the blood-brain barrier (BBB). For all selected compounds, the $tPSA$ values were ranging between 32.0 and 70.7 \AA^2 , and therefore, they are expected to be orally bioavailable. Furthermore, compounds with a PSA value lower or equal to 61 \AA^2 are classified as “good” for brain penetration.⁵⁷ The PSA for most of the selected compounds (except for **32**, **34** and **36**) did not exceed the required limit for brain permeability of 60 \AA^2 , and therefore, these may be considered as promising central nervous system (CNS) drug candidates.⁵² A further parameter frequently applied in the lead generation and optimization process is the ligand-lipophilicity efficiency (LLE) that combines potency and lipophilicity.⁵⁴ For most of the selected compounds (except for **54** and **59**), the LLE value was found to be within the range of 5–7. Compounds with a LLE >5 can be considered as suitable drug candidates.⁵⁴ In case of the selected new compounds, **28-30** possessed an optimal LLE value of more than 6, and may therefore serve as drug candidates suitable for further in vivo evaluation. To assess the relationship between lipophilicity and bioactivity, we plotted the $\text{clog}P$ values versus the pIC_{50} values (human MAO-B) for all target compounds as well as reference drugs **1-3** (Figure 8).

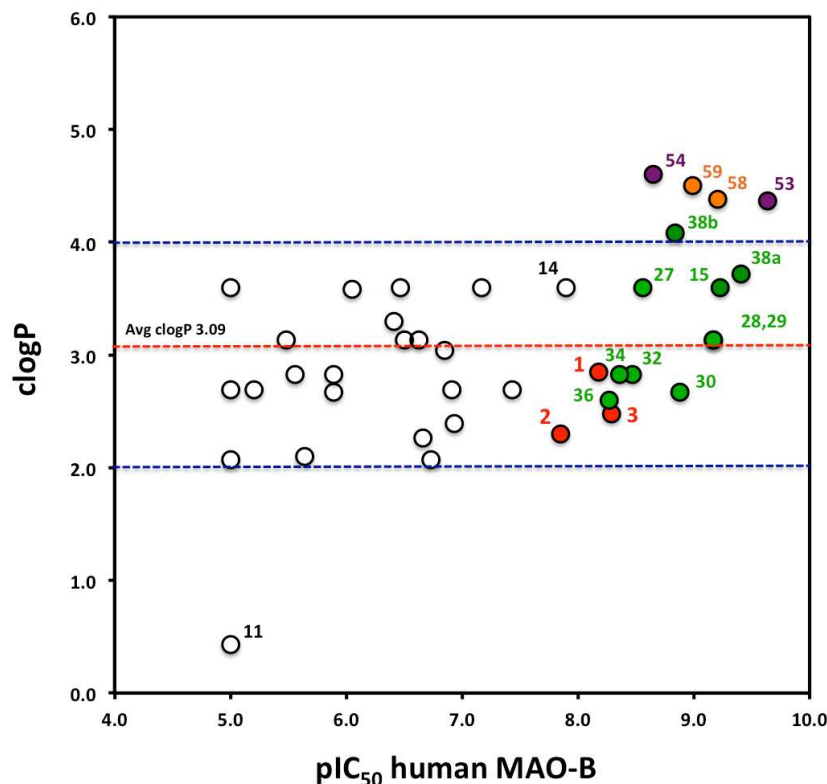


Figure 8. Distribution of clogP versus pIC₅₀ values (human MAO-B) for reference compounds and newly developed inhibitors. The reference drugs and selected novel classes of MAO-B inhibitors are indicated in red (**1**, **2** and **3**), green (indazole-5-carboxamides, class I), violet (indole-5-carboxamides, class II) and orange (indazol-5-yl)methanimines, class III) circles, respectively (also see Table 3). The blue dashed lines represent the preferred range for clogP values. The red dashed line indicates the average clogP value of 3.09 of all synthesized compounds.

The reference drugs and the structurally novel MAO-B inhibitors (class I, II and III) are shown in colored circles. The white circles represent compounds that are only weakly active at human MAO-B. All compounds with the exception of **53**, **54**, **58** and **59**, display acceptable clogP values within the preferred range for CNS drugs of 2-4 (blue dashed lines).⁵⁸ The clogP value for compound **38b** is at the upper limit (4.08), while **11** is a highly hydrophilic compound with a clogP of 0.43. There was a significant correlation between the pIC₅₀ values of indole-5-carboxamides (**53** and **54**) and (indazol-5-yl)methanimines (**58** and **59**) at human MAO-B and their high lipophilicity with clogP values in the range of 4.36-4.60. Among all presented compounds, **53** was not only identified as the most potent (pIC₅₀ = 9.64) but also as one of the most highly lipophilic MAO-B inhibitors of the present series of compounds. The N1-methyl-substituted derivative **54** (clogP 4.60) is even more lipophilic and represents the most lipophilic compound of all series of inhibitors investigated in this study. The

1 distribution of the clogP values plotted versus M_R and $tPSA$ values indicates that newly developed class
2 II (**53** and **54**) and class III (**58** and **59**) MAO-B inhibitors possessing $tPSA$ values between 32.0 and
3 44.9 Å² are less polar than class I inhibitors (for more details, see Figure S10, Supporting Information).
4
5 The plotted pIC_{50} and clogP values demonstrate that highly potent MAO-B inhibitors (e.g., compounds
6
7 **28-30** and **34**) with an optimal lipophilicity suitable for further CNS drug development were discovered
8
9 (Figure 8).
10
11
12
13
14
15
16

17 Additional physicochemical values, known as important predictors of drug-likeness⁵⁸ were calculated,
18 including pK_a values, distribution coefficients (clogD_{7.4}), hydrogen bond donor/acceptor (HBD/HBA)
19 counts, rotatable bonds (Rot.), water solubility (S_w), and molar volume (V_m) (for details, see Tables S3
20 and S4, Supporting Information). The properties of the new MAO-B inhibitors were compared to the
21 profiles of the top-selling 25 CNS drugs, and many of them were found to perform similarly well. The
22 physicochemical properties for the new compounds are in the suggested limits (clogP = 2–5, $tPSA < 90$
23 Å², $M_R < 500$, HBD < 3).⁵⁸ The mean clogP value for all new compounds was 3.09, whereas the mean
24 MW and $tPSA$ values were 229.1 and 60.5 Å², respectively (see Supporting Information). Of all new
25 compounds, **30** are predicted to possess oral bioavailability ($S_w = 0.36$ mg/mL at pH 7.4),⁵⁵ lead
26 likeness,^{52,54,55} and fulfill the rule-of-3 criteria ($M_R \leq 300$, $\log P \leq 3$, acceptor counts ≤ 3 , rotatable bond
27 counts ≤ 3 , $tPSA \leq 60$)⁵² for CNS drug candidates (for details, see Supporting Information Table S5 and
28 S6).
29
30
31
32
33
34
35
36
37
38
39
40
41
42
43
44
45
46

47 **The Most Promising Lead Structures.** As the most promising MAO-B inhibitors of the present series
48 with drug-like properties, compounds **29** and **30** have to be highlighted (Figure 10). In order to improve
49 their physicochemical properties while maintaining high potency and selectivity at human MAO-B, **29**
50 and **30** were designed and evaluated in a two-step drug optimization process. In addition to the already
51 discussed physicochemical properties (e.g., M_R , clogP, and the number of heavy atoms HA) and ligand-
52 lipophilicity efficiency (LLE), we also used the binding efficiency index (BEI)^{51,53,54} as a metric value to
53
54
55
56
57
58
59
60

assess the properties of lead structure **15** optimized derivatives. Additionally, the indazole-5-carboxamide derivatives **15**, **29** and **30** were aligned and characterized by high shape and field similarity.⁵⁹

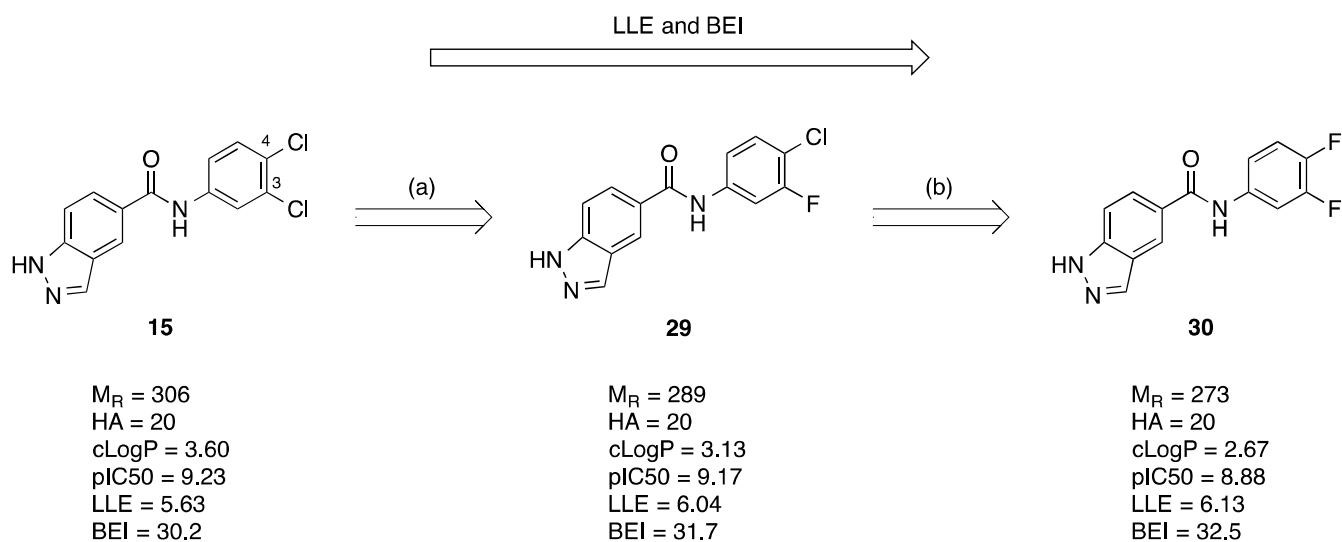


Figure 9. Structure optimization process of lead structure **15** towards derivative **30** with improved properties by replacement of the 3-Cl (step a), or the 3,4-di-Cl atoms (step b) with one (**29**) or two fluorine atoms (**30**). The binding efficiency index (BEI) is defined as $BEI = pIC_{50}/M_R$ (in 1/kDa).

Starting from **15**, we stepwise replaced the chlorine atoms at the phenyl ring in position 4 (compound **28**, not shown), and position 3 (compound **29**, Figure 9), respectively, with fluorine atoms (step a). In the following step b, both fluorine atoms at positions 3 and 4 of **15** were replaced resulting in **30**. During both steps the relative molar mass (M_R) was consequently decreased from 306 (**15**) to 273 (**30**). Since the number of heavy atoms (HA) for all three compounds is equal to 20 (see Figure 9), we additionally applied the binding efficiency index (BEI) as an alternative metric value to the ligand efficiency index (LE) in order to quantify the drug optimization of **15**, which showed the same trend.⁶⁰ The BEI values were calculated by using the measured binding affinity (pIC₅₀ at human MAO-B) dividing it by the M_R (in kDa). It is well known, that during a drug optimization from hit to lead to clinical candidate an increase in M_R is typically observed.⁶⁰ In contrast, in the presented series of MAO-B inhibitors the potency within the chemical series of indazole-5-carboxamides is not strongly correlated with molecular weight. Because of its well-balanced profile compound **30** may be considered as a promising CNS drug

1 candidate for further development. Similar features were observed by several compounds of the series
2 of indazole-5-carboxamides (class I MAO-B inhibitors) like 3,4-chlormethoxyphenyl-substituted
3 derivatives **32** and **34** as well as 3,4-dichloropyridine containing analogue **36**.
4
5
6
7
8

9
10 The selected MAO-B inhibitor **30** was analyzed by a superposition onto both the reference ligand
11 safinamide (**3**) and lead compound **15**. For this purpose, the 3D alignments were computed with flexible
12 ligands and **3** as the template bioactive structure (for details, see Table S7 and Figure S11, Supporting
13 Information). Based on their physicochemical interaction model (e.g., reflecting donors, acceptors,
14 delocalization, and amide character of the molecules), compounds **15** and **30** showed a 72% and 75%
15 identity to **3**, respectively. Furthermore, the volume overlaps reflect a spatial coverage of **3** in the range
16 of 85%. The overlays give a hint to the higher MAO-B potency of **15** and **30** in comparison to **3**. In
17 addition, the superposition experiment supports the assumption of a relatively rare (compare Docking
18 results) interplanar twist between the phenyl and the indazole ring planes, enforcing a non-planarity
19 between the amide function and at least one of the ring systems.
20
21
22
23
24
25
26
27
28
29
30
31
32
33
34

35 CONCLUSIONS

36
37 In conclusion, we discovered indazol-5-carboxamides, indol-5-carboxamide and (1*H*-indazol-5-
38 yl)methanimine derivatives as structurally novel classes of MAO-B inhibitors. Structural optimization
39 and SAR analyses led to the discovery of remarkably potent competitive and reversible MAO-B
40 inhibitors with subnanomolar potency. Furthermore, the binding mode of selected C5- versus C6-
41 substituted indazole-carboxamide derivatives within the binding pocket of the human MAO-B enzyme
42 was investigated. The molecular modeling studies provided insights into the main interactions and
43 structural requirements of enzyme-inhibitor binding and broadened our understanding of the
44 compounds' requirements for achieving high MAO-B affinity and selectivity. Thus, several indazole-5-
45 and indole-5-carboxamide analogues with different substituents at the phenyl 3- and 4-positions (e.g.,
46 compounds **28-30**, **32**, **34**, **36** and **53**) and those with an *N*1-methylated indole or indazole moiety (e.g.,
47
48
49
50
51
52
53
54
55
56
57
58
59
60

1 compounds **38a** and **54**) were identified that may serve as promising lead structures or even drug
2 candidates e.g., for the treatment of PD and AD. Moreover, they will be highly useful as
3 pharmacological tools for in vitro and in vivo studies, and may be suitable for the development of
4 radioligands, including diagnostics for positron emission tomography (PET). As an example, compound
5 **30** can be highlighted because of its remarkable in vitro MAO-B inhibitory activity and its well-
6 balanced physicochemical profile, which is predictive of CNS bioavailability. Future efforts will be
7 directed towards further improving the compounds' drug-like properties with regard to water-solubility,
8 bioavailability, metabolism and toxicity, and to evaluate the new MAO-B inhibitors in relevant animal
9 models.
10
11
12
13
14
15
16
17
18
19
20
21
22
23
24
25
26
27
28
29
30
31
32
33
34
35
36
37
38
39
40
41
42
43
44
45
46
47
48
49
50
51
52
53
54
55
56
57
58
59
60

EXPERIMENTAL SECTION

Chemistry. All reagents including 5-amino-indazole (**17**), different substituted anilines (**23a-k** and **25**), 2,3-dichloro-5-aminopyridine (**24**), carboxylic acids (**20**, **21a-c**, **22**, **39**, and **50-52**), and indazole-5-carboxaldehydes (**57a** and **57b**) were obtained from various producers (Acros, Sigma Aldrich, Alfa Aesar, and TCI) and used without further purification. The experimental procedures and spectroscopic analysis for the carboxylic acids **18** and **19** are provided in the Supporting Information. Solvents were used without additional purification or drying unless otherwise noted. Reactions were monitored by thin layer chromatography (TLC) using aluminum sheets coated with silica gel 60 F₂₅₄ (Merck). Compounds were visualized under UV light (254 nm). Preparative column chromatography was performed on silica gel 60 (Acros Organics) 0.060–0.200 mm. Mass spectra were recorded on an API 2000 mass spectrometer (electron spray ion source ESI, Applied Biosystems, Darmstadt, Germany) coupled with an Agilent 1100 HPLC system using a Phenomenex Luna HPLC C18 column (50 × 2.00 mm, particle size 3.0 μm). Purification by RP-HPLC of final products was performed on a Eurospher 100-10 C18 column (250 × 20 mm, particle size 10.0 μm, flow rate 10 mL/min) using Knauer Advanced Scientific Instruments (Berlin, Germany) preparative pump 1800/100 coupled with a Smartline 2600 UV diode array detector (DAD) with an UV detection in the range from 220 to 400 nm. The purity of the tested compounds and stability control of selected compounds **54** and **59** was determined by HPLC-UV obtained on an LC-MS instrument (Applied Biosystems API 2000 LC-MS/MS, HPLC Agilent 1100) using the standard or modified LC/ESI-MS method as described in the Supporting Information. All tested compounds possessed a purity of not less than 95%. ¹H and ¹³C NMR spectra were recorded on a Bruker Avance 500 MHz NMR spectrometer. DMSO-*d*₆ was used as a solvent as indicated below. NMR spectra were recorded at room temperature (303 K). Chemical shifts (δ) are given in parts per million (ppm) related to that of the solvent. Coupling constants *J* are given in Hertz (Hz), and spin multiplicities are given as singlet (s), doublet (d), triplet (t), quartet (q), multiplet (m), and broad (br). Melting points were determined on a Büchi Melting Point B-545 apparatus and are uncorrected. The carboxylic acids **18** and **19** were prepared as described in the Supporting Information.

1
2
3 *General Procedure A for the Amide Coupling to Produce Compounds 10-16, 26-37, 40-49, 53, 55 and*
4
5 **56. Method 1.** A solution of the corresponding carboxylic acids **18-20** and **22** (1.0 equiv.), different
6
7 substituted anilines **17** and **23a** (1,2 equiv.) and TBTU (1.2 equiv.) in acetonitrile (2–3 mL/mmol) was
8
9 treated with DIPEA (1.2 equiv.), and the reaction was allowed to stir over night at room temperature.
10
11 The precipitate formed was filtered, dried at 70 °C and purified by column chromatography on silica gel
12
13 (eluent: CH₂Cl₂/MeOH, 9:1 v/v).
14

15
16 *Method 2.* A solution of the corresponding carboxylic acid **21a-c**, **22**, **39** and **50-52** (1.0 equiv.),
17
18 different substituted anilines **23a-k**, **24** and **25** (1.0 equiv.) and EDC-HCl (1.1 equiv.) in methanol (3–5
19
20 mL/mmol) was stirred over night at room temperature. The reaction was concentrated in vacuo, the
21
22 residue was treated with a water/ether-mixture (5:1, 12 mL/mmol), and the mixture was stirred for 30
23
24 min at room temperature. The precipitate formed was filtered under reduced pressure and dried at 70 °C.
25
26 The crude product was purified by column chromatography on silica gel (eluent: CH₂Cl₂/MeOH, 9:1
27
28 v/v).
29
30
31
32

33
34 *5-Chloro-N-(1H-indazol-6-yl)-6-morpholinonicotinamide (10).* The compound was prepared following
35
36 Method 1. Purification by silica gel chromatography (CH₂Cl₂/MeOH, 9:1 v/v) following by
37
38 recrystallization two times from petroleum ether/CH₂Cl₂ afforded **10** as colorless crystals (241 mg,
39
40 37%), mp: 238-239 °C; ¹H NMR (500 MHz, DMSO-*d*₆) δ = 3.43 (t, *J* = 4.72 Hz, 4H, Morph.), 3.74 (t, *J*
41
42 = 4.42 Hz, 4H, Morph.), 7.51 (d, *J* = 8.83 Hz, 1H, Ph), 7.68 (dd, *J* = 1.26 / 8.83 Hz, 1H, Ph), 8.03 (s,
43
44 1H, Ph), 8.24 (s, 1H, Ind.-Het.), 8.40 (d, *J* = 1.89 Hz, 1H, Pyr.), 8.85 (d, *J* = 1.89 Hz, 1H, Pyr.), 10.44 (s,
45
46 1H, -NHCO-), 13,11 (s, 1H, NH); ¹³C NMR (125 MHz, DMSO-*d*₆) δ = 44.0 (2C, Morph.), 66.1 (2C,
47
48 Morph.), 110.1, 111.4, 119.7, 121.5, 122.8, 124.8, 132.0, 133.5, 137.3, 138.5, 146.1, 158.7, 162.6;
49
50 LC/ESI-MS (*m/z*): negative mode 356 [M-H]⁻, positive mode 358 [M+H]⁺.
51
52

53
54
55 *N-(1H-indazol-5-yl)-1-methyl-6-oxo-1,6-dihydropyridine-3-carboxamide (11).* The compound was
56
57 prepared following Method 1. Purification by silica gel chromatography (CH₂Cl₂/MeOH, 9:1 v/v)
58
59
60

1 following by recrystallization three times from petroleum ether/CH₂Cl₂ afforded **11** as a white solid (61
2 mg, 45%), mp: 247-249 °C; ¹H NMR (500 MHz, DMSO-*d*₆) δ = 3.52 (s, 3H, Me), 6.43 (d, *J* = 9.46 Hz,
3 1H, Pyr.), 7.49 (d, *J* = 8.82 Hz, 1H, Ph), 7.68 (dd, *J* = 1.58 / 8.83 Hz, 1H, Ph), 8.10 (s, 1H, Ph), 8.05 (dd,
4 *J* = 2.53 / 9.46 Hz, 1H, Pyr.), 8.20 (d, *J* = 1.27 Hz, 1H, Ind.-Het.), 8.80 (d, *J* = 2.52 Hz, 1H, Pyr.), 10.29
5 (s, 1H, -NHCO-), 13.09 (s, 1H, NH); ¹³C NMR (125 MHz, DMSO-*d*₆) δ = 37.4, 53.3, 110.1, 111.1,
6 112.8, 117.9, 121.6, 122.8, 132.2, 133.4, 138.5, 142.7, 162.0, 163.0; LC/ESI-MS (*m/z*): negative mode
7 267 [M-H]⁻, positive mode 269 [M+H]⁺.
8
9

10 *2-Chloro-6-fluoro-N-(1H-indazol-5-yl)benzamide (12)*. The compound was prepared following Method
11 1. Purification by silica gel chromatography (CH₂Cl₂/MeOH, 9:1 v/v) following by recrystallization two
12 times from petroleum ether/CH₂Cl₂ afforded **12** as a white solid (128 mg, 72%), mp: 270-271 °C; ¹H
13 NMR (500 MHz, DMSO-*d*₆) δ = 7.37 (dt, *J* = 0.95 / 8.36 Hz, 1H, Ph), 7.44 (d, *J* = 8.19 Hz, 1H, Ph),
14 7.49 (dd, *J* = 1.89 / 9.14 Hz, 1H, Ph), 7.52 (s, 1H, Ph), 7.52–7.56 (m, 1H, Ph), 8.06 (s, 1H, Ph), 8.23 (s,
15 1H, Ind.-Het.), 10.72 (s, 1H, -NHCO-), 13.0 (s, 1H, NH); ¹³C NMR (125 MHz, DMSO-*d*₆) δ = 110.5 (d,
16 *J* = 6.24 Hz), 114.9 (d *J* = 21.7 Hz), 120.4, 122.8, 125.7 (d, *J* = 2.99 Hz), 126.2, 126.4, 131.3 (d, *J* =
17 5.99 Hz), 131.6, 131.7 (d, *J* = 8.98 Hz), 133.7, 157.9, 159.9, 160.0; LC/ESI-MS (*m/z*): negative mode
18 288 [M-H]⁻, positive mode 290 [M+H]⁺.
19
20

21 *2,3-Dichloro-N-(1H-indazol-5-yl)benzamide (13)*. The compound was prepared following Method 1.
22 Purification by silica gel chromatography (CH₂Cl₂/MeOH, 9:1 v/v) following by recrystallization two
23 times from petroleum ether/CH₂Cl₂ afforded **13** as a white solid (127 mg, 73%), mp: 265-266 °C; ¹H
24 NMR (500 MHz, DMSO-*d*₆) δ = 7.49 (t, *J* = 7.88 Hz, 1H, Ph), 7.52 (s, 2H, Ph), 7.58 (dd, *J* = 1.57 / 7.56
25 Hz, 1H, Ph), 7.75 (dd, *J* = 1.27 / 7.89 Hz, 1H, Ph), 8.06 (s, 1H, Ph), 8.23 (s, 1H, Ind.-Het.), 10.55 (s, 1H,
26 -NHCO-), 13.0 (s, 1H, NH); ¹³C NMR (125 MHz, DMSO-*d*₆) δ = 110.4, 110.5, 120.6, 122.8, 127.5,
27 128.3, 128.8, 131.3, 131.8, 132.2, 133.7, 137.3, 139.6, 164.1; LC/ESI-MS (*m/z*): negative mode 304 [M-
28 H]⁻, positive mode 306 [M+H]⁺.
29
30

31 *3,4-Dichloro-N-(1H-indazol-5-yl)benzamide (14)*. The compound was prepared following Method 1.
32 Purification by silica gel chromatography (CH₂Cl₂/MeOH, 9:1 v/v) following by recrystallization two
33
34
35
36
37
38
39
40
41
42
43
44
45
46
47
48
49
50
51
52
53
54
55
56
57
58
59
60

times from petroleum ether/CH₂Cl₂ afforded **14** as a white solid (101 mg, 41%), mp: 277-278 °C; ¹H NMR (500 MHz, DMSO-*d*₆) δ = 7.52 (d, *J* = 8.83 Hz, 1H, Ph), 7.61 (dd, *J* = 1.9 / 8.83 Hz, 1H, Ph), 7.81 (d, *J* = 8.51 Hz, 1H, Ph), 7.96 (dd, *J* = 1.89 / 8.2 Hz, 1H, Ph), 8.06 (s, 1H, Ph), 8.22 (d, *J* = 1.27 Hz, 1H, Ind.-Het.), 8.24 (d, *J* = 2.21 Hz, 1H, Ph), 10.38 (s, 1H, -NHCO-), 13.0 (s, 1H, NH); ¹³C NMR (125 MHz, DMSO-*d*₆) δ = 110.2, 111.6, 121.5, 122.8, 128.1, 129.7, 130.9, 131.4, 131.7, 133.7, 134.3, 135.5, 137.4, 163.1; LC/ESI-MS (*m/z*): negative mode 304 [M-H]⁻, positive mode 306 [M+H]⁺.

N-(3,4-Dichlorophenyl)-1*H*-indazole-5-carboxamide (**15**). The compound was prepared following Method 2. Purification by silica gel chromatography (CH₂Cl₂/MeOH, 9:1 v/v) following by recrystallization two times from petroleum ether/CH₂Cl₂ afforded **15** as a white crystalline solid (336 mg, 76%), mp: 271-272 °C; ¹H NMR (500 MHz, DMSO-*d*₆) δ = 7.60 (d, *J* = 8.83 Hz, 1H, Ph), 7.65 (d, *J* = 8.83 Hz, 1H, Ph), 7.78 (dd, *J* = 2.52 / 8.83 Hz, 1H, Ph), 7.94 (dd, *J* = 1.58 / 8.83 Hz, 1H, Ph), 8.18 (d, *J* = 2.52 Hz, 1H), 8.28 (s, 1H, Ind.-Het.), 8.48 (s, 1H, Ph), 10.49 (s, 1H, -CONH-), 13.35 (s, 1H, NH); ¹³C NMR (125 MHz, DMSO-*d*₆) δ = 110.2, 120.3, 121.5, 121.6, 122.5, 125.0, 125.7, 126.8, 130.7, 131.0, 135.2, 139.8, 141.3, 166.2; LC/ESI-MS (*m/z*): negative mode 304 [M-H]⁻, positive mode 306 [M+H]⁺.

2-(3,4-dichlorophenyl)-*N*-(1*H*-indazol-5-yl)acetamide (**16**). The compound was prepared following Method 2. Purification by silica gel chromatography (CH₂Cl₂/MeOH, 9:1 v/v) following by recrystallization three times from petroleum ether/ CH₂Cl₂ afforded **16** as a white solid (145 mg, 56%), mp: 274-275 °C; ¹H NMR (500 MHz, DMSO-*d*₆) δ = 3.69 (s, 2H, CH₂), 7.33 (dd, *J* = 1.89 / 8.19 Hz, 1H, Ph), 7.41 (dd, *J* = 1.58 / 8.83 Hz, 1H, Ph), 7.47 (d, *J* = 8.83 Hz, 1H, Ph), 7.58 (d, *J* = 8.20 Hz, 1H, Ph), 7.61 (d, *J* = 1.89 Hz, 1H, Ph), 7.99 (s, 1H, Ph), 8.08 (d, *J* = 1.26 Hz, 1H, Ind.-Het.), 10.15 (s, 1H, -NHCO-), 12.94 (s, 1H, NH); ¹³C NMR (125 MHz, DMSO-*d*₆) δ = 42.1, 110.0, 110.3, 120.4, 122.8, 129.4, 129.8, 130.5, 130.8, 131.4, 132.1, 133.5, 137.1, 137.4, 168.1; LC/ESI-MS (*m/z*): negative mode 318 [M-H]⁻, positive mode 320 [M+H]⁺.

N-Phenyl-1*H*-indazole-5-carboxamide (**26**). The compound was prepared following Method 2. Purification by silica gel chromatography (CH₂Cl₂/MeOH, 9:1 v/v) following by recrystallization two

times from petroleum ether/CH₂Cl₂ afforded **26** as a white crystalline solid (180 mg, 76%), mp: 285-286 °C; ¹H NMR (500 MHz, DMSO-*d*₆) δ = 7.08 (dt, *J* = 0.94 / 7.57 Hz, 1H, Ph), 7.33 (t, *J* = 6.3 Hz, 1H, Ph), 7.34 (t, *J* = 7.25 Hz, 1H, Ph), 7.63 (d, *J* = 8.83 Hz, 1H, Ph), 7.74 (dt, *J* = 1.53 / 7.57 Hz, 1H, Ph), (dd, *J* = 1.26 / 8.83 Hz, 1H, Ph), 7.95 (dd, *J* = 1.58 / 8.83 Hz, 1H, Ph), 8.25 (s, 1H, Ind.-Het.), 8.52 (s, 1H, Ph), 10.22 (s, 1H, -CONH-), 13.30 (s, 1H, NH); ¹³C NMR (125 MHz, DMSO-*d*₆) δ = 110.1, 120.4 (2C), 121.3, 122.4, 123.5, 125.8, 127.5, 128.7 (2C), 135.1, 139.6, 141.2, 165.9; LC/ESI-MS (*m/z*): negative mode 236 [M-H]⁻, positive mode 238 [M+H]⁺.

N-(3,5-Dichlorophenyl)-1*H*-indazole-5-carboxamide (**27**). The compound was prepared following Method 2. Purification by silica gel chromatography (CH₂Cl₂/MeOH, 9:1 v/v) following by recrystallization four times from petroleum ether/CH₂Cl₂ afforded **27** as a white solid (190 mg, 62%), mp: 303-305 °C; ¹H NMR (500 MHz, DMSO-*d*₆) δ = 7.30 (t, *J* = 1.89 Hz, 1H, Ph), 7.65 (d, *J* = 8.51 Hz, 1H, Ph), 7.51 (d, *J* = 2.52 Hz, 1H, Ph), 7.91 (dd, *J* = 1.57 / 3.15 Hz, 1H, Ph), 7.92 (d, *J* = 1.89 Hz, 1H, Ph), 8.28 (d, *J* = 0.63 Hz, 1H, Ind.-Het.), 8.48 (dd, *J* = 0.63 / 1.58 Hz, 1H, Ph), 10.51 (s, 1H, -CONH-), 13.35 (s, 1H, NH); ¹³C NMR (125 MHz, DMSO-*d*₆) δ = 110.1, 110.3, 118.3 (2C), 121.7, 122.4, 122.7, 125.7, 126.6, 126.7, 134.1, 142.0, 145.2, 166.4; LC/ESI-MS (*m/z*): negative mode 304 [M-H]⁻, positive mode 306 [M+H]⁺.

N-(3-Chloro-4-fluorophenyl)-1*H*-indazole-5-carboxamide (**28**). The compound was prepared following Method 2. Purification by silica gel chromatography (CH₂Cl₂/MeOH, 9:1 v/v) following by recrystallization two times from petroleum ether/CH₂Cl₂ afforded **28** as a white solid (190 mg, 66%), mp: 240-241 °C; ¹H NMR (500 MHz, DMSO-*d*₆) δ = 7.40 (t, *J* = 9.15 Hz, 1H, Ph), 7.64 (d, *J* = 8.82 Hz, 1H, Ph), 7.71-7.77 (m, 1H, Ph), 7.93 (dd, *J* = 1.27 / 8.83 Hz, 1H, Ph), 8.11 (dd, *J* = 2.53 / 6.94 Hz, 1H, Ph), 8.26 (s, 1H, Ind.-Het.), 8.47 (s, 1H, Ph), 10.41 (s, 1H, -CONH-), 13.33 (s, 1H, NH); ¹³C NMR (125 MHz, DMSO-*d*₆) δ = 110.2, 116.9 (d, *J* = 21.7 Hz), 119.1 (d, *J* = 18.2 Hz), 120.6 (d, *J* = 6.73 Hz), 121.5, 121.8, 122.5, 125.7, 126.9, 135.1, 136.9 (d, *J* = 2.99 Hz), 141.3, 153.4 (d, *J* = 242.84 Hz), 166.1; LC/ESI-MS (*m/z*): negative mode 288 [M-H]⁻, positive mode 290 [M+H]⁺.

N-(4-Chloro-3-fluorophenyl)-1*H*-indazole-5-carboxamide (**29**). The compound was prepared following Method 2. Purification by silica gel chromatography (CH₂Cl₂/MeOH, 9:1 v/v) following by recrystallization two times from PE/CH₂Cl₂ afforded **29** as a white solid (95 mg, 33%), mp: 247-248 °C; ¹H NMR (500 MHz, DMSO-*d*₆) δ = 7.54 (t, *J* = 8.52 Hz, 1H, Ph), 7.63 (dd, *J* = 1.57 / 8.82 Hz, 1H, Ph), 7.65 (d, *J* = 8.82 Hz, 1H, Ph), 7.93 (dd, *J* = 1.58 / 8.51 Hz, 1H, Ph), 7.97 (dd, *J* = 2.21 / 11.98 Hz, 1H, Ph), 8.27 (s, 1H, Ind.-Het.), 8.47 (s, 1H, Ph), 10.52 (s, 1H, -CONH-), 13.34 (s, 1H, NH); ¹³C NMR (125 MHz, DMSO-*d*₆) δ = 108.3 (d, *J* = 25.7 Hz), 110.3, 113.1 (d, *J* = 17.95 Hz), 117.1 (d, *J* = 2.99 Hz), 120.5, 121.6, 122.4, 125.7, 126.8, 130.5, 135.2, 140.2 (d, *J* = 10.22 Hz), 157.0 (d, *J* = 243.35 Hz), 166.3; LC/ESI-MS (*m/z*): negative mode 288 [M-H]⁻, positive mode 290 [M+H]⁺.

N-(3,4-Difluorophenyl)-1*H*-indazole-5-carboxamide (**30**). The compound was prepared following Method 2. Purification by silica gel chromatography (CH₂Cl₂/MeOH, 9:1 v/v) following by recrystallization two times from petroleum ether/CH₂Cl₂ afforded **30** as a white solid (163 mg, 60%), mp: 239-240 °C; ¹H NMR (500 MHz, DMSO-*d*₆) δ = 7.41 (q, *J* = 9.14 Hz, 1H, Ph), 7.54–7.59 (m, 1H, Ph), 7.64 (d, *J* = 8.45 Hz, 1H, Ph), 7.93 (dd, *J* = 1.26 / 8.51 Hz, 1H, Ph), 7.96 (ddd, *J* = 2.52 / 7.57 / 13.24 Hz, 1H), 8.27 (s, 1H, Ind.-Het.), 8.47 (d, *J* = 0.63 Hz, 1H, Ph), 10.42 (s, 1H, -CONH-), 13.33 (s, 1H, NH); ¹³C NMR (125 MHz, DMSO-*d*₆) δ = 109.3 (d, *J* = 21.7 Hz), 110.2, 116.6 (q, *J* = 3.24 Hz), 117.4 (d, *J* = 17.7 Hz), 121.5, 122.5, 125.7, 126.9, 135.1, 136.7 (dd, *J* = 2.74 / 9.22 Hz), 141.2, 145.5 (dd, *J* = 12.71 / 241.59 Hz), 149.0 (dd, *J* = 13.22 / 242.85 Hz), 166.1; LC/ESI-MS (*m/z*): negative mode 272 [M-H]⁻, positive mode 274 [M+H]⁺.

N-(3,4-Dimethoxyphenyl)-1*H*-indazole-5-carboxamide (**31**). The compound was prepared following Method 2. Purification by silica gel chromatography (CH₂Cl₂/MeOH, 9:1 v/v) following by recrystallization three times from petroleum ether/CH₂Cl₂ afforded **31** as a brownish solid (183 mg, 61%), mp: 258-262 °C; ¹H NMR (500 MHz, DMSO-*d*₆) δ = 3.74 (s, 3H, OMe), 3.76 (s, 3H, OMe), 6.93 (d, *J* = 8.83 Hz, 1H, Ph), 7.36 (dd, *J* = 2.53 / 8.83 Hz, 1H, Ph), 7.51 (d, *J* = 2.52 Hz, 1H, Ph), 7.63 (td, *J* = 0.94 / 8.83 Hz, 1H, Ph), 7.94 (dd, *J* = 1.58 / 8.83 Hz, 1H, Ph), 8.24 (d, *J* = 0.63 Hz, 1H, Ind.-Het.), 8.46 (dd, *J* = 0.63 / 1.58 Hz, 1H, Ph), 10.1 (s, 1H, -CONH-), 13.35 (s, 1H, NH); ¹³C NMR (125 MHz,

1 DMSO- d_6) δ = 55.6 (OMe), 55.9 (OMe), 105.8, 110.0, 112.2, 112.4, 121.1, 122.5, 125.7, 127.6, 133.2,
2
3 135.0, 141.1, 145.2, 148.6, 165.5; LC/ESI-MS (m/z): negative mode 296 [M-H]⁻, positive mode 298
4
5 [M+H]⁺.
6

7 *N*-(3-Chloro-4-methoxyphenyl)-1*H*-indazole-5-carboxamide (**32**). The compound was prepared following
8
9 Method 1. Repeated purification by silica gel chromatography (CH₂Cl₂/MeOH, 9:1 v/v) following by
10
11 recrystallization three times from petroleum ether/CH₂Cl₂ afforded **32** as a white solid (33 mg, 11%),
12
13 mp: 276-278 °C; ¹H NMR (500 MHz, DMSO- d_6) δ = 3.84 (s, 3H, 4-MeO), 7.15 (d, J = 9.15 Hz, 1H,
14
15 Ph), 7.65 (d, J = 8.83 Hz, 1H, Ph), 7.68 (dd, J = 2.53 / 8.83 Hz, 1H, Ph), 7.94 (dd, J = 1.57 / 8.83 Hz,
16
17 1H, Ph), 7.97 (d, J = 2.52 Hz, 1H, Ph), 8.24 (s, 1H, Ind.-Het.), 8.48 (s, 1H, Ph), 10.25 (s, 1H, -CONH-),
18
19 13.34 (s, 1H, NH); ¹³C NMR (125 MHz, DMSO- d_6) δ = 56.3 (OMe), 110.1, 113.0, 120.2, 120.6, 121.3,
20
21 122.0, 122.5, 125.7, 127.2, 133.3, 135.1, 141.2, 150.8, 165.7; LC/ESI-MS (m/z): negative mode 300 [M-
22
23 H]⁻, positive mode 302 [M+H]⁺.
24
25
26
27

28 *N*-(3-Chloro-4-hydroxyphenyl)-1*H*-indazole-5-carboxamide (**33**). The compound was prepared following
29
30 Method 2. Purification by silica gel chromatography (CH₂Cl₂/MeOH, 9:1 v/v) following by
31
32 recrystallization three times from petroleum ether/CH₂Cl₂ afforded **33** as a yellowish solid (169 mg,
33
34 59%), mp: 272-274 °C; ¹H NMR (500 MHz, DMSO- d_6) δ = 6.94 (d, J = 8.82 Hz, 1H, Ph), 7.50 (dd, J =
35
36 2.53 / 8.83 Hz, 1H, Ph), 7.62 (d, J = 0.95 / 8.82 Hz, 1H, Ph), 7.85 (d, J = 2.53 Hz, 1H, Ph), 7.92 (dd, J
37
38 = 1.57 / 8.82 Hz, 1H, Ph), 8.24 (s, 1H, Ind.-Het.), 8.43 (dd, J = 0.95 / 1.58 Hz, 1H, Ph), 9.92 (bs, 1H,
39
40 OH), 10.12 (s, 1H, -CONH-), 13.29 (s, 1H, NH); ¹³C NMR (125 MHz, DMSO- d_6) δ = 110.1, 116.5,
41
42 119.1, 120.6, 121.2, 122.0, 122.5, 125.7, 127.3, 132.0, 135.0, 141.1, 149.3, 165.6; LC/ESI-MS (m/z):
43
44 negative mode 286 [M-H]⁻, positive mode 288 [M+H]⁺.
45
46
47
48
49

50 *N*-(4-Chloro-3-methoxyphenyl)-1*H*-indazole-5-carboxamide (**34**). The compound was prepared following
51
52 Method 1. Repeated purification by silica gel chromatography (CH₂Cl₂/MeOH, 9:1 v/v) following by
53
54 recrystallization three times from petroleum ether/CH₂Cl₂ afforded **34** as a white solid (34 mg, 11%),
55
56 mp: 280-282 °C; ¹H NMR (500 MHz, DMSO- d_6) δ = 3.85 (s, 3H, 4-MeO), 7.36 (d, J = 8.82 Hz, 1H,
57
58 Ph), 7.46 (dd, J = 2.53 / 8.83 Hz, 1H, Ph), 7.64 (d, J = 8.51 Hz, 1H, Ph), 7.71 (dd, J = 2.21 Hz, 1H, Ph),
59
60

7.94 (dd, $J = 1.57 / 8.82$ Hz, 1H, Ph), 8.27 (s, 1H, Ind.-Het.), 8.47 (d, $J = 0.63$ Hz, 1H, Ph), 10.32 (s, 1H, -CONH-), 13.32 (s, 1H, NH); ^{13}C NMR (125 MHz, DMSO- d_6) $\delta = 56.0$ (OMe), 105.0, 110.1, 113.0, 115.2, 121.4, 122.5, 125.7, 127.2, 129.7, 135.1, 139.8, 141.2, 154.5, 166.0; LC/ESI-MS (m/z): negative mode 300 $[\text{M}-\text{H}]^-$, positive mode 302 $[\text{M}+\text{H}]^+$.

N-(4-Chloro-3-hydroxyphenyl)-1H-indazole-5-carboxamide (**35**). The compound was prepared following Method 2. Purification by silica gel chromatography ($\text{CH}_2\text{Cl}_2/\text{MeOH}$, 9:1 v/v) following by recrystallization three times from petroleum ether/ CH_2Cl_2 afforded **35** as a brownish solid (151 mg, 53%), mp: 307-308 °C; ^1H NMR (500 MHz, DMSO- d_6) $\delta = 7.19$ (dd, $J = 2.52 / 8.83$ Hz, 1H, Ph), 7.25 (d, $J = 8.51$ Hz, 1H, Ph), 7.62 (td, $J = 0.95 / 8.82$ Hz, 1H, Ph), 7.68 (d, $J = 2.21$ Hz, 1H, Ph), 7.92 (dd, $J = 1.89 / 8.83$ Hz, 1H, Ph), 8.25 (s, 1H, Ind.-Het.), 8.45 (dd, $J = 0.95 / 1.58$ Hz, 1H, Ph), 10.16 (bs, 1H, OH), 10.22 (s, 1H, -CONH), 13.32 (s, 1H, NH); ^{13}C NMR (125 MHz, DMSO- d_6) $\delta = 108.6$, 110.1, 112.2, 114.1, 121.4, 122.4, 125.8, 127.3, 129.5, 135.1, 139.3, 141.2, 153.1, 166.0; LC/ESI-MS (m/z): negative mode 286 $[\text{M}-\text{H}]^-$, positive mode 288 $[\text{M}+\text{H}]^+$.

N-(5,6-Dichloropyridin-3-yl)-1H-indazole-5-carboxamide (**36**). The compound was prepared following Method 2. Purification by silica gel chromatography ($\text{CH}_2\text{Cl}_2/\text{MeOH}$, 9:1 v/v) following by recrystallization three times from petroleum ether/ CH_2Cl_2 afforded **36** as a brownish solid (112 mg, 53%), mp: >290 °C (dec.); ^1H NMR (500 MHz, DMSO- d_6) $\delta = 7.67$ (d, $J = 8.82$ Hz, 1H, Ph), 8.05 (d, $J = 8.51$ Hz, 1H, Ph), 8.21 (s, 1H, Ind.-Het.), 8.34 (s, 1H, Pyr.), 8.44 (s, 1H, Ph), 8.74 (s, 1H, Pyr), 12.8 (s, 1H, -CONH-), 13.55 (s, 1H, NH); ^{13}C NMR (125 MHz, DMSO- d_6) $\delta = 110.1$, 111.1, 120.5, 123.0, 123.2, 123.9, 126.3, 126.7, 127.1, 135.3, 136.1, 141.4, 163.1; LC/ESI-MS (m/z): negative mode 305 $[\text{M}-\text{H}]^-$, positive mode 307 $[\text{M}+\text{H}]^+$.

N-(3,4-Dichlorobenzyl)-1H-indazole-5-carboxamide (**37**). The compound was prepared following Method 2. Purification by silica gel chromatography ($\text{CH}_2\text{Cl}_2/\text{MeOH}$, 9:1 v/v) following by recrystallization three times from petroleum ether/ CH_2Cl_2 afforded **37** as a brownish solid (196 mg, 61%), mp: 205-206 °C; ^1H NMR (500 MHz, DMSO- d_6) $\delta = 4.48$ (d, $J = 5.99$ Hz, 2H, CH_2), 7.33 (dd, $J = 1.89 / 8.20$ Hz, 1H, Ph), 7.57 (s, 1H, Ph), 7.59 (s, 1H, Ph), 7.88 (dd, $J = 1.26 / 8.82$ Hz, 1H, Ph), 8.20

(s, 1H, Ind.-Het.), 8.38 (s, 1H, Ph), 9.06 (t, $J = 5.99$ Hz, 1H, -CONH-), 13.26 (s, 1H, NH); ^{13}C NMR (125 MHz, DMSO- d_6) $\delta = 41.9, 109.9, 120.8, 122.5, 125.4, 126.6, 127.8, 129.3, 129.4, 130.6, 130.9, 135.0, 141.1, 141.3, 166.8$; LC/ESI-MS (m/z): negative mode 318 $[\text{M-H}]^-$, positive mode 320 $[\text{M+H}]^+$.

N-(3,4-Dichlorophenyl)-1H-indazole-6-carboxamide (**40**). The compound was prepared following Method 2. Purification by silica gel chromatography ($\text{CH}_2\text{Cl}_2/\text{MeOH}$, 9:1 v/v) following by recrystallization two times from petroleum ether/ CH_2Cl_2 afforded **40** as a white crystalline solid (161 mg, 52%), mp: 272-274 °C; ^1H NMR (500 MHz, DMSO- d_6) $\delta = 7.62$ (d, $J = 8.83$ Hz, 1H, Ph), 7.67 (dd, $J = 1.26 / 8.51$ Hz, 1H, Ph), 7.79 (dd, $J = 2.52 / 8.83$ Hz, 1H, Ph), 7.90 (dd, $J = 0.94 / 8.51$ Hz, 1H, Ph), 8.16 (s, 1H, Ind.-Het.), 8.18 (s, 1H, Ph), 8.19 (s, 1H, Ph), 10.59 (s, 1H, -CONH-), 13.44 (s, 1H, NH); ^{13}C NMR (125 MHz, DMSO- d_6) $\delta = 110.4, 119.7, 120.4, 120.8, 121.6, 124.8, 125.2, 130.7, 131.0, 132.1, 133.8, 139.3, 139.6, 166.3$; LC/ESI-MS (m/z): negative mode 304 $[\text{M-H}]^-$, positive mode 306 $[\text{M+H}]^+$.

N-(3,5-Dichlorophenyl)-1H-indazole-6-carboxamide (**41**). The compound was prepared following Method 2. Purification by silica gel chromatography ($\text{CH}_2\text{Cl}_2/\text{MeOH}$, 9:1 v/v) following by recrystallization two times from petroleum ether/ CH_2Cl_2 afforded **41** as grey crystals (173 mg, 57%), mp: 277-279 °C; ^1H NMR (500 MHz, DMSO- d_6) $\delta = 7.32$ (t, $J = 1.89$ Hz, 1H, Ph), 7.66 (dd, $J = 1.26 / 8.51$ Hz, 1H, Ph), 7.90 (d, $J = 0.63 / 8.19$ Hz, 1H, Ph), 7.92 (s, 1H, Ph), 7.93 (s, 1H, Ph), 8.16 (s, 1H, Ind.-Het.), 8.19 (s, 1H, Ph), 10.61 (s, 1H, -CONH-), 13.46 (s, 1H, NH); ^{13}C NMR (125 MHz, DMSO- d_6) $\delta = 110.4, 118.5$ (2C), 119.7, 120.8, 122.9, 124.8, 131.9, 133.8, 134.1 (2C), 139.3, 141.8, 166.5; LC/ESI-MS (m/z): negative mode 304 $[\text{M-H}]^-$, positive mode 306 $[\text{M+H}]^+$.

N-(3-Chloro-4-fluorophenyl)-1H-indazole-6-carboxamide (**42**). The compound was prepared following Method 2. Purification by silica gel chromatography ($\text{CH}_2\text{Cl}_2/\text{MeOH}$, 9:1 v/v) following by recrystallization two times from petroleum ether/ CH_2Cl_2 afforded **42** as an ecru solid (205 mg, 71%), mp: 257-259 °C; ^1H NMR (500 MHz, DMSO- d_6) $\delta = 7.42$ (t, $J = 9.14$ Hz, 1H, Ph), 7.68 (d, $J = 8.51$ Hz, 1H, Ph), 7.73–7.78 (m, 1H, Ph), 7.89 (d, $J = 8.51$ Hz, 1H, Ph), 8.10 (dd, $J = 2.53 / 6.62$ Hz, 1H, Ph), 8.16 (s, 1H, Ind.-Het.), 8.19 (s, 1H, Ph), 10.52 (s, 1H, -CONH-), 13.44 (s, 1H, NH); ^{13}C NMR (125

1 MHz, DMSO- d_6) δ = 109.5, 116.2 (d, J = 21.69 Hz), 118.4 (d, J = 18.2 Hz), 118.9, 120.0, 120.03 (d, J =
2 6.98 Hz), 121.2, 124.0, 131.5, 133.1, 135.9 (d, J = 2.99 Hz), 138.6, 152.7 (d, J = 243.09 Hz), 165.4;
3
4 LC/ESI-MS (m/z): negative mode 288 [M-H]⁻, positive mode 290 [M+H]⁺.
5
6

7 *N*-(4-Chloro-3-fluorophenyl)-1*H*-indazole-6-carboxamide (**43**). The compound was prepared following
8
9 Method 2. Purification by silica gel chromatography (CH₂Cl₂/MeOH, 9:1 v/v) following by
10
11 recrystallization two times from petroleum ether/CH₂Cl₂ afforded **43** as a white solid (64 mg, 22%), mp:
12
13 281-282 °C; ¹H NMR (500 MHz, DMSO- d_6) δ = 7.56 (t, J = 8.51 Hz, 1H, Ph), 7.63 (dd, J = 1.89 / 9.14
14
15 Hz, 1H, Ph), 7.67 (dd, J = 1.26 / 8.51 Hz, 1H, Ph), 7.89 (d, J = 8.51 Hz, 1H, Ph), 7.97 (dd, J = 2.21 /
16
17 11.98 Hz, 1H, Ph), 8.16 (s, 1H, Ind.-Het.), 8.19 (s, 1H, Ph), 10.62 (s, 1H, -CONH-), 13.45 (s, 1H, NH);
18
19 ¹³C NMR (125 MHz, DMSO- d_6) δ = 108.4 (d, J = 25.7 Hz), 110.4, 113.4 (d, J = 17.7 Hz), 117.3 (d, J =
20
21 2.99 Hz), 119.7, 120.8, 124.8, 130.5, 132.2, 133.8, 139.3, 140.0 (d, J = 10.22 Hz), 157.0 (d, J = 243.59
22
23 Hz), 166.4; LC/ESI-MS (m/z): negative mode 288 [M-H]⁻, positive mode 290 [M+H]⁺.
24
25
26
27

28 *N*-(3,4-Difluorophenyl)-1*H*-indazole-6-carboxamide (**44**). The compound was prepared following
29
30 Method 2. Purification by silica gel chromatography (CH₂Cl₂/MeOH, 9:1 v/v) following by
31
32 recrystallization two times from petroleum ether/CH₂Cl₂ afforded **44** as a white solid (186 mg, 68%),
33
34 mp: 264-266 °C; ¹H NMR (500 MHz, DMSO- d_6) δ = 7.43 (q, J = 9.14 Hz, 1H, Ph), 7.56–7.60 (m, 1H,
35
36 Ph), 7.66 (dd, J = 0.95 / 8.20 Hz, 1H, Ph), 7.89 (dd, J = 8.19 Hz, 1H, Ph), 7.96 (ddd, J = 2.52 / 7.57 /
37
38 13.24 Hz, 1H, Ph), 8.15 (s, 1H, Ind.-Het.), 8.18 (s, 1H, Ph), 10.54 (s, 1H, -CONH-), 13.43 (s, 1H, NH);
39
40 ¹³C NMR (125 MHz, DMSO- d_6) δ = 109.4 (d, J = 21.44 Hz), 110.3, 116.8 (q, J = 3.24 Hz), 117.4 (d, J
41
42 = 17.7 Hz), 119.7, 120.7, 124.7, 132.3, 133.8, 136.5 (dd, J = 2.49 / 8.98 Hz), 139.4, 145.6 (dd, J = 12.72
43
44 / 242.1 Hz), 149.0 (dd, J = 13.22 / 242.85 Hz), 166.2; LC/ESI-MS (m/z): negative mode 272 [M-H]⁻,
45
46
47
48 positive mode 274 [M+H]⁺.
49
50
51

52 *N*-(3,4-Dimethoxyphenyl)-1*H*-indazole-6-carboxamide (**45**). The compound was prepared following
53
54 Method 2. Purification by silica gel chromatography (CH₂Cl₂/MeOH, 9:1 v/v) following by
55
56 recrystallization three times from petroleum ether/CH₂Cl₂ afforded **45** as a grey solid (174 mg, 59%),
57
58 mp: 204-206 °C; ¹H NMR (500 MHz, DMSO- d_6) δ = 3.74 (s, 3H, OMe), 3.76 (s, 3H, OMe), 6.94 (d, J
59
60

1
2
3
4
5
6
7
8
9
10
11
12
13
14
15
16
17
18
19
20
21
22
23
24
25
26
27
28
29
30
31
32
33
34
35
36
37
38
39
40
41
42
43
44
45
46
47
48
49
50
51
52
53
54
55
56
57
58
59
60

= 8.51 Hz, 1H, Ph), 7.35 (dd, $J = 2.52 / 8.83$ Hz, 1H, Ph), 7.50 (d, $J = 2.52$ Hz, 1H, Ph), 7.67 (dd, $J = 1.26 / 8.51$ Hz, 1H, Ph), 7.87 (dd, $J = 0.63 / 8.51$ Hz, 1H, Ph), 8.14 (s, 1H, Ind.-Het.), 8.17 (s, 1H, Ph), 10.19 (s, 1H, -CONH-), 13.36 (s, 1H, NH); ^{13}C NMR (125 MHz, DMSO- d_6) $\delta = 55.6$ (OMe), 55.9 (OMe), 105.8, 110.0, 112.2, 112.6, 119.7, 120.5, 124.5, 132.9, 133.0, 133.7, 139.5, 145.3, 148.6, 165.6; LC/ESI-MS (m/z): negative mode 296 [M-H] $^-$, positive mode 298 [M+H] $^+$.

N-(3-Chloro-4-methoxyphenyl)-1*H*-indazole-6-carboxamide (**46**). The compound was prepared following Method 2. Repeated purification by silica gel chromatography (CH₂Cl₂/MeOH, 9:1 v/v) following by recrystallization three times from petroleum ether/CH₂Cl₂ afforded **46** as a white solid (144 mg, 48%), mp: 160-161 °C; ^1H NMR (500 MHz, DMSO- d_6) $\delta = 3.84$ (s, 3H, 4-MeO), 7.15 (d, $J = 9.14$ Hz, 1H, Ph), 7.67 (dd, $J = 1.26 / 8.51$ Hz, 1H, Ph), 7.70 (dd, $J = 2.52 / 9.14$ Hz, 1H, Ph), 7.87 (dd, $J = 0.94 / 8.51$ Hz, 1H, Ph), 7.96 (d, $J = 2.52$ Hz, 1H, Ph), 8.15 (s, 1H, Ind.-Het.), 8.17 (s, 1H, Ph), 10.33 (s, 1H, -CONH-), 13.41 (s, 1H, NH); ^{13}C NMR (125 MHz, DMSO- d_6) $\delta = 56.4$ (OMe), 110.1, 113.0, 116.5, 119.7, 120.4, 120.6, 122.1, 124.6, 132.5, 133.1, 133.8, 139.4, 150.9, 165.8; LC/ESI-MS (m/z): negative mode 300 [M-H] $^-$, positive mode 302 [M+H] $^+$.

N-(3-Chloro-4-hydroxyphenyl)-1*H*-indazole-6-carboxamide (**47**). The compound was prepared following Method 2. Purification by silica gel chromatography (CH₂Cl₂/MeOH, 9:1 v/v) following by recrystallization three times from petroleum ether/CH₂Cl₂ afforded **47** as a brownish solid (160 mg, 54%), mp: 263-265 °C; ^1H NMR (500 MHz, DMSO- d_6) $\delta = 6.95$ (d, $J = 8.51$ Hz, 1H, Ph), 7.52 (dd, $J = 2.52 / 8.51$ Hz, 1H, Ph), 7.65 (dd, $J = 1.26 / 8.51$ Hz, 1H, Ph), 7.85 (s, 1H, Ph), 7.86 (dd, $J = 1.26 / 8.51$ Hz, 1H, Ph), 8.13 (s, 1H, Ph), 8.16 (s, 1H, Ind.-Het.), 9.93 (bs, 1H, OH), 10.23 (s, 1H, -CONH-), 13.39 (s, 1H, NH); ^{13}C NMR (125 MHz, DMSO- d_6) $\delta = 110.1, 116.5, 119.2, 119.7, 120.6, 120.7, 122.1, 124.5, 131.8, 132.7, 133.7, 139.4, 149.4, 165.6$; LC/ESI-MS (m/z): negative mode 286 [M-H] $^-$, positive mode 288 [M+H] $^+$.

N-(4-Chloro-3-methoxyphenyl)-1*H*-indazole-6-carboxamide (**48**). The compound was prepared following Method 2. Repeated purification by silica gel chromatography (CH₂Cl₂/MeOH, 9:1 v/v) following by recrystallization three times from petroleum ether/CH₂Cl₂ afforded **48** as a white solid (203 mg, 71%),

mp: 156-157 °C; ¹H NMR (500 MHz, DMSO-*d*₆) δ = 3.86 (s, 3H, 3-MeO), 7.38 (d, *J* = 8.83 Hz, 1H, Ph), 7.45 (dd, *J* = 2.20 / 8.51 Hz, 1H, Ph), 7.68 (dd, *J* = 1.26 / 8.51 Hz, 1H, Ph), 7.72 (d, *J* = 2.21 Hz, 1H), 7.89 (dd, *J* = 0.63 / 8.52 Hz, 1H, Ph), 8.16 (s, 1H), 8.18 (s, 1H, Ph), 10.44 (s, 1H, -CONH-), 13.42 (s, 1H, NH); ¹³C NMR (125 MHz, DMSO-*d*₆) δ = 56.0 (OMe), 105.1, 110.2, 113.1, 115.4, 119.7, 120.7, 124.7, 129.7, 132.5, 133.8, 139.4, 139.6, 154.5, 166.1; LC/ESI-MS (*m/z*): negative mode 300 [M-H]⁻, positive mode 302 [M+H]⁺.

N-(4-Chloro-3-hydroxyphenyl)-1*H*-indazole-6-carboxamide (**49**). The compound was prepared following Method 2. Purification by silica gel chromatography (CH₂Cl₂/MeOH, 9:1 v/v) following by recrystallization three times from petroleum ether/CH₂Cl₂ afforded **49** as an ecru solid (150 mg, 52%), mp: 257-258 °C; ¹H NMR (500 MHz, DMSO-*d*₆) δ = 6.95 (d, *J* = 8.51 Hz, 1H, Ph), 7.52 (dd, *J* = 2.52 / 8.51 Hz, 1H, Ph), 7.65 (dd, *J* = 1.26 / 8.51 Hz, 1H, Ph), 7.85 (s, 1H, Ph), 7.86 (dd, *J* = 1.26 / 8.51 Hz, 1H, Ph), 8.13 (s, 1H, Ph), 8.16 (s, 1H, Ind.-Het.), 9.93 (bs, 1H, OH), 10.23 (s, 1H, -CONH-), 13.39 (s, 1H, NH); ¹³C NMR (125 MHz, DMSO-*d*₆) δ = 110.1, 116.5, 119.2, 119.7, 120.6, 120.7, 122.1, 124.5, 131.8, 132.7, 133.7, 139.4, 149.4, 165.6; LC/ESI-MS (*m/z*): negative mode 286 [M-H]⁻, positive mode 288 [M+H]⁺.

N-(3,4-Dichlorophenyl)-1*H*-indole-5-carboxamide (**53**). The compound was prepared following Method 2. Purification by repeated silica gel chromatography (petroleum ether/ethyl acetate, 1:1 v/v) following by recrystallization two times from petroleum ether/CH₂Cl₂ afforded **53** as a white crystalline solid (52 mg, 17%), mp: 234-235 °C; ¹H NMR (500 MHz, DMSO-*d*₆) δ = 6.59 (m, 1H, Indol.-Het.), 7.46 (t, *J* = 3.16 Hz, 1H, Indol.-Het.), 7.49 (d, *J* = 8.51 Hz, 1H, Ph), 7.58 (d, *J* = 8.82 Hz, 1H, Ph), 7.72 (dd, *J* = 1.89 / 8.83 Hz, 1H, Ph), 7.79 (dd, *J* = 2.53 / 8.83 Hz, 1H, Ph), 8.20 (d, *J* = 2.21 Hz, 1H, Ph), 8.26 (d, *J* = 1.89 Hz, 1H, Ph), 10.34 (s, 1H, -CONH-), 11.39 (s, 1H, NH); ¹³C NMR (125 MHz, DMSO-*d*₆) δ = 102.5, 111.3, 120.2, 120.8, 121.1, 121.3, 124.6, 125.2, 127.2, 127.2, 130.6, 130.9, 138.0, 140.1, 167.0; LC/ESI-MS (*m/z*): negative mode 303 [M-H]⁻, positive mode 305 [M+H]⁺.

N-(3,4-Dichlorophenyl)imidazo[1,2-*a*]pyridine-6-carboxamide (**55**). The compound was prepared following Method 2. Purification by repeated silica gel chromatography (CH₂Cl₂/MeOH, 9:1 v/v)

1 following by recrystallization two times from petroleum ether/CH₂Cl₂ afforded **55** as a white solid (93
2 mg, 36%), mp: 268-269 °C; ¹H NMR (500 MHz, DMSO-*d*₆) δ = 7.63 (d, *J* = 8.83 Hz, 1H, Ph), 7.67 (d,
3 *J* = 9.46 Hz, 1H, Het.), 7.69 (d, *J* = 0.95 Hz, 1H), 7.72 (d, *J* = 1.89 / 9.46 Hz, 1H, Het.), 7.73 (dd, *J* =
4 2.21 / 8.52 Hz, 1H, Ph), 8.10 (s, 1H, Het.), 8.13 (d, *J* = 2.52 Hz, 1H, Ph), 9.25 (dd, *J* = 0.94 / 1.89 Hz,
5 1H, Het.), 10.58 (s, 1H, -CONH-); ¹³C NMR (125 MHz, DMSO-*d*₆) δ = 114.6, 116.4, 119.8, 120.4,
6 121.6, 123.1, 125.4, 129.3, 130.8, 131.1, 134.9, 139.2, 144.8, 163.9; LC/ESI-MS (*m/z*): negative mode
7 304 [M-H]⁻, positive mode 306 [M+H]⁺.

8
9
10
11
12
13
14
15
16
17 *N*-(3,4-Dichlorophenyl)-[1,2,4]triazolo[4,3-*a*]pyridine-6-carboxamide (**56**). The compound was
18 prepared following Method 2. Purification by repeated silica gel chromatography (CH₂Cl₂/MeOH, 9:1
19 v/v) following by recrystallization two times from petroleum ether/CH₂Cl₂ afforded **56** as a yellowish
20 solid (111 mg, 36%), mp: 326-327 °C; ¹H NMR (500 MHz, DMSO-*d*₆) δ = 6.63 (d, *J* = 8.83 Hz, 1H,
21 Ph), 7.71 (dd, *J* = 2.20 / 8.83 Hz, 1H, Ph), 7.82 (dd, *J* = 1.26 / 9.45 Hz, 1H, Het.), 7.89 (d, *J* = 9.46 Hz,
22 1H, Het.), 8.10 (d, *J* = 2.20 Hz, 1H, Ph), 9.24 (s, 1H, Het.), 9.42 (s, 1H, Het.), 10.67 (s, 1H, -CONH-);
23 ¹³C NMR (125 MHz, DMSO-*d*₆) δ = 114.8, 120.5, 121.4, 121.7, 125.8, 126.8, 127.6, 130.9, 131.2,
24 137.8, 139.0, 148.5, 163.2; LC/ESI-MS (*m/z*): negative mode 305 [M-H]⁻, positive mode 307 [M+H]⁺.

25
26
27
28
29
30
31
32
33
34
35
36 *General Procedure B for the Preparation of N-Methylated Compounds 38a,b and 54*. To a solution of
37 the respective *N*-(3,4-dichlorophenyl)-1*H*-indazole-5-carboxamide (**15**) or *N*-(3,4-dichlorophenyl)-1*H*-
38 indole-5-carboxamide (**53**) (1.0 equiv.) and potassium carbonate (1.2 equiv.) in DMF (10.0 mL/mmol;
39 extra dry over molecular sieves, 99.8%, Acros) was added methyl iodide (1.3–2.0 equiv.). The mixture
40 was stirred at room temperature until completed conversion could be detected (TLC control:
41 CH₂Cl₂/MeOH, 9:1 v/v), hydrolyzed with water (20 mL/mmol), and acidified with hydrochloric acid
42 (2*N*, 2.0 mL/mmol). The precipitate formed was filtered, washed three times with water (10 mL) and
43 dried at 70 °C. The crude product was purified by column chromatography on silica gel and
44 recrystallized as indicated below.

45
46
47
48
49
50
51
52
53
54
55
56
57 *N*-(3,4-Dichlorophenyl)-1-methyl-1*H*-indazole-5-carboxamide (**38a**). Purification by silica gel
58 chromatography (CH₂Cl₂/MeOH, 9:1 v/v) following by recrystallization two times from petroleum
59
60

1 ether/CH₂Cl₂ afforded **38a** as a white crystalline solid (37 mg, 47%), mp: 193-194 °C; ¹H NMR (500
2 MHz, DMSO-*d*₆) δ = 4.09 (s, 3H, N1Me), 7.61 (d, *J* = 8.82 Hz, 1H, Ph), 7.76 (d, *J* = 8.20 Hz, 1H, Ph),
3 7.78 (dd, *J* = 2.21 / 8.83 Hz, 1H, Ph), 7.98 (dd, *J* = 1.57 / 8.82 Hz, 1H, Ph), 8.18 (d, *J* = 2.52 Hz, 1H,
4 Ph), 8.24 (d, *J* = 0.63 Hz, 1H, Ind.-Het.), 8.46 (dd, *J* = 0.63 / 1.57 Hz, 1H, Ph), 10.49 (s, 1H, -CONH-);
5 ¹³C NMR (125 MHz, DMSO-*d*₆) δ = 35.7 (N1Me), 109.8, 120.3, 121.5, 121.9, 123.1, 125.0, 125.6,
6 126.7, 130.7, 131.0, 134.2, 139.7, 140.9, 166.1; LC/ESI-MS (*m/z*): negative mode 318 [M-H]⁻, positive
7 mode 320 [M+H]⁺.
8

9
10
11
12
13
14
15
16
17 *N*-(3,4-Dichlorophenyl)-2-methyl-1*H*-indazole-5-carboxamide (**38b**). Purification by silica gel
18 chromatography (CH₂Cl₂/MeOH, 9:1 v/v) following by recrystallization two times from petroleum
19 ether/CH₂Cl₂ afforded **38a** as a white solid (8 mg, 9%), mp: 181-182 °C; ¹H NMR (500 MHz, DMSO-
20 *d*₆) δ = 4.23 (s, 3H, N2Me), 7.60 (d, *J* = 8.82 Hz, 1H, Ph), 7.68 (dt, *J* = 0.95 / 8.82 Hz, 1H), 7.75 (s, 1H,
21 Ph), 7.76 (dd, *J* = 2.21 / 8.83 Hz, 1H, Ph), 8.16 (d, *J* = 0.63 Hz, 1H, Ph), 8.44 (dd, *J* = 0.94 / 1.89 Hz,
22 1H, Ph), 8.58 (s, 1H, Ind.-Het.), 10.44 (s, 1H, -CONH-); ¹³C NMR (125 MHz, DMSO-*d*₆) δ = 48.8
23 (N2Me), 116.9, 120.4, 120.9, 121.5, 122.4, 124.6, 125.0, 127.1, 127.2, 130.7, 131.0, 139.8, 149.1,
24 166.4; LC/ESI-MS (*m/z*): negative mode 318 [M-H]⁻, positive mode 320 [M+H]⁺.
25
26
27
28
29
30
31
32
33
34
35

36 *N*-(3,4-Dichlorophenyl)-2-methyl-1*H*-indole-5-carboxamide (**54**). Purification by silica gel
37 chromatography (CH₂Cl₂/MeOH, 9:1 v/v) following by recrystallization two times from petroleum
38 ether/CH₂Cl₂ afforded **54** as a white solid (17 mg, 68%), mp: 179-180 °C; ¹H NMR (500 MHz, DMSO-
39 *d*₆) δ = 3.83 (s, 3H, N1Me), 6.59 (dd, *J* = 0.95 / 3.16 Hz, 1H, Indol.-Het.), 7.44 (d, *J* = 3.16 Hz, 1H,
40 Indol.-Het.), 7.55 (d, *J* = 8.83 Hz, 1H, Ph), 7.59 (d, *J* = 8.82 Hz, 1H, Ph), 7.78 (dd, *J* = 2.52 / 3.15 Hz,
41 1H, Ph), 7.80 (dd, *J* = 2.52 / 3.47 Hz, 1H, Ph), 8.20 (d, *J* = 2.21 Hz, 1H, Ph), 8.26 (d, *J* = 1.26 Hz, 1H,
42 Ph), 10.35 (s, 1H, -CONH-); ¹³C NMR (125 MHz, DMSO-*d*₆) δ = 32.8 (NMe), 101.9, 109.7, 120.2,
43 121.0, 121.1, 121.4, 124.7, 125.2, 127.5, 130.6, 130.9, 131.5, 138.3, 140.0, 166.9; LC/ESI-MS (*m/z*):
44 negative mode 317 [M-H]⁻, positive mode 319 [M+H]⁺.
45
46
47
48
49
50
51
52
53
54
55
56

57 *General Procedure C for the Preparation Compounds 58 and 59*. A solution of the corresponding 1*H*-
58 indazole-5-carboxaldehyde (**57**, 1.0 equiv.), 3,4-dichloroaniline (**23a**, 1.0 equiv.) and acetic acid (0.2
59
60

mL) in ethanol (3.0 mL/mmol) was stirred under reflux until a precipitation took place. After cooling to room temperature, water (30 mL) was added and the reaction mixture was sonicated for 5 min. The precipitate formed was filtered and dried at 70 °C and purified by column chromatography on silica gel (CH₂Cl₂/MeOH, 9:1 v/v) and recrystallized from petroleum ether/CH₂Cl₂.

(*E*)-*N*-(3,4-dichlorophenyl)-1-(1*H*-indazol-5-yl)methanimine (**58**). White solid (258 mg, 90%), mp: 207-208 °C; ¹H NMR (500 MHz, DMSO-*d*₆) δ = 7.27 (dd, *J* = 2.52 / 8.51 Hz, 1H, Ph), 7.55 (d, *J* = 2.53 Hz, 1H, Ph), 7.63 (s, 1H, Ph), 7.65 (s, 1H, Ph), 8.12 (dd, *J* = 1.26 / 8.83 Hz, 1H, Ph), 8.24 (s, 1H, Ind.-Het.), 8.29 (s, 1H, Ph), 8.73 (s, 1H, CH=N), 13.35 (s, 1H, NH); ¹³C NMR (125 MHz, DMSO-*d*₆) δ = 110.9, 122.1, 122.7, 123.0, 125.1, 125.2, 127.7, 128.9, 131.1, 131.7, 135.2, 141.5, 151.9, 163.2; LC/ESI-MS (*m/z*): negative mode 288 [M-H]⁻, positive mode 290 [M+H]⁺.

(*E*)-*N*-(3,4-dichlorophenyl)-1-(1-methyl-1*H*-indazol-5-yl)methanimine (**59**). Light yellowish solid (275 mg, 91%), mp: 145-146 °C; ¹H NMR (500 MHz, DMSO-*d*₆) δ = 4.09 (s, 3H, N1Me), 7.28 (dd, *J* = 2.53 / 8.52 Hz, 1H, Ph), 7.56 (d, *J* = 2.53 Hz, 1H, Ph), 7.63 (s, 1H, Ph), 7.65 (s, 1H, Ph), 7.75 (dd, *J* = 0.63 / 8.83 Hz, 1H, Ph), 8.05 (dd, *J* = 1.58 / 8.83 Hz, 1H, Ph), 8.22 (d, *J* = 0.94 Hz, 1H, Ind.-Het.), 8.28 (s, 1H, Ph), 8.74 (s, 1H, CH=N); ¹³C NMR (125 MHz, DMSO-*d*₆) δ = 35.7, 110.5, 122.1, 122.7, 123.6, 125.0, 125.3, 125.2, 127.8, 128.9, 131.1, 131.7, 134.2, 141.1, 151.8, 163.0; LC/ESI-MS (*m/z*): negative mode 302 [M-H]⁻, positive mode 304 [M+H]⁺.

Biological Experiments.

MAO-A and MAO-B Inhibition Assays. Stock solutions of the compounds (10 mM) in DMSO were used to prepare the test samples for the MAO assays with a final DMSO concentration of 1.0 % as described in the Supporting Information. The MAO-A and MAO-B enzymatic activity of the compounds was measured using a continuous fluorescence-based assay.⁴³ The MAO experiments were performed using the commercial assay kit Amplex Red (compare Supporting Information). The kit was stored frozen at ≤ -20 °C and protected from light. To ensure an optimal efficiency of the Amplex Red reagent, the rat and human MAO assay was performed at pH 7.4. The quantification of hydrogen peroxide released from the

1 biological sample and the subsequent production of resorufin was monitored using a microplate
2 fluorescence reader (PHERAstar BMG Labtech, Germany) with an excitation at 544 nm and an
3 emission at 590 nm. The MAO experiments were performed in triplicate or quadruplicate at room
4 temperature.
5
6
7
8

9
10 *Rat MAO Inhibition Assays.* To obtain MAO enzyme-containing mitochondrial-enriched fractions of rat,
11 livers from male Sprague-Dawley rats (250–300 g, Harlan Sprague Dawley, Dublin, VA, US) were
12 obtained. These were livers that were left-over from control rats that had been used for other
13 experiments. The livers (10.0 g) were dissected, given into 15.0 mL of an ice-cold 5.0 mM Hepes buffer
14 (pH 7.4), containing 210 mM of mannitol, 70 mM of sucrose, 0.5 mM of ethyleneglycoltetraacetic acid
15 (EGTA) and 2.0 mg/mL of bovine serum albumin (BSA), and homogenized using a glass/Teflon potter
16 (10 ups and downs at 1100 rpm). After homogenization, the volume was adjusted to 100 mL with the
17 same buffer. After a low speed centrifugation (10 min at 600 g; 4°C), the supernatant was further
18 centrifuged at 15,000 rpm for 5 min at +4°C. The resulting pellet was re-suspended in 2.0 mL of a 50
19 mM sodium phosphate buffer (pH 7.4) and stored at -80°C in aliquots of 1.0 mL until further use.
20
21 Assays were performed in 96-well plates in a final volume of 200 µL at RT. Rat liver mitochondria
22 were pre-treated for 15 min at RT with an aqueous solution of clorgyline (30 nM) or selegiline (300 nM)
23 to irreversibly block MAO-A or MAO-B activity, respectively. Test compounds (2.0 µL), dissolved in
24 DMSO (100%), were added to 90.0 µL of mitochondrial preparation (25.0 µg of protein for rat MAO-A
25 and 5.0 µg protein for rat MAO-B) and incubated for 30 min prior to the addition of 90 µL of freshly
26 prepared Amplex Red reagent. The Amplex Red reagent was used as follows: for a 96-well plate, 1.0
27 mg of Amplex Red, dissolved in 200 µL of DMSO (100%) and 100 µL of reconstituted horse-radish
28 peroxidase (HRP 200 U/mL) stock solution (kit vial + 1.0 mL of 50 mM sodium phosphate buffer) were
29 added to 9700 µL of sodium phosphate buffer (250 mM, pH 7.4). The enzymatic reaction was started by
30 the addition of 20 µL/well of an aqueous solution of the substrate *p*-tyramine (300 µM final
31 concentration). Selegiline and clorgyline (each in a final concentration of 1.0 µM) were used to
32 determine non-MAO-B and non-MAO-A enzyme activity, respectively. Fluorescence measurements
33
34
35
36
37
38
39
40
41
42
43
44
45
46
47
48
49
50
51
52
53
54
55
56
57
58
59
60

1 were performed for 45 min and the concentration-response curves of clorgyline and selegiline served as
2 positive controls for the rat MAO-A and rat MAO-B assay, respectively.
3

4
5 *Human MAO Inhibition Assays.* Recombinant human MAO-A and MAO-B enzymes, expressed in
6 baculovirus-infected insect cells, were purchased from Sigma Aldrich (M7441, M7316). The assays
7 were carried out in 96-well plates in a final volume of 200 μL at RT. According to the experimental
8 protocol, a solution of test compound (2.0 μL) in DMSO (100%) was added to 90.0 μL of protein
9 solution (for MAO-A: 0.3 μg protein/well, containing 6.6 μL of protein and 9.993 μL of phosphate
10 buffer, 50 mM; for MAO-B: 2.3 μg protein/well containing 51.0 μL of protein and 9.949 μL of buffer)
11 and incubated for 30 min prior to the addition of 90 μL of freshly prepared Amplex Red reagent. The
12 Amplex Red reagent was prepared as described above. The enzymatic reaction was started by the
13 addition of 20 μL /well of an aqueous solution of the substrate *p*-tyramine (150 μM final concentration).
14 Non-MAO-B and non-MAO-A enzyme activity was determined in the presence of selegiline and
15 clorgyline (each in a final concentration of 1.0 μM) and subtracted from the total activity measured. A
16 sample with DMSO (2.0 μL) was used as a negative control. Fluorescence measurements were
17 performed for 45 min and the concentration-response curves of clorgyline and selegiline served as
18 positive controls for the human MAO-A and human MAO-B assay, respectively.
19
20
21
22
23
24
25
26
27
28
29
30
31
32
33
34
35
36

37
38 *Reversibility of MAO-B.* To investigate the reversibility of MAO-B inhibition by compound **15**, we
39 performed time-dependent inhibition experiments using human MAO-B. Compound **15** as well as
40 reference compounds selegiline¹⁵ and safinamide¹⁷ were examined at their corresponding IC_{80} values
41 (determined with 150 μM of the substrate *p*-tyramine). The human MAO-B enzyme/inhibitor mixtures
42 were not pre-incubated. The enzyme reaction was started by the addition of a low substrate
43 concentration of 10 μM and the enzymatic activity of the test compounds was measured for 22 min
44 followed by an increase in the substrate concentration to 1.0 mM final concentration of *p*-tyramine. The
45 enzyme reactivation was monitored by fluorescence measurements over a period of 5 h.
46
47
48
49
50
51
52
53
54
55

56
57 *Kinetic MAO-B Experiments.* To evaluate the mode of MAO-B inhibition, the representative inhibitor
58 *N*-(3,4-dichlorophenyl)-1*H*-indazole-5-carboxamide (**15**) was evaluated in substrate-dependent kinetic
59
60

1 experiments and the corresponding progression curves as well as sets of Lineweaver–Burk plots were
2 generated. The reciprocal MAO-B activity was plotted against the reciprocal substrate concentration.
3
4 The initial catalytic rates of human MAO-B were measured at six different concentrations of the
5 substrate *p*-tyramine (0.05, 0.1, 0.25, 0.5, 1.0, and 1.5 mM) in the absence (basal sample) and in the
6
7 presence of three different concentrations (0.1, 0.5 and 1.0 nM) of the inhibitor **15**. The enzymatic
8
9 reactions and measurements were performed using human MAO-B assay conditions as described above
10
11 for the determination of IC₅₀ values.
12
13
14
15
16
17
18

19 **Data Analysis.** Enzyme inhibition was initially determined with at least two different concentrations
20
21 (10 μM and 0.1 μM) of test compound, each performed in triplicate and, if necessary, in quadruplicate.
22
23 For potent compounds, full concentration-inhibition curves were determined and IC₅₀ values were
24
25 calculated by nonlinear regression (curve fit) analysis. Data were expressed as mean IC₅₀ value ± SEM
26
27 (standard error of the mean). Generally, SEM values were lower than 10% of the calculated mean.
28
29 Preparation of the corresponding dose-response curves as well as the non-linear and linear regression
30
31 analysis was performed using GraphPad Prism Version 4.0 software (San Diego, CA, USA).
32
33
34
35
36
37

38 **Molecular Modeling Studies.**

39 **Data Preparation and Optimization.**

40
41 *MAO-B Protein.* The crystal structure (PDB code 2V5Z) of the human MAO-B in complex with
42
43 safinamide (**3**) was obtained from the PDB web page and prepared using the LeadIT v.2.1.6 software
44
45 from BioSolveIT GmbH, Germany.^{44,47} To decide which chain (A or B) should be considered for the
46
47 docking experiments, we computed an initial HYDE Visual Affinity Assessment for the two
48
49 crystallographically recorded ligand positions (SAG_A vs. SAG_B). It turned out that, owing to small
50
51 differences in atomic positions, the ligand crystallized in the pocket formed by chain B exhibited a
52
53 slightly better agreement between experiment and computation; therefore we chose chain B for all
54
55 further computations. The protein preparation used defaults throughout, with the exception of a slight
56
57
58
59
60

1 increase regarding the radius of the binding site definition, which was set to 7 Å (default: 6.5 Å),
2 motivated by consistency to other experiments (unpublished). Protonation and tautomer selection were
3 carried out automatically by the integrated ProToss functionality in LeadIT. Water selection was
4 determined also automatically by LeadIT; unless otherwise mentioned, this preparation was used for all
5 crystal structure computations, dockings, and scorings.^{61,62}

6
7
8
9
10
11 *Ligands.* To obtain valid 3D input structures for docking experiments, starting structures of the ligands
12 **15**, **40** and **53** were drawn in Titan v.1.05 (Wevefunction Inc. 2000), subsequently energy-optimized
13 using the MMFF94 force field, and saved as mol2 files.

14 15 16 17 18 19 **Computational Details.**

20
21 *Docking.* All computations were carried out using the FlexX docking module in LeadIT v.2.1.6 applying
22 the binding size definitions and water handling described above. A LeadIT Project File (*.fxx) was
23 created and saved on disk. The docking algorithms in LeadIT incorporate both a triangle-based
24 placement algorithm and the so-called Single-Interaction-Scan (FlexSIS), which are activated by
25 default. This way, a 50:50 merge process of poses (triangle vs. SIS) is executed. A maximum of 32
26 poses was stored for post-processing with HYDE. Computational experiments using a receptor-based
27 pharmacophore, which would force any halogen into the 2V5Z-known halogen binding pocket (HBP)
28 yielded essentially the same poses as the unconstrained docking on high ranks – both as a function of
29 the docking score, as well as in terms of the HYDE computation.

30
31
32
33
34
35
36
37
38
39
40
41
42 *HYDE Rescoring and HYDE Visual Affinities.* Hyde is a recently developed mechanism to rapidly
43 compute estimations of binding affinities (Binding Free Energies). It is based solely on a (weighting-
44 parameter free) description of hydrogen bonds, salt bridges etc. on the one hand side, and desolvation
45 (dehydration) terms on the other, as given by equation 1:

$$46
47
48
49
50
51
52
53
54
55
56
57
58
59
60$$
$$(1) \quad \Delta G_{\text{HYDE}}^i = \sum_{\text{atom } i} \Delta G_{\text{dehydration}}^i + \Delta G_{\text{H-bond}}^i$$

Herein, i is an atom counter running over all contributing protein and ligand atoms. The final, reported
affinity estimate corresponds to the sum over all atoms. In contrast to requiring weighting against each

other using fitted parameters, these two terms are connected using an atomic logP increment system which enables the user to visualize atom-based contributions to the affinity – and thus to explain unexplained SAR and/or point to room for lead optimization (LO). The individual terms of equation 1 take the form:

$$(2) \quad \Delta G_{\text{H-bond}}^i = 2.3RT \frac{p \log P_{\text{atom}}^i}{f_{\text{sat}}(T)} \Delta_{\text{interact}}^i$$

and

$$(3) \quad \Delta G_{\text{dehydration}}^i = -2.3RT \cdot p \log P_{\text{atom}}^i \cdot \Delta_{\text{accessibility}}^i$$

Where $p \log P$ is the “partial logP” for a given atom type, $f_{\text{sat}}(T)$ describes the temperature-dependent amount of defects in tetrahedral coordination in bulk water and is constant for a given temperature. The Δ_{interact} term ensures that only differences between the unbound and the bound states in terms of H-bonds are captured, and the $\Delta_{\text{accessibility}}$ term captures the “buriedness” of a certain group (calculated by a term based on the difference of solvent accessible surface). For further details regarding the methods, refer to the recent publication by Schneider et al.⁴⁸

HYDE calculations run within a very few seconds per compound on a standard CPU core; their output is an estimated binding affinity, the respective ligand efficiency (LE_{HYDE}), and certainly the visualization of an atom-colored molecule in 3D. HYDE-based Ligand Efficiency values (LE_{HYDE}) were calculated in kcal/mol using equation 4:

$$(4) \quad \text{LE}_{\text{Hyde}} = \left| \frac{\Delta G_{\text{Hyde}}}{\text{HA}} \right|$$

Herein, HA is the number of non-hydrogen atoms of the respective ligand (heavy atoms). The atom colors range from dark green (contributes favorably to affinity) over white (no contribution) to dark red (unfavorable contribution to affinity). Since HYDE receptor contributions are projected onto the relevant ligand molecule in the 3D visualization, it may occur that, e.g., a red atom is red because close receptor atoms contribute with a high desolvation penalty. A table in the software enables a quantitative split-up of HYDE atomic energies with respect to their originating atoms (receptor or ligand). Since

1 other important terms such as inter-/intra-molecular clash and torsional strain are not included in the
2 HYDE kernel mathematics, it is highly advisable to pre-optimize respective molecular input so that
3 these terms are negligibly small. This optimization is based on a linear combination of HYDE and
4 classical force field terms, and by default it is automatically carried out upon evoking a HYDE
5 calculation.
6
7
8
9
10

11 For rescoring, previous experience proposed to file 32 FlexX/-SIS placements into HYDE. For this
12 study, however, it turned out indeed, that the HYDE best-scored pose for all ligands was always
13 amongst the top 10 docking solutions (compare Section Discussion and Results).⁴⁸ Since the former is
14 considered best practice, we filed a maximum of 32 poses into HYDE and selected the best-scored ones
15 thereafter.
16
17
18
19
20
21
22

23 *Visual Inspection of Computed Results.* Since the HYDE kernel, as mentioned above, does not contain
24 torsional energy terms, we (additionally to the pre-optimizer) double-checked the torsional conspicuous
25 arrangements visually. Results were therefore visualized using the TorsionAnalyzer software allowing a
26 quick assessment of the statistical significance of torsion patterns.^{63,64,65} A multi-SD file of the relevant
27 poses was loaded into TorsionAnalyzer and briefly controlled. It should be stressed that the respective
28 coloring (*red* = rarely/not observed; *orange* = observed sometimes; *green* = observed often) is based on
29 statistics rooting in Cambridge Structural Database (CSD) occurrence and not on any energetics.⁴⁷
30
31
32
33
34
35
36
37
38
39
40
41
42
43
44
45
46
47
48
49
50
51
52
53
54
55
56
57
58
59
60

ACKNOWLEDGEMENTS

We thank Dr. Jag Heer and Dr. Miriam Schlenk for helpful discussions and suggestions, Angelika Fischer and Anika Püsche for expert technical assistance in performing MAO inhibition assays, Marion Schneider for performing LC/MS analyses, and Sabine Terhart-Krabbe and Annette Reiner for recording NMR spectra.

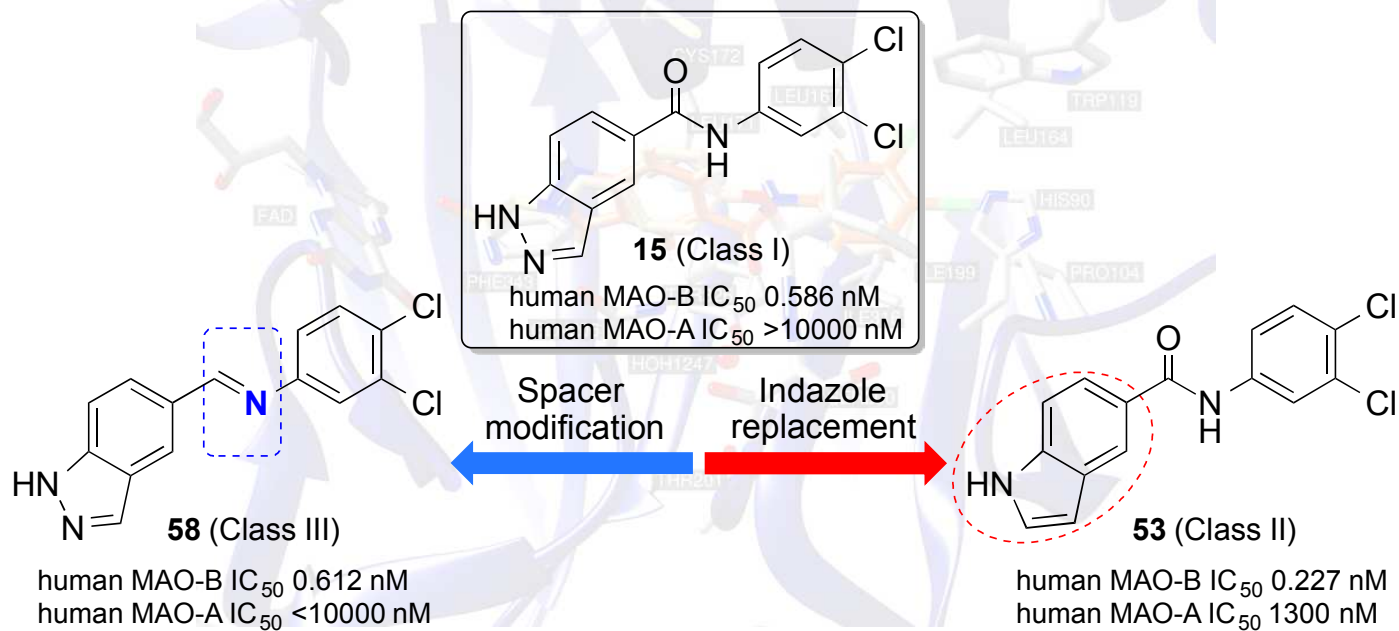
SUPPORTING INFORMATION. Synthetic procedures and analytic data of carboxylic acids **18** and **19**; ^1H and ^{13}C NMR spectra of compounds **10** and **11**, conditions for chromatography; LC/ESI-MS data for all new compounds; stability studies for compounds **54** and **59**; analysis of *E/Z* isomers stability for **58**; physicochemical profiling of all new compounds including calculated important parameters and plots; pharmacological studies and correlation of inhibition data of rat versus human MAO-B for all tested compounds, and computational analysis of compounds **15** and **30** in comparison with safinamide **3**. This material is available free of charge via the Internet at <http://pubs.acs.org>.

ABBREVIATIONS USED

AChE, acetylcholinesterase; AD, Alzheimer's disease; AR, adenosine receptor; BEI, binding efficiency index; BBB, blood-brain barrier; CHO, Chinese hamster ovary; CNS, central nervous system; COMT, catechol-*O*-methyltransferase; DA, dopamine; DIPEA, *N,N*-diisopropylethylamine; DMF, *N,N*-dimethylformamide; DMSO, dimethylsulfoxide; EDC, 1-ethyl-3-(3-dimethylaminopropyl)-carbodiimide; EGTA, ethyleneglycoltetraacetic acid; ESI, electrospray ionization; FAD, flavin adenine dinucleotide; h, human; HBP, hydrogen binding pocket; HMBC, heteronuclear multiple bond correlation; HRP, horseradish peroxidase; HYDE, hydrogen dehydration; LE, ligand efficiency; LLE, lipophilic ligand efficiency; MAO, monoamine oxidase; PD, Parkinson's disease; PE, petroleum ether; r, rat; PET, positron emission tomography; ROS, reactive oxygen species; SAR, structure-activity relationship; SIS, Single-Interaction-Scan; TBTU, *O*-(benzotriazol-1-yl)-*N,N,N',N'*-tetramethyluronium tetrafluoroborate; TLC, thin-layer chromatography

1
2
3
4
5
6
7
8
9
10
11
12
13
14
15
16
17
18
19
20
21
22
23
24
25
26
27
28
29
30
31
32
33
34
35
36
37
38
39
40
41
42
43
44
45
46
47
48
49
50
51
52
53
54
55
56
57
58
59
60

TABLE OF CONTENTS GRAPHIC



REFERENCES

- 1 a) Castagnoli, N., Jr.; Petzer, J. P.; Steyn, S.; Castagnoli, K.; Chen, J.-F.; Schwarzschild, M. A.;
2
3
4
5
6
7
8
9
10
11
12
13
14
15
16
17
18
19
20
21
22
23
24
25
26
27
28
29
30
31
32
33
34
35
36
37
38
39
40
41
42
43
44
45
46
47
48
49
50
51
52
53
54
55
56
57
58
59
60
Van der Schyf, C. J. Monoamine oxidase B inhibition and neuroprotection. *Neurology* **2003**, *61*
(Suppl. 6), S62–S68.
- 2 a) Shih, J. C.; Chen, K.; Ridd, M. J. Monoamine oxidase: from genes to behavior. *Annu. Rev.*
Neurosci. **1999**, *22*, 197–217. b) Binda, C.; Newton-Vinson, P.; Hubálek, F.; Edmondson, D. E.;
Mattevi, A. Structure of human monoamine oxidase B, a drug target for the treatment of
neurological disorders. *Nat. Struct. Biol.* **2002**, *9*, 22–26. c) Hubálek, F.; Pohl, J.; Edmondson, D. E.
Structural comparison of human monoamine oxidases A and B. *J. Biol. Chem.* **2003**, *278*, 28612–
28618.
- 3 a) Youdim, M. B. H.; Lavie, L. Selective MAO-A and MAO-B inhibitors, radical scavengers and
nitric oxide synthase inhibitors in Parkinson's disease. *Life Sci.* **1994**, *55*, 2077–2082. b)
Hauptmann, N.; Grimsby, J.; Shih, J. C.; Cadenas E. The metabolism of tyramine by monoamine
oxidase A/B causes oxidative damage to mitochondrial DNA. *Arch. Biochem. Biophys.* **1996**, *335*,
295–304. c) Sayre, L. M.; Perry, G.; Smith, M. A. Oxidative stress and neurotoxicity. *Chem. Res.*
Toxicol. **2008**, *21*, 172–188.
- 4 a) Youdim, M. B. H.; Finberg, J. P. M. New directions in monoamine oxidase A and B selective
inhibitors and substrates. *Biochem. Pharmacol.* **1991**, *41*, 155–162. b) Shih, J. C.; Chen, K.
Regulation of MAO-A and MAO-B gene expression. *Curr. Med. Chem.* **2004**, *11*, 1995–2005. c)
Edmondson, D. E.; Binda, C.; Wang, J.; Upadhyay, A. K.; Mattevi, A. Molecular and mechanistic
properties of the membrane-bound mitochondrial monoamine oxidases. *Biochemistry* **2009**, *48*,
4210–4230.

- 1
2
3
4 5 a) Levitt, P.; Pintar, J. E.; Breakefield, X. O. Immunocytochemical demonstration of monoamine
6 oxidase B in brain astrocytes and serotonergic neurons. *Proc. Natl. Acad. Sci. USA* **1982**, *79*, 6385–
7 6389. b) O'Carroll, A.-M.; Fowler, C. J.; Phillips, J. P.; Tobbia, I.; Tipton, K. F. The deamination
8 of dopamine by human brain monoamine oxidase. Specificity for the two enzyme forms in seven
9 brain regions. *Nounyn Schmiedeberg's Arch. Pharmacol.* **1983**, *322*, 198–202. c) Lin, J. S.;
10 Kitahama, K.; Fort, P.; Panula, P.; Denney, R. M.; Jouvett, M. Histaminergic system in the cat
11 hypothalamus with reference to type B monoamine oxidase. *J. Comp. Neurol.* **1993**, *330*, 405–420.
12 d) Westlund, K. N.; Denney, R. M.; Kochersperger, L. M.; Rose, R. M.; Abell, C. W. Distinct
13 monoamine oxidase A and B populations in primate brain. *Science* **1985**, *230*, 181–183.
14
15 6 a) Fowler, C. J.; Wiberg, A.; Orelund, L.; Marcusson, J.; Winblad, B. The effect of age on the
16 activity and molecular properties of human brain monoamine oxidase. *J. Neural Transm.* **1980**, *49*,
17 1–20. b) Nicotra, A.; Pierucci, F.; Parvez, H.; Senatori, O. Monoamine oxidase expression during
18 development and aging. *NeuroToxicology* **2004**, *25*, 155–165.
19
20 7 a) Nagatsu, T. Progress in monoamine oxidase (MAO) research and relation to genetic engineering.
21 *NeuroToxicology* **2004**, *25*, 11–20. b) Bortolato, M.; Chen, K.; Shih, J. C. Monoamine oxidase
22 inactivation: From pathophysiology to therapeutics. *Adv. Drug Deliv. Rev.* **2008**, *60*, 1527–1533.
23
24 8 a) Riederer, P.; Lachenmayer, L.; Laux, G. Clinical applications of MAO-inhibitors. *Curr. Med.*
25 *Chem.* **2004**, *11*, 2033–2043. b) Youdim, M. B. H.; Bakhle, Y. S. Monoamine oxidase: isoforms
26 and inhibitors in Parkinson's disease and depressive illness. *Br. J. Pharmacol.* **2006**, *147*, S287–
27 S296. c) Schapira, A. H. V. Treatment options in the modern management of Parkinson's disease.
28 *Arch. Neurol. Rev.* **2007**, *64*, 1083–1088. d) Hoskini, J.; Shenfield, G.; Murray, M.; Gross, A.
29 Characterization of moclobemide *N*-oxidation in human microsomes. *Xenobiotica* **2001**, *31*, 387–
30 397.
31
32
33
34
35
36
37
38
39
40
41
42
43
44
45
46
47
48
49
50
51
52
53
54
55
56
57
58
59
60

- 1
2
3
4
5
6
7
8
9
10
11
12
13
14
15
16
17
18
19
20
21
22
23
24
25
26
27
28
29
30
31
32
33
34
35
36
37
38
39
40
41
42
43
44
45
46
47
48
49
50
51
52
53
54
55
56
57
58
59
60
- 9 Finberg, J. P. M. Update on the pharmacology of selective inhibitors of MAO-A and MAO-B: Focus on modulation of CNS monoamine neurotransmitter release. *Pharmacol. Ther.* **2014**, <http://dx.doi.org/10.1016/j.pharmthera.2014.02.010>.
- 10 a) Schapira, A. H. V. Treatment options in the modern management of Parkinson's disease. *Arch. Neurol.* **2007**, *64*, 1083–1088. b) Singer, C. Managing the patient with newly diagnosed Parkinson's disease. *Clev. Clin. J. Med.* **2012**, *79* (Suppl. 2), S3–S7. c) Jankovic, J.; Poewe, W. Therapies in Parkinson's disease. *Curr. Opin. Neurol.* **2012**, *25*, 433–447. d) Youdim, M. B. H.; Kupersmidt, L.; Amit, T.; Weinreb, O. Promises of novel multi-target neuroprotective and neurorestorative drugs for Parkinson's disease. *Parkinsonism Rel. Disord.* **2014**, *20* (Suppl. 1), S132–S136.
- 11 Pisani, L.; Catto, M.; Leonetti, F.; Nicolotti, O.; Stefanachi, A.; Campagna, F.; Carotti, A. Targeting monoamine oxidases with multipotent ligands: An emerging strategy in the search of new drugs against neurodegenerative diseases. *Curr. Med. Chem.* **2011**, *18*, 4568–4587.
- 12 a) Patyar, S.; Prakash, A.; Medhi, B. Dual inhibition: a novel promising pharmacological approach for different disease conditions. *J. Pharm. Pharmacol.* **2011**, *63*, 459–471. b) Youdim, M. B. H. Multi target neuroprotective and neurorestorative anti-Parkinson and anti-Alzheimer drugs ladostigil and M30 derived from rasagiline. *Exp. Neurobiol.* **2013**, *22*, 1–10. c) Sterling, J.; Herzig, Y.; Goren, T.; Finkelstein, N.; Lerner, D.; Goldenberg, W.; Miskolczi, I.; Molnar, S.; Rantal, F.; Tamas, T.; Toth, G.; Zagyva, A.; Zekany, A.; Lavian, G.; Gross, A.; Friedman, R.; Razin, M.; Huang, W.; Kraus, B.; Chorev, M.; Youdim, M. B.; Weinstock, M. Novel dual inhibitors of AChE and MAO derived from hydroxyl aminoindan and phenethylamine as potential treatment for Alzheimer's disease. *J. Med. Chem.* **2002**, *45*, 5260–5279. d) Bolea, I.; Juárez-Jiménez, J.; de los Rios, C.; Chioua, M.; Pouplana, R.; Luque, F. J.; Unzeta, M.; Marco-Contelles, J.; Samadi, A. Synthesis, biological evaluation, and molecular modeling of donepezil and *N*-[(5-(benzyloxy)-1-methyl-1*H*-indol-2-yl)methyl]-*N*-methylprop-2-yn-1-amine hybrids as new multipotent

- 1 cholinesterase/monoamine oxidase inhibitors for the treatment of Alzheimer's disease. *J. Med.*
2
3
4 *Chem.* **2011**, *54*, 8251–8270. E) Bautista-Aguilera, O. M.; Esteban, G.; Bolea, I.; Nikolic, K.;
5
6 Agbabe, D.; Moraleda, I.; Iriepa, I.; Smadi, A.; Soriano, E.; Unzeta, M.; Marco-Contelles, J.
7
8 Design, synthesis, pharmacological evaluation, QSAR analysis, molecular modeling and ADMET
9
10 of novel donepezil-indoyl hybrids as multipotent cholinesterase/monoamine oxidase inhibitors for
11
12 the potential treatment of Alzheimer's disease. *Eur. J. Med. Chem.* **2014**, *75*, 82–95.
- 13 a) Petzer, J. P.; Castagnoli, N., Jr.; Schwarzschild, M. A.; Chen, J.-F.; Van der Schyf, C. J. Dual-
14
15 target-directed drugs that block monoamine oxidase B and adenosine A_{2A} receptors for Parkinson's
16
17 disease. *Neurotherapeutics* **2009**, *6*, 141–151. b) Rivara, S.; Piersanti, G.; Bartoccini, F.;
18
19 Diamantini, G.; Pala, D.; Riccioni, T.; Stasi, M. A.; Cabri, W.; Borsini, F.; Mor, M.; Tarzia, G.;
20
21 Minetti, P. Synthesis of (*E*)-8-(3-chlorostyryl)caffeine analogues leading to 9-deazaxanthine
22
23 derivatives as dual A_{2A} antagonists/MAO-B inhibitors. *J. Med. Chem.* **2013**, *56*, 1247–1261.
- 24
25
26
27
28
29
30 a) Petzer, J. P.; Steyn, S.; Castagnoli, K. P.; Chen, J.-F.; Schwarzschild, M. A.; Van der Schyf, C.
31
32 J.; Castagnoli, N. Inhibition of monoamine oxidase B by selective adenosine A_{2A} receptor
33
34 antagonists. *Bioorg. Med. Chem.* **2003**, *11*, 1299–1310. b) Vlok, N.; Malan, S. F.; Castagnoli, N.,
35
36 Jr.; Bergh, J. J.; Petzer, J. P. Inhibition of monoamine oxidase B by analogues of the adenosine A_{2A}
37
38 receptor antagonists (*E*)-8-(3-chlorostyryl)caffeine (CSC). *Bioorg. Med. Chem.* **2006**, *14*, 3512–
39
40 3521. c) Pretorius, J.; Malan, S. F.; Castagnoli, N. Jr.; Bergh, J. J.; Petzer, J. P. Dual inhibition of
41
42 monoamine oxidase B and antagonism of the adenosine A_{2A} receptor by (*E,E*)-8-(4-phenylbutadien-
43
44 1-yl)caffeine analogues. *Bioorg. Med. Chem.* **2008**, *16*, 8876–8684. d) Stöbel, A.; Schlenk, M.;
45
46 Hinz, S.; Küppers, P.; Heer, J.; Gütschow, M.; Müller, C. E. Dual targeting of adenosine A_{2A}
47
48 receptors and monoamine oxidase B by 4*H*-3,1-benzothiazin-4-ones. *J. Med. Chem.* **2013**, *56*,
49
50 4580–4596. e) Brunschweiler, A.; Koch, P.; Schlenk, M.; Pineda, F.; Küppers, P.; Hinz, S.; Köse,
51
52 M.; Ullrich, S.; Hockemeyer, J.; Wiese, M.; Müller, C. E. 8-Benzyltetrahydropyrazino[2,1-
53
54
55
56
57
58
59
60

- 1
2
3
4
5
6
7
8
9
10
11
12
13
14
15
16
17
18
19
20
21
22
23
24
25
26
27
28
29
30
31
32
33
34
35
36
37
38
39
40
41
42
43
44
45
46
47
48
49
50
51
52
53
54
55
56
57
58
59
60
- flupuridiones: water-soluble tricyclic xanthine derivatives as multitarget drugs for neurodegenerative diseases. *ChemMedChem*, DOI: 10.1002/cmdc.201402082.
- 15 a) Knoll, J.; Magyar, K. Some puzzling pharmacological effects of monoamine oxidase inhibitors. *Adv. Biochem. Psychopharmacol.* **1972**, *5*, 393–408. b) Birkmayer, W.; Riederer, P.; Ambrozi, I.; Youdim, M. B. H. Implications of combined treatment with Madopar and l-deprenyl in Parkinson's disease. *Lancet* **1977**, *2*, 439–443. c) Reynolds, G. P.; Riederer, P.; Sandler, M.; Jellinger, K.; Seemann, D. Amphetamine and 2-phenylethylamine in post-mortem Parkinsonian brain after (*L*)-deprenyl administration. *J. Neural. Transm.* **1978**, *43*, 271–277. d) Riederer, P.; Lachenmayer L. Selegiline's neuroprotective capacity revisited. *J. Neural. Transm.* **2003**, *110*, 1273–1278. e) Pålhagen, S.; Heinonen, E.; Hägglund, J. Selegiline slows the progression of the symptoms of Parkinson disease. *Neurology* **2006**, *66*, 1200–1206.
- 16 a) Lakhan, S. E. From a Parkinson's disease expert: Rasagiline and the future of therapy. *Mol. Neurodegen.* **2007**, *2*, 1–3. b) Teo, K. C.; Ho, S.-L. Monoamine oxidase-B (MAO-B) inhibitors: implications for disease-modification in Parkinson's disease. *Transl. Neurodegener.* **2013**, 2–10.
- 17 a) Marzo, A.; Bo, L. D.; Monti, N. C.; Crivelli, F.; Ismaili, S.; Caccia, C.; Cattaneo, C.; Fariello, R. G. Pharmacokinetics and pharmacodynamics of safinamide, a neuroprotectant with antiparkinsonian and anticonvulsant activity. *Pharmacol. Res.* **2004**, *50*, 77–85. b) Fariello, R. G. Safinamide. *Neurotherapeutics* **2007**, *4*, 110–116. c) Onofrij, M.; Bonanni, L.; Thomas, A. An expert opinion on safinamide in Parkinson's disease. *Expert Opin. Investig. Drugs* **2008**, *17*, 1115–1125. d) Schapira, A. H. V. Safinamide in the treatment of Parkinson's disease. *Expert Opin. Pharmacother.* **2010**, *11*, 2261–2268. e) Seithel-Keuth, A.; Johne, A.; Freisleben, A.; Kupas, K.; Lissy, M.; Krösser, A. Absolute bioavailability and effect of food on the disposition of safinamide immediate release tablets in healthy adult subjects. *Clin. Pharmacol. Drug Dev.* **2013**, *2*, 79–89.

- 1
2
3
4
5
6
7
8
9
10
11
12
13
14
15
16
17
18
19
20
21
22
23
24
25
26
27
28
29
30
31
32
33
34
35
36
37
38
39
40
41
42
43
44
45
46
47
48
49
50
51
52
53
54
55
56
57
58
59
60
- 18 Youdim, M. B. H.; Gross, A.; Finberg, J. P. M. Rasagiline [*N*-propargyl-1*R*(+)-aminoindan], a selective and potent inhibitor of mitochondrial monoamine oxidase B. *Br. J. Pharmacol.* **2001**, *132*, 500–506.
- 19 a) Clarke, A.; Brewer, F.; Johnson, E. S.; Mallard, N.; Hartig, F.; Taylor, S.; Corn, T. H. A new formulation of selegiline: improved bioavailability and selectivity for MAO-B inhibition. *J. Neural Transm.* **2003**, *110*, 1241–1255. b) Clarke, A.; Johnson, E. S.; Mallard, N.; Corn, T. H.; Johnston, A.; Boce, M.; Warrington, S.; MacMahon, D. G. A new low-dose formulation of selegiline: clinical efficacy, patient preference and selectivity for MAO-B inhibition. *J. Neural Transm.* **2003**, *110*, 1257–1271.
- 20 Lees, A. Alternatives to levodopa in the initial treatment of early Parkinson's disease. *Drugs Aging* **2005**, *22*, 731–740.
- 21 Parkinson Study Group. A controlled, randomized, delayed-start study of rasagiline in early Parkinson's disease. *Arch. Neurol.* **2004**, *61*, 561–566.
- 22 a) Hubálek, F.; Binda, C.; Li, M.; Herzig, Y.; Sterling, J.; Youdim, M. B. H.; Mattevi, A.; Edmondson, D. E. Inactivation of purified human recombinant monoamine oxidases A and B by rasagiline and its analogues. *J. Med. Chem.* **2004**, *47*, 1760–1766. b) Prins, L. H. A.; Petzer, J. P.; Malan, S. F. Inhibition of monoamine oxidase by indole and benzofuran derivatives. *Eur. J. Med. Chem.* **2010**, *45*, 4458–4466.
- 23 Hampel, H.; Berger, C.; Buch, K.; Möller, H.-J. A review of the reversible MAO-A inhibitor moclobemide in geriatric patients. *Hum. Psychopharm.* **1998**, *12*, 43–51.
- 24 Malek, N. M.; Grosset, D. G. Investigational agents in the treatment of Parkinson's disease: focus on safinamide. *J. Exp. Pharmacol.* **2012**, *4*, 85–90.
- 25 Schapira, A. H.; Stocchi, F.; Borgohain, R.; Onofri, M.; Bhatt, M.; Lorenzana, P.; Lucini, V.; Giuliani, R.; Anand, R.; Study 017 Investigators. Long-term efficacy and safety of safinamide as add-on therapy in early Parkinson's disease. *Eur. J. Neurol.* **2013**, *20*, 271–280.

- 1
2
3
4
5
6
7
8
9
10
11
12
13
14
15
16
17
18
19
20
21
22
23
24
25
26
27
28
29
30
31
32
33
34
35
36
37
38
39
40
41
42
43
44
45
46
47
48
49
50
51
52
53
54
55
56
57
58
59
60
- 26 a) Caccia, C.; Maj, R.; Calabresi, M.; Maestroni, S.; Faravelli, L.; Curatolo, L.; Salvati, P.; Fariello, R. G. Safinamide: From molecular targets to a new anti-parkinson drug. *Neurology* **2006**, *67* (7_suppl_2), S18–S23. b) Schapira, A. H. V. Monoamine oxidase B inhibitors for the treatment of Parkinson's disease: a review of symptomatic and potential disease-modifying effects. *CNS Drugs* **2011**, *25*, 1061–1071.
- 27 Leonetti, F.; Capaldi, C.; Pisani, L.; Nicolotti, O.; Muncipinto, G.; Stefanachi, A.; Cellamare, S.; Caccia, C.; Carotti, A. Solid-phase synthesis and insights into structure-activity relationships of safinamide analogues as potent and selective inhibitors of type B monoamine oxidase. *J. Med. Chem.* **2007**, *50*, 4909–4916.
- 28 Mertens, M. D.; Hinz, S.; Müller, C. E.; Gütschow, M. Alkynyl-coumarinyl ethers as MAO-B inhibitors. *Bioorg. Med. Chem.* **2014**, *22*, 1916–1928.
- 29 Pérez, V.; Marco, J. L.; Fernández-Álvarez, E.; Unzeta, M. Relevance of benzyloxy group in 2-indoyl methylamines in the selective MAO-B inhibition. *Br. J. Pharmacol.* **1999**, *127*, 869–876.
- 30 Herraiz, T.; Arán, V. J.; Guillén, H. Nitroindazole compounds inhibit the oxidative activation of 1-methyl-4-phenyl-1,2,3,6-tetrahydropyridine (MPTP) neurotoxin to neurotoxic pyridinium cations by human monoamine oxidase (MAO). *Free Radical Res.* **2009**, *43*, 975–984.
- 31 Pisani, L.; Muncipinto, G.; Miscioscia, T. F.; Nicolotti, O.; Leonetti, F.; Catto, M.; Caccia, C.; Salvati, P.; Soto-Otero, R.; Mendez-Alvarez, E.; Passeleu, C.; Carotti, A. Discovery of a novel class of potent coumarin monoamine oxidase B inhibitors: development and biopharmacological profiling of 7-[(3-chlorobenzyl)oxy]-4-[(methylamino)methyl]-2H-chromen-2-one methanesulfonate (NW-1772) as a highly potent, selective, reversible, and orally active monoamine oxidase B inhibitor. *J. Med. Chem.* **2009**, *52*, 6685–6706.
- 32 a) Van der Walt, E. M.; Milczek, E. M.; Malan, S. F.; Edmondson, D. E.; Castagnoli, Jr., N.; Bergh, J. J.; Petzer, J. P. Inhibition of monoamine oxidase by (*E*)-styrylisatin analogues. *Bioorg. Med. Chem. Lett.* **2009**, *19*, 2509–2513. b) Manley-King, C. I.; Bergh, J. J.; Petzer, J. P. Inhibition of

- 1 monoamine oxidase by selected C5- and C6-substituted isatin analogues. *Bioorg. Med. Chem.* **2011**,
2
3
4 *19*, 261–274.
- 5
6 33 a) Prat, G.; Pérez, V.; Rubi, A.; Casas, M.; Unzeta, M. The novel type B MAO inhibitor PF9601N
7
8 enhances the duration of L-DOPA-induced contralateral turning in 6-hydroxydopamine lesioned
9
10 rats. *J. Neural Transm.* **2000**, *107*, 409–417. b) Bellik, L.; Dragoni, S.; Pessina, F.; Sanz, E.;
11
12 Unzeta, M.; Valoti, M. Antioxidant properties of PF9601N, a novel MAO-B inhibitor: assessment
13
14 of its ability to interact with reactive nitrogen species. *Acta Biochim. Pol.* **2010**, *57*, 235–239. c)
15
16 Unzeta, M.; Sanz, E.; Novel MAO-B inhibitors: potential therapeutic use of the selective MAO-B
17
18 inhibitor PF9601N in Parkinson's disease. In *International Review of Neurobiology*, 1st Edition;
19
20 Youdim, M. B. H.; Riederer, P., Eds.; Monoamine oxidases and their inhibitors; Elsevier: London,
21
22 2011; Vol. 100, pp 218–229.
- 23
24
25
26
27 34 Müller, C. E.; Hockemeyer, J.; Tzvetkov, N. T.; Burbiel, J. 8-Ethynyl-xanthine derivatives as
28
29 selective A_{2A} receptor antagonists. PCT Int. Appl. WO 2008077557, 2008.
- 30
31
32 35 Binda, C.; Aldeco, M.; Geldenhuys, W. J.; Tortorici, M.; Mattevi, A.; Edmondson, D. E. Molecular
33
34 insights into human monoamine oxidase B inhibition by the glitazone anti-diabetes drugs. *ACS*
35
36 *Med. Chem. Lett.* **2011**, *3*, 39–42.
- 37
38
39 36 Raffa, D.; Daidone, G.; Maggio, B.; Schillaci, D.; Plescia, S.; Torta, L. Synthesis and antifungal
40
41 activity of new *N*-isoxazolyl-2-iodomenzamides. *Il Farmaco* **1999**, *54*, 90–94.
- 42
43
44 37 Tzvetkov, N. T.; Euler, H.; Müller, C. E. Regioselective synthesis of 7,8-dihydroimidazo[5,1-
45
46 *c*][1,2,4]triazine-3,6-(2*H*,4*H*)-dione derivatives: A new drug-like heterocyclic scaffold. *Beilstein J.*
47
48 *Org. Chem.* **2012**, *8*, 1584–1593.
- 49
50
51 38 Pevarello, P.; Bonsignori, A.; Dostert, P.; Heidempergher, F.; Pinciroli, V.; Colombo, M.;
52
53 AcArthur, R. A.; Salvati, P.; Post, C.; Fariello, R. G.; Varasi, M. Synthesis and anticonvulsant
54
55 activity of a new class of 2-[(arylalkyl)amino]alkanamide derivatives. *J. Med. Chem.* **1998**, *41*,
56
57 579–590.
58
59
60

- 1
2
3
4
5
6
7
8
9
10
11
12
13
14
15
16
17
18
19
20
21
22
23
24
25
26
27
28
29
30
31
32
33
34
35
36
37
38
39
40
41
42
43
44
45
46
47
48
49
50
51
52
53
54
55
56
57
58
59
60
- 39 Raffa, D.; Maggio, B.; Cascioferro, S.; Raimondi, M. V.; Daidone, G.; Plescia, S.; Schillaci, D.; Cusimano, M. G.; Titone, L.; Colomba, C.; Tolomeo, M. N-(Indazolyl)benzamido derivatives as CDK1 inhibitors: design, synthesis, biological activity, and molecular docking studies. *Arch. Pharm. Chem. Lett. Sci.* **2009**, *342*, 265–273.
- 40 a) Barbanti, E.; Caccia, C.; Salvati, P.; Velardi, F.; Ruffilli, T.; Bogogna, L. Process for the production of 2-[4-(3- and 2-fluorobenzyloxy)benzylamino]propanamides. U.S. Patent 8076515, 2011. b) Zhang, K.; Xue, N.; Shi, X.; Liu, W.; Meng, J.; Du, Y. A validated chiral liquid chromatographic method for the enantiomeric separation of safinamide mesylate, a new anti-Parkinson drug. *J. Pharm. Biomed. Anal.* **2011**, *55*, 220–234.
- 41 a) Hockemeyer, J.; Burbiel, J. C.; Müller, C. E. Multigram-scale syntheses, stability, and photoreactions of A_{2A} adenosine receptor antagonists with 8-styrylxanthine structure: Potential drugs for Parkinson's disease. *J. Org. Chem.* **2004**, *69*, 3308–3318. b) Müller, C. E.; Geis, U.; Hipp, J.; Schobert, U. Frobenius, W.; Pawlowski, M.; Suzuki, F.; Sandoval-Ramirez, J. Synthesis and structure-activity relationships of 3,7-dimethyl-1-propargylxanthine derivatives, A_{2A}-selective adenosine receptor antagonists. *J. Med. Chem.* **1997**, *40*, 4396–4405.
- 42 Yáñez, M.; Fraiz, N.; Cano, E.; Orallo, F. Inhibitory effects of *cis*- and *trans*-resveratrol on noradrenaline and 5-hydroxytryptamine uptake and on monoamine oxidase activity. *Biochem. Biophys. Res. Commun.* **2006**, *344*, 688–695.
- 43 Holt, A.; Sharman, D. F.; Baker, G. B.; Palcie, M. M. A continuous spectrophotometric assay for monoamine oxidase and related enzymes in tissue homogenates. *Anal. Biochem.* **1997**, *244*, 384–392.
- 44 Binda, C.; Wang, J.; Pisani, L.; Caccia, C.; Carotti, A.; Salvati, P.; Edmondson D. E.; Mattevi, A. Structures of monoamine oxidase B complexes with selective noncovalent inhibitors: safinamide and coumarin analogs. *J. Med. Chem.* **2007**, *50*, 5848–5852.

- 1
2
3
4
5
6
7
8
9
10
11
12
13
14
15
16
17
18
19
20
21
22
23
24
25
26
27
28
29
30
31
32
33
34
35
36
37
38
39
40
41
42
43
44
45
46
47
48
49
50
51
52
53
54
55
56
57
58
59
60
- 45 Binda, C.; Hubálek, F.; Min, L.; Herzig, Y.; Sterling, J.; Salvati, P.; Edmondson D. E.; Mattevi, A. Crystal structures of monoamine oxidase B in complex with four inhibitors of the *N*-propargylaminoindan class. *J. Med. Chem.* **2004**, *47*, 1767–1774.
- 46 Novaroli, L.; Daina, A.; Favre, E.; Bravo, J.; Carotti, A.; Leonetti, F.; Catto, M.; Carrupt, P. A.; Reist, M. Impact of species-dependent differences on screening, design, and development of MAO B inhibitors. *J. Med. Chem.* **2006**, *49*, 6264–6272.
- 47 FlexS/FlexV v.2.1.2, BioSolveIT GmbH, Germany, 2013; <http://www.biosolveit.de>.
- 48 Schneider, N.; Lange, G.; Hindle, S.; Klein, R.; Rarey, M. A consistent description of HYdrogen bond and DEhydratation energies in protein-ligand complexes: methods behind the HYDE scoring function. *J. Comput.-Aided Mol. Des.* **2013**, *27*, 15–29.
- 49 Schneider, N.; Hindle, S.; Lange, G.; Klein, R.; Albrecht, J.; Briem, H.; Beyer, K.; Claußen, H.; Gastreich, M.; Lemmen, C.; Rarey, M. Substantial improvements in large-scale redocking and screening using the novel HYDE scoring function. *J. Comput.-Aided Mol. Des.* **2012**, *26*, 701–723.
- 50 a) The docking pose graphics were performed with the UCSF Chimera package. Chimera is developed by the Resource for Biocomputing, Visualization, and Informatics at the University of California, San Francisco (supported by NIGMS P41-GM103311). b) Pettersen, E. F.; Goddard, T. D.; Huang, C. C.; Couch, G. S.; Greenblatt, D. M.; Meng, E. C.; Ferrin, T. E. UCSF Chimera – A visualization system for exploratory research and analysis. *J. Comput. Chem.* **2004**, *25*, 1605–1612.
- 51 Hopkins, A. L.; Groom, C. R. Ligand efficiency: a useful metric for lead selection. *Drug Discov. Today* **2004**, *9*, 430–431.
- 52 Abad-Zapatero, C. Ligand efficiency indices for effective drug discovery. *Expert Opin. Drug Discov.* **2007**, *2*, 469–488.
- 53 Schultes, S.; de Graaf, C.; Haaksma, E. E. J.; de Esch, I. J. P.; Leurs, R.; Krämer, O. Ligand efficiency as a guide in fragment hit selection and optimization. *Drug Discov. Today Technol.* **2010**, *7*, e157–e162.

- 1
2
3
4
5
6
7
8
9
10
11
12
13
14
15
16
17
18
19
20
21
22
23
24
25
26
27
28
29
30
31
32
33
34
35
36
37
38
39
40
41
42
43
44
45
46
47
48
49
50
51
52
53
54
55
56
57
58
59
60
- 54 Leeson, P. D.; Springthorpe, B. The influence of drug-like concepts on decision-making in medicinal chemistry. *Nat. Rev. Drug Discov.* **2007**, *6*, 881–890.
- 55 Lipinski, C. A.; Lombardo, F.; Dominy, B. W.; Feeney, P. J. Experimental and computational approaches to estimate solubility and permeability in drug discovery and development settings. *Adv. Drug Delivery Rev.* **1997**, *23*, 3–25.
- 56 Wager, T. T.; Hou, X.; Verhoest, P. R.; Villalobos, A. Moving beyond rules: The development of a central nervous system multiparameter optimization (CNS MPO) approach to enhance alignment of drug-like properties. *ACS Chem. Neurosci.* **2010**, *1*, 435–449.
- 57 Clark, D. E. Rapid calculation of polar molecular surface area and its application to the prediction of transport phenomena. 1. Prediction of intestinal absorption. *J. Pharm. Sci.* **1999**, *88*, 807–814.
- 58 Hitchcock, S. A.; Pennington, L. D. Structure-brain exposure relationships. *J. Med. Chem.* **2006**, *49*, 7559–7583.
- 59 Sally, R.; Vinter, A. Molecular field technology and its applications in drug discovery. *Innov. Pharm. Technol.* **2007**, 14–18.
- 60 Abad-Zapatero, C.; Metz, J. Ligand efficiency indices as guideposts for drug discovery. *Drug Discov. Today* **2005**, *10*, 464–469.
- 61 Lippert, T.; Rarey, M. Fast automated placement of polar hydrogen atoms in protein-ligand complexes. *J. Cheminform.* **2009**, *1*, 13–24.
- 62 Bietz, S.; Urbaczek, S.; Rarey, M. Hydrogen placement in protein-ligand complexes under consideration of tautomerism. *J. Cheminform.* **2011**, *3* (Suppl. 1), P13.
- 63 Schärfer, C.; Schulz-Gasch, T.; Hert, J.; Heinzerling, L.; Schulz, B.; Inhester, T.; Stahl, M.; Rarey, M. CONFECT: Conformations from an expert collection of torsion patterns. *ChemMedChem.* **2013**, *8*, 1690–1700.

-
- 1
2
3
4
5
6
7
8
9
10
11
12
13
14
15
16
17
18
19
20
21
22
23
24
25
26
27
28
29
30
31
32
33
34
35
36
37
38
39
40
41
42
43
44
45
46
47
48
49
50
51
52
53
54
55
56
57
58
59
60
- 64 Schärfer, C.; Schulz-Gasch, T.; Ehrlich, H. C.; Guba, W.; Rarey, M.; Stahl, M. Torsion angle preferences in drug-like chemical space: A comprehensive guide. *J. Med. Chem.* **2013**, *56*, 2016–2028.
- 65 TorsionAnalyzer was developed in collaboration between F.A. Hoffmann-LaRoche, Switzerland, and the Center for Bioinformatics (ZBH) of the University of Hamburg; <http://www.biosolveit.de/TorsionAnalyzer/>.

